



PONTIFICIA UNIVERSIDAD CATOLICA DE CHILE
ESCUELA DE INGENIERIA

**PHYSIOLOGY OF OXYGEN CONSUMPTION
BY AN INDUSTRIAL STRAIN OF
SACCHAROMYCES CEREVISIAE UNDER
ENOLOGICAL FERMENTATION CONDITIONS**

MARCELO ANDRÉS ORELLANA ACUÑA

Thesis submitted to the Office of Research and Graduate Studies in partial fulfillment of the requirements for the Degree of Doctor in Engineering Sciences

Advisor:

EDUARDO AGOSIN TRUMPER

Santiago de Chile, August, 2013

© 2013, Marcelo Orellana Acuña



PONTIFICIA UNIVERSIDAD CATOLICA DE CHILE
ESCUELA DE INGENIERIA

**PHYSIOLOGY OF OXYGEN CONSUMPTION
BY AN INDUSTRIAL STRAIN OF
SACCHAROMYCES CEREVISIAE UNDER
ENOLOGICAL FERMENTATION CONDITIONS**

MARCELO ANDRÉS ORELLANA ACUÑA

Members of the Committee:

EDUARDO AGOSIN T., PHD

RICARDO PEREZ C., PHD

CLAUDIO GELMI W., PHD

FELIPE LAURIE G., PHD

FLORIAN BAUER, PHD

CRISTIAN VIAL E., PHD

Thesis submitted to the Office of Research and Graduate Studies in partial fulfillment of the requirements for the Degree of Doctor in Engineering Sciences

Santiago de Chile, August, 2013

*A mi familia...
por su apoyo incondicional.*

ACKNOWLEDGMENTS

I would like to thank all people who have contributed to this work either in the research area or with everyday support. Many thanks also to everyone in the Biotechnology laboratory, the Chemical Engineering and Bioprocess Department, for their friendship and for making the laboratory an agreeable place to work.

Special thanks to Professor Eduardo Agosin for his continuous support and patience, his valuable supervision, his sharp observations and good advice throughout this thesis.

Also thanks to PhD. Felipe Aceituno, MSc. Isabel Moenne, Eng. Marianna Delgado and Eng. Waldo Acevedo for their support in different stages of this thesis and for their comments and discussions to improve the final version of this manuscript and the oral presentation.

Thanks to the Comisión Nacional de Investigación Científica y Tecnológica (CONICYT), the Vicerrectoría de Investigación (VRI) and Pontificia Universidad Católica de Chile for providing the necessary funding to make this research possible.

Finally, I would like to say thanks to my family: Fernando, Cynthia, Cristina and Consuelo for their unconditional love and support, and thanks to Milena for her support and love in the last part of this long trip.

INDEX OF CONTENTS

ACKNOWLEDGMENTS.....	i
INDEX OF CONTENTS.....	ii
FIGURE INDEX.....	vi
TABLE INDEX.....	ix
ABBREVIATION INDEX.....	x
ABSTRACT.....	xii
RESUMEN.....	xiv
I. INTRODUCTION.....	1
I.1 Motivation.....	1
I.2 Oxygen management during winemaking.....	1
I.3 Metabolic role of oxygen during wine yeast fermentation.....	4
I.4 Metabolism of <i>Saccharomyces cerevisiae</i> in aerobic and anaerobic conditions.....	6
I.5 Oxygen regulatory effects on the physiology of <i>S. cerevisiae</i>	9
I.5.1 Gene expression regulated by oxygen.....	9
I.5.2 Crabtree effect and cytosol-mitochondria redox shuttles.....	14
I.5.3 Effect of oxygen availability on tricarboxylic acid (TCA) cycle.....	16
I.6 Continuous cultures as a tool for conducting physiological studies.....	18
I.7 Dynamic response of <i>Saccharomyces cerevisiae</i> physiology to environmental perturbations.....	22
I.8 Metabolic flux analysis (MFA) as a tool for research.....	23
I.9 Yeast oxygen consumption under winemaking conditions.....	26
I.10 Working hypotheses.....	28
I.11 Objectives.....	29
I.12 Approach.....	29
II. MATERIALS AND METHODS.....	31
II.1 Yeast strain and culture conditions.....	31
II.2 Culture media.....	31
II.3 Gas measurement and control.....	33

II.3.1 Dissolved oxygen levels	33
II.3.2 Oxygen impulses generation and sampling time	34
II.4 Bioreactor sampling	35
II.5 Analytical techniques.....	35
II.5.1 High pressure liquid chromatography (HPLC).....	35
II.5.2 Dry cell weight determination	36
II.5.3 Assimilable nitrogen and proline determination.....	36
II.5.4 Ergosterol extraction and determination.....	36
II.5.5 Biomass components determination	37
II.6 RNA extraction and quantification	37
II.7 Transcriptome analysis	38
II.7.1 Microarray analysis of dissolved oxygen levels	38
II.7.2 Data clustering analysis of dissolved oxygen levels.....	39
II.7.3 Microarray analysis through dissolved oxygen impulse.....	40
II.7.4 Data clustering analysis for dissolved oxygen impulse	40
II.7.5 Transcriptional network analysis	41
I.8 Metabolic flux analysis	42
II.8.1 Stoichiometric matrix	42
II.8.2 Flux estimation	43
II.8.3 Consistency and sensibility analysis.....	43
III. RESULTS	45
III.1 Long-term impact of increasing concentrations of dissolved oxygen on wine yeast physiology under enological conditions.....	45
III.1.1 Simulation of dissolved oxygen concentrations and oxygen uptake rates under enological conditions.....	45
III.1.2 Carbon balances at different dissolved oxygen concentration	46
III.1.3 Relationship between biomass increase and proline consumption in the presence of oxygen	47
III.1.4 Impact of dissolved oxygen concentration on specific rates and respiratory quotient (RQ).....	48
III.1.5 Metabolic flux analysis.....	49

III.1.5.1. Sources and sinks of NADH and NADPH	52
III.1.5.2 Sources and sinks of ATP.....	53
III.1.6 Gene expression analysis of dissolved oxygen levels	54
III.1.6.1 Analysis of oxygen level transitions.....	55
III.1.6.1.1 Genes differentially expressed between 0 and 1.2 μ M dissolved oxygen	55
III.1.6.1.2 Genes differentially expressed between 1.2 μ M and 2.7 μ M dissolved oxygen	55
III.1.6.1.3 Genes differentially expressed between 5 and 21 μ M dissolved oxygen.	56
III.1.6.1.4 Other gene expression changes	56
III.1.6.2 Clustering analysis.....	58
III.1.6.2.1 Genes down-regulated at 21 μ M dissolved oxygen	58
III.1.6.2.2 Genes down-regulated with 1.2 μ M dissolved oxygen	58
III.1.6.2.3 Genes negatively correlated with dissolved oxygen	59
III.1.6.2.4 Genes positively correlated with dissolved oxygen	59
III.2 Transient effect of oxygen on wine yeast physiology, in anaerobic conditions using an impulse of oxygen.....	62
III.2.1 Dissolved oxygen dynamics under wine fermentation conditions at laboratory scale.	62
III.2.2 Metabolic dynamics of the yeast cells throughout the oxygen impulse	63
III.2.3. Transcriptomic dynamics of the yeast cells before and after the oxygen impulse	65
III.2.3.1 Characterization of yeast transcriptome after the oxygen impulse	65
III.2.3.1.1 Genes of immediate response to oxygen	67
III.2.3.1.2 Genes of delayed response to oxygen	67
III.2.3.1.3 Genes of over-delayed response to oxygen	68
III.2.3.2 Gene ontology analysis.....	68
III.2.3.3 Transcriptional networks controlling the oxygen response.....	69
III.2.3.3.1 Master transcriptional regulators	69
III.2.3.3.2 Hap1p regulatory network.....	70
III.2.3.3.3 Skn7p regulatory network	71

IV. DISCUSSION	73
IV.1 Impact of different oxygen levels in wine yeast extracellular metabolism.....	73
IV.2 Effect of different oxygen concentration in the transition between fermentative and respiro-fermentative metabolism	74
IV.3 Succinic acid transport under different dissolved oxygen levels	75
IV.4 Role of cytosol-mitochondria redox shuttles in respiro-fermentative metabolism	76
IV.5 Respiratory related genes are expressed under steady state oxygen levels despite high sugar concentrations	77
IV.6 Physiological response of wine yeast at the highest dissolved oxygen concentration.	78
IV.7 Yeast cell wall remodeling by different steady state dissolved oxygen concentration	79
IV.8 Dissolved oxygen levels impact for winemaking process.	80
IV.9 Physiological response of the wine yeast <i>S. cerevisiae</i> EC1118 to an oxygen impulse under enological conditions.	81
IV.10 Gene expression response and regulatory networks throughout dissolved oxygen impulse.....	82
IV.11 Master transcription factors controlling the short-term oxygen yeast response.	82
IV.11.1 Beneficial oxygen impulse effects from a winemaking perspective: the role of Hap1p.	83
IV.11.2 Other yeast oxidative stress response upon oxygen addition in wine fermentation conditions: the role of Skn7p.	85
IV.12 Other stress related responses and effect of oxygen impulse on the yeast cell wall.	86
V. CONCLUSIONS AND FUTURE DIRECTIONS	87
VI. ANNEXES	91
VII. REFERENCES	102

FIGURE INDEX

Figure I.1: Aerated pump over operation. The arrows indicate the direction of the fermenting must flow (P= pump). (Adapted from (Ribéreau-Gayon, et al., 2006))......2

Figure I.2: The oxygen dependent steps of sterol synthesis in *S. cerevisiae*: intermediates and oxygen requirements. Enzymes: Erg1p, squalene epoxidase; Erg7p, lanosterol synthase; Erg11p (Cyp51p), lanosterol C-14 demethylase; Erg24p, sterol C-14 reductase; Erg25p, sterol C-4 methyloxidase; Erg26p, sterol C-3 dehydrogenase (C4-decarboxylase);Erg27p, sterol C-3 ketoreductase; Erg6p, sterol C-24 methyltransferase; Erg2p, sterol C-8 isomerase; Erg3p, sterol C-5 desaturase; Erg5p, sterol C-22 desaturase; Erg4p, sterol C-24 reductase. (Adapted from (Rosenfeld & Beauvoit, 2003)).5

Figure I.3: Electron transfer and energy generation from glucose in aerobic and anaerobic conditions by *S. cerevisiae*. (Adapted from (Walker, 1998)).....7

Figure I.4: Diagram showing two mechanisms in which heme may mediate oxygen control of transcription in *S. cerevisiae*. In the first case (1), heme serves as a ligand for a transcription factor and heme concentration regulates transcription. In the second case (2), heme is a prosthetic group of a transcription factor and up- or down regulates transcription in response to changes in its redox state. (Adapted from (Bunn & Poyton, 1996)). 11

Figure I.5: Hap1p and Hap2/3/4/5p (represented by HAP) interacts with upstream activator sites (UAS) to activate the transcription of aerobic genes. Furthermore, Hap1p also activates transcription of some hypoxic genes. Rox1p represses the transcription of hypoxic genes interacting with upstream repressor sites (URS). (Adapted from (Kwast et al., 1998)). 12

Figure I.6: Three main redox shuttles that have been proposed to work in *S. cerevisiae* 1) the glycerol-3-phosphate shuttle (Gut2p), 2) the external NADH dehydrogenase (Nde1p) shuttle and 3) the mitochondrial alcohol dehydrogenase (Adh3p) shuttle. (Adapted from (Bakker, et al., 2001))..... 16

Figure I.7: TCA pathways during respiration and fermentation. Black arrows, the TCA pathway functions as a cycle during respiration. Grey arrows, the TCA pathway operates as an oxidative branch and a reductive branch during fermentative metabolism. FR,

fumarate reductase; SDH, Succinate dehydrogenase complex; OGDH, Oxoglutarate dehydrogenase complex. (Taken from (Camarasa, et al., 2003)). 17

Figure I.8: Representation of a continuous culture in a stirred tank bioreactor. The liquid medium from the feed reservoir, containing known concentrations of substrates (S_0), biomass (X_0 , commonly =0), and products (P_0), is pumped into the bioreactor at a flow rate v . Gaseous feed can also be used (not shown). The concentrations of biomass (X), substrates (S) and products (P) inside the bioreactor are equal to those in the effluent. The effluent is pumped out at the same rate as the feed rate, v . The volume of medium in the bioreactor, V , is constant. The dilution rate D is defined as v/V (Adapted from (Acevedo, et al., 2004)). 19

Figure III.1: Relationship between dissolved oxygen concentration and specific oxygen uptake rate (OUR) of *Saccharomyces cerevisiae* strain EC1118. Blue symbols correspond to steady state nitrogen limited continuous cultures with increasing dissolved oxygen concentrations. The corresponding OURs were determined in the same cultures. Brown squares represent the five dissolved oxygen conditions evaluated in this research. 46

Figure III.2: Flux distributions in *S. cerevisiae* EC1118 strain grown in nitrogen limited chemostats at $D = 0.1 \text{ h}^{-1}$ from anaerobic (top) to 21 μM (bottom) dissolved oxygen concentrations. Numbers indicate specific reactions related with oxygen consumption: 1) Respiration, 2) Unsaturated lipid synthesis, 3) Ergosterol synthesis, 4) Proline uptake. The fluxes are expressed as percentage of the total carbon uptake. Negative numbers indicate flux in the reverse direction. The flux for maintenance is expressed as a percentage of the total ATP produced. CARB, carbohydrates; GLC, glucose; FRUC, fructose; F6P, fructose 6-phosphate; R5P, ribose 5-phosphate; DHAP, dihydroxyacetone phosphate; G3P, glyceraldehyde 3-phosphate; E4P, erythrose 4-phosphate; GLY3P, glycerol 3-phosphate; 3PG, 3-phosphoglycerate; GLYC, glycerol; SER, serine; PEP, phosphoenolpyruvate; AC, acetate; ACCoA, acetyl coenzyme A; LIP, lipids; OAA, oxaloacetate; PYR, pyruvate; ADE, acetaldehyde; ETOH, ethanol; ASP, aspartate; ISOCIT, isocitrate; GLN, glutamine; FUM, fumarate; AKG, α -ketoglutarate; GLU, glutamic acid; PROT, protein; SUC, succinate; SUCEX, extracellular succinate; mATP, maintenance ATP; PRO, proline; NADH_{mit}, mitochondrial NADH; NADH_{cyt}, cytosolic NADH; ERG, ergosterol; UN_LIP, unsaturated lipids. 51

Figure III.3: Hierarchical clustering of the *S. cerevisiae* transcriptome data obtained for the five dissolved oxygen conditions. From center to outside, the dendrogram depicts: 1) Hierarchical clustering tree; 2) Color ribbons indicate each of the 56 clusters; 3) Heatmaps of gene expression values, where black and green represent low and high gene

expression levels, respectively. Increasing dissolved oxygen concentrations, from 0 (most internal) to 21 μM (most external), are shown. The scale of the calculated distances in the dendrogram is also illustrated.....61

Figure III.4: a) Dissolved oxygen dynamics during dissolved oxygen impulse. Time zero corresponds to anaerobic, steady state anaerobic conditions. The curve is the dissolved oxygen average value of three independent experiments. b) Sampling points before and after oxygen impulse.....63

Figure III.5: Metabolic dynamics of wine yeast throughout a dissolved oxygen impulse within the first hour (upper panel) and within the first residence time (bottom panel). Specific rates of glucose consumption (open diamond), glycerol production (close square), ethanol production (close triangle) and CO_2 production (open circle) are indicated. Each point represents the average value of three independent experiments during the time course (0 (steady state), 10 min, 20 min, 30 min, 45 min, 60 min, 300 min and 600 min (one residence time)).....64

Figure III.6: Mean time-dependent profiles of clustered genes. Differentially expressed genes through dissolved oxygen pulse were clustered in six groups according to their time dependent expression profiles. Grey lines represent the expression level of each gene in that cluster during the time course. Black line represents the average expression level of all genes in that cluster during the time course (0 (steady state), 4 min, 10 min, 1 hour, 5 hours and 10 hours). Absolute intensity values were mean normalized for each gene and for each time-point.....66

Figure III.7: Genes regulated by Hap1p. Master transcription factor and target genes are illustrated from the top to the bottom of the figure. Nodes were identified according to the cluster to which they belong: Cluster 1 (light diamond), Cluster 4 (grey hexagon) and Cluster 5 (grey square). a) Genes directly regulated by Hap1p, b) Genes regulated by Hap1p through transcription factors related to stress and c) Genes regulated by Hap1p through Yap1p/Rox1p.....71

Figure III.8: Genes regulated by Skn7p. Master transcription factor and target genes are illustrated from the top to the bottom of the figure. Nodes were identified according to the cluster they belong: Cluster 1 (light diamond), Cluster 4 (grey hexagon) and Cluster 5 (grey square). a) Skn7p regulatory network and b) Genes regulated by Skn7p and Hap1p.72

TABLE INDEX

Table II.1: Conditions used to generate the steady state dissolved oxygen levels evaluated in this study.....	34
Table II.2: Estimation of ethanol and CO ₂ specific production rates by the MFA model.....	44
Table III.1: Dissolved oxygen concentrations and specific oxygen uptake rate of <i>S. cerevisiae</i> EC 1118 grown under different oxygen levels.	45
Table III.2: Dissolved oxygen concentration and glucose yields in different oxygen feeding conditions ^a	47
Table III.3: Proline consumption and nitrogen yields.	48
Table III.4: a) Specific consumption and production rates and b) Steady-state metabolite concentration in <i>S. cerevisiae</i> EC 1118 grown under increasing dissolved oxygen culture conditions.	49
Table III.5: Specific production rates of major biomass components at different dissolved oxygen concentrations ^a	50
Table III.6: Contribution to NADH and ATP turnover of different metabolic pathways in <i>S. cerevisiae</i> EC1118 grown under different dissolved oxygen culture conditions.....	54
Table III.7: Characterization of differentially expressed genes across the different oxygen levels.....	57
Table III.8: Functional terms enrichment for the genes in each cluster	60
Table III.9: Functional terms enrichment for the genes in each cluster	69

ABBREVIATION INDEX

CCC	Cophenetic Correlation Coefficient
ChIP	Chromatin Immunoprecipitation
CWI	Cell Wall Integrity
DCW	Dry Cell Weight
DEPC	Diethylpyrocarbonate
DNA	Deoxyribonucleic Acid
FAD	Flavin Adenine Dinucleotide
FDR	False Discovery Rate
GEO	Gene Expression Omnibus
GO	Gene Ontology
HPLC	High Pressure Liquid Chromatography
MFA	Metabolic Flux Analysis
NMR	Nuclear Magnetic Resonance
NOPA	Nitrogen by o-phthaldialdehyde
OUR	Specific Oxygen Uptake Rate
RMA	Robust Multiarray Analysis
RNA	Ribonucleic Acid
RPM	Revolutions Per Minute
RQ	Respiratory Quotient
SGD	Saccharomyces Genome Database
TCA	Tricarboxylic Acid
UFA	Unsaturated Fatty Acids

YAN

Yeast Assimilable Nitrogen

YPD

Yeast extract Peptone Dextrose

PONTIFICIA UNIVERSIDAD CATOLICA DE CHILE
ESCUELA DE INGENIERIA

PHYSIOLOGY OF OXYGEN CONSUMPTION BY AN INDUSTRIAL STRAIN OF
SACCHAROMYCES CEREVISIAE UNDER ENOLOGICAL FERMENTATION
CONDITIONS

Thesis submitted to the Office of Research and Graduate Studies in partial fulfillment of
the requirements for the Degree of Doctor in Engineering Sciences by

MARCELO ANDRES ORELLANA ACUÑA

ABSTRACT

Discrete oxygen additions play a critical role in wine fermentation process. However, no system biology studies have been conducted so far about how oxygen modifies yeast metabolism under wine fermentation conditions. We proposed here the first systemic approach for the quantitative understanding of the impact of oxygen on wine yeast physiology, under enological conditions. In order to do this, transcriptomic, fluxomic and metabolomic effects of dissolved oxygen on wine yeast physiology were evaluated.

We simulated the range of dissolved oxygen concentrations that occur after an enological pump-over, by sparging nitrogen-limited continuous cultures with oxygen-nitrogen gaseous mixtures to achieve increasing steady-state dissolved oxygen concentrations. When the dissolved oxygen increases from 1.2 to 2.7 μM (20 °C), yeast cells change from a fully fermentative to a mixed respiro-fermentative metabolism. This transition is characterized by a switch in the operation of the tricarboxylic acid (TCA) cycle and an activation of NADH shuttling from the cytosol to mitochondria. Nevertheless, fermentative ethanol production remained the major cytosolic NADH sink for all oxygen conditions, suggesting the limitation of mitochondrial NADH reoxidation as the major cause of the Crabtree effect, instead of glucose repression. This is reinforced by the induction of several key respiratory genes by oxygen, despite the high sugar concentration.

On the other hand, we simulated typical enological operations for oxygen addition by carrying out an impulse of pure oxygen for 30 seconds, under anaerobic conditions, employing nitrogen limited continuous cultures. Respiratory and ergosterol biosynthetic genes were induced after oxygen impulse. Moreover, genes involved in yeast cell wall remodeling and oxidative stress among others were significantly induced and/or repressed by oxygen impulse. The changes in expression of these genes are coordinated responses that share common elements at the level of transcriptional regulation.

The results of this study indicate that mitochondrial respiration is responsible for a substantial part of the oxygen response in yeast cells during alcoholic fermentation. Furthermore, genes involved in proline uptake, mannoprotein composition of yeast cell and oxidative stress were significantly induced and/or repressed both short and long term by oxygen, highlighting the dual role of oxygen in “making or breaking wines.” These findings will facilitate the development of oxygen addition strategies to optimize yeast performance in industrial fermentations.

Members of the Doctoral Thesis Committee:

Eduardo Agosin T.

Ricardo Pérez C.

Claudio Gelmi W.

Felipe Laurie G.

Florian Bauer

Cristian Vial E.

Santiago, August, 2013

PONTIFICIA UNIVERSIDAD CATOLICA DE CHILE
ESCUELA DE INGENIERIA

FISIOLOGIA DEL CONSUMO DEL CONSUMO DE OXIGENO EN UNA CEPA
INDUSTRIAL DE *SACCHAROMYCES CEREVISIAE* EN CONDICIONES DE
FERMETACION ENOLOGICA

Tesis enviada a la Dirección de Investigación y Postgrado en cumplimiento parcial de los requisitos para el grado de Doctor en Ciencias de la Ingeniería.

MARCELO ANDRES ORELLANA ACUÑA

RESUMEN

Las adiciones discretas de oxígeno juegan un papel crítico en el proceso de fermentación del vino. Sin embargo, hasta ahora, no se han llevado a cabo estudios de biología de sistemas, acerca de cómo el oxígeno modifica el metabolismo de la levadura vínica bajo condiciones de fermentación vínica. Proponemos aquí la primera aproximación sistémica para el entendimiento cuantitativo del impacto del oxígeno sobre la fisiología de la levadura vínica, bajo condiciones enológicas. Para este fin, los efectos del oxígeno disuelto en el transcriptoma, fluxoma y metabóloma sobre la fisiología de la levadura vínica fueron evaluados.

Simulamos el rango de concentraciones de oxígeno que se producen después de un remontaje enológico, burbujeando cultivos continuos limitados en nitrógeno con mezclas gaseosas oxígeno-nitrógeno, para alcanzar concentraciones crecientes de oxígeno en estado estacionario. Cuando el oxígeno disuelto aumenta desde 1.2 a 2.7 μM (20 °C), el metabolismo de la levadura cambia desde totalmente fermentativo a mixto respiro-fermentativo. Esta transición se caracteriza por un cambio en la operación de ciclo del ácido tricarbóxico y el aumento del transporte de NADH desde el citosol a la mitocondria. Sin embargo, la producción fermentativa de etanol sigue siendo el principal sumidero del NADH citosólico para todas las condiciones con oxígeno, sugiriendo la limitación de la reoxidación mitocondrial de NADH como la principal causa del efecto Crabtree, en lugar de la represión por glucosa. Esto es reforzado por la inducción de varios genes respiratorios clave por oxígeno, a pesar de la alta concentración de azúcar.

Por otro lado, simulamos las típicas operaciones enológicas de adición de oxígeno realizando un impulso de oxígeno puro por 30 segundos, en condiciones anaeróbicas, utilizando cultivos continuos limitados en nitrógeno. Genes respiratorios y de biosíntesis de ergosterol fueron inducidos después del impulso de oxígeno. Además, genes involucrados en remodelamiento de pared celular y estrés oxidativo entre otros, fueron significativamente inducidos y/o reprimidos por el impulso de oxígeno. Los cambios en la expresión de estos genes son respuestas coordinadas que comparten elementos comunes a nivel de regulación transcripcional.

Los resultados de este estudio indican que la respiración mitocondrial es responsable de parte sustancial de la respuesta al oxígeno en células de levadura durante la fermentación alcohólica. Además, genes involucrados en consumo de prolina, remodelamiento de pared celular y estrés oxidativo fueron significativamente inducidos y/o reprimidos, tanto a corto como a largo plazo por oxígeno, destacando el papel dual del oxígeno en “crear o destruir vinos”. Estos hallazgos facilitaran el desarrollo de estrategias de adición de oxígeno para optimizar el desempeño de la levadura en fermentaciones industriales.

Miembros de la Comisión de Tesis Doctoral

Eduardo Agosin T.

Ricardo Pérez C.

Claudio Gelmi W.

Felipe Laurie G.

Florian Bauer

Cristian Vial E.

Santiago, Agosto, 2013

I. INTRODUCTION

I.1 Motivation

Oxygen is frequently added during enological fermentation at an industrial scale in order to improve fermentative rate, yeast viability and biomass concentration (Julien et al., 2000). Oxygen additions during enological fermentation are particularly effective at the end of the yeast growth phase (Sablayrolles et al., 1996). From a yeast perspective, oxygen is required for the synthesis of the so-called “anaerobic” growth factors, i.e. ergosterol and unsaturated fatty acids (Fornairon-Bonnefond et al., 2002; Rosenfeld et al., 2003). Furthermore, oxygen is essential for proline consumption as nitrogen source (Ingledeu et al., 1987). To the best of our knowledge, no systemic studies have been conducted so far about how oxygen modifies yeast metabolism under wine fermentation conditions. The aim of this work is to use a systemic approach for a quantitative understanding of the impact of dissolved oxygen on yeast cells physiology, under enological conditions. These findings will facilitate the development of oxygen addition strategies to optimize yeast performance in industrial fermentations.

I.2 Oxygen management during winemaking

“Oxygen can make or break wines” (Ribereau-Gayon, 1933). Indeed, winemakers are aware that oxygen is a critical factor to consider over the whole winemaking process. During wine production, oxygen is always encountered. From the onset of harvest through several winery operations such as crushing, pressing, racking and fermentation, oxygen will be always present (DuToit et al., 2006). The consequences of significant oxygen exposure range from notorious flavor changes to acetification (Oszmianski et al., 1996; Ribéreau-Gayon et al., 2006). Conversely, moderate oxygen exposure could benefit some wines by, for instance, improving

yeast performance and contributing to the stabilization of colour and reduction of astringency and bitterness (Atanasova et al., 2002; Castellari et al., 1998; Danilewicz, 2003; Waterhouse & Laurie, 2006). Thus, the optimal management of oxygen incorporation during the winemaking process is essential to produce a high quality product.

Oxygen addition during wine fermentation is generally achieved through aerated pump overs. An aerated pump over consists in letting fermenting must flow out of the tank in contact with atmospheric air and then pumping it back into the upper part of the tank (Figure I.1) (Ribéreau-Gayon et al, 2006).

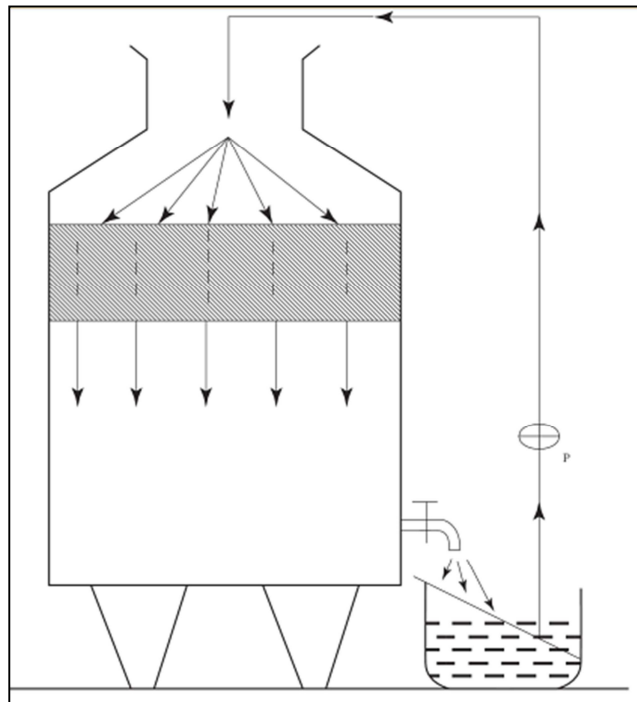


Figure I.1: Aerated pump over operation. The arrows indicate the direction of the fermenting must flow (P= pump). (Adapted from (Ribéreau-Gayon, et al., 2006)).

Controlled oxygen additions during wine fermentations also can be beneficial for wine aromatic diversity. For instance, Valero et al., (2002) compared the higher alcohols

and esters content of wines fermented with and without oxygenated musts. They found higher aroma contents in wines produced with oxygenated musts, although they showed a lower esters/higher-alcohols ratio. Moreover, oxygen additions during wine fermentation significantly reduce the capacity of oxygen consumption by the yeast lees (Salmon, 2006).

Another technique aiming to introduce small and controlled quantities of oxygen after alcoholic fermentation, called micro-oxygenation, is common practice in many wineries (Salmon, 2006). Micro-oxygenation was initially developed with the aim of bringing about desirable changes in aroma and texture which cannot readily be obtained by traditional ageing techniques (Parish et al., 2000)

The main benefits of this technique for wine are the elimination of sulphide aromas, as well as an improvement in color stability and “tannin structure” (Pérez-Magariño et al., 2007; Sánchez-Iglesias et al., 2009). The general principle of micro-oxygenation is the addition of small and controlled amounts of oxygen into the wine by means of a sparger that distributes the gas in the form of small bubbles (Parish et al., 2000; Schmidtke et al., 2011; Zoecklein et al., 2002).

However, oxygen could also be detrimental when added at the wrong moment or in too high concentrations, resulting in wine oxidation, white wine color degradation due to its low antioxidant capacity, off-flavors synthesis and growth of undesirable microorganisms such as acetic acid bacteria (Devatine et al., 2007; Du Toit et al., 2006).

It is therefore clear that oxygen plays a critical role during the winemaking process, which could be either beneficial or detrimental for the quality of the final product, depending on the moment and amount of exposure to dissolved oxygen. Therefore, to develop oxygen addition strategies, that maximize wine yeast performance in industrial fermentations and minimize the detrimental effects of oxygen on wine yeast metabolism and wine quality, it is essential to understand the molecular mechanisms involved in wine yeast oxygen consumption under wine fermentation conditions.

I.3 Metabolic role of oxygen during wine yeast fermentation

Wine fermentation is a complex and dynamic process during which sugar is transformed to ethanol due to the biological activity of the fermenting yeast. Upon inoculation, wine yeast adapts to adverse conditions found in grape must, such as low pH (2.9-3.8), and high sugar concentrations (up to 300 g·L⁻¹). After the onset of fermentation, the biological activity of yeast produce additional stressful conditions, such as nitrogen limitation and increasing ethanol concentration in the fermenting must.

The adverse conditions that the wine yeast faces throughout winemaking are the main reasons for sluggish and stuck fermentations – i.e. fermentations in which the rate of sugar consumption is extremely slow, especially towards the end of the fermentation (Ingledew et al., 1985), avoiding the completion of the fermentation process. Sluggish and stuck fermentations are a frequent and major problem for the winemaking industry, due to the economic losses that they can causes.

Many authors have highlighted that oxygen additions are an efficient method to avoid sluggish and stuck fermentations (Alexandre & Charpentier, 1998; Bisson & Butzke, 2000; Blateyron & Sablayrolles, 2001; Sablayrolles et al., 1996). Furthermore, Sablayrolles (Sablayrolles, et al., 1996) demonstrated that the most effective oxygenation results are obtained by adding approximately 5 mg·L⁻¹ at the end of the cell growth phase.

From the wine yeast perspective, oxygen addition has a positive effect on yeast metabolism because it helps to improve the fermentative rate, yeast viability and biomass concentration (Julien et al., 2000; Valero et al., 2001). Yeast cells need oxygen to produce anaerobic growth factors such as ergosterol and mono-unsaturated fatty acids (Fornairon-Bonnefond et al., 2002; Rosenfeld et al, 2003). Molecular oxygen is required for squalene conversion to ergosterol at the level of six enzymatic steps catalysed by five enzymes: a non P450 mono-oxygenase (Erg1p), two hydroxylases/desaturases (Erg25p and Erg3p) and two cytochromes P450 (Erg11p and Erg25p) (Rosenfeld & Beauvoit, 2003). In other words, 12 oxygen molecules are required for the conversion of one squalene to ergosterol (Figure I.2). Meanwhile, the biosynthesis of mono-unsaturated

fatty acids, such as palmitoleate (C16:1^{Δ9}) and oleate (C18:1^{Δ9}) requires ½O₂ per double bond formation, as an electron acceptor. These reactions are catalyzed by the unique microsomal acyl-CoA desaturase Ole1p (Fornairon-Bonnefond, et al., 2002; Rosenfeld & Beauvoit, 2003).

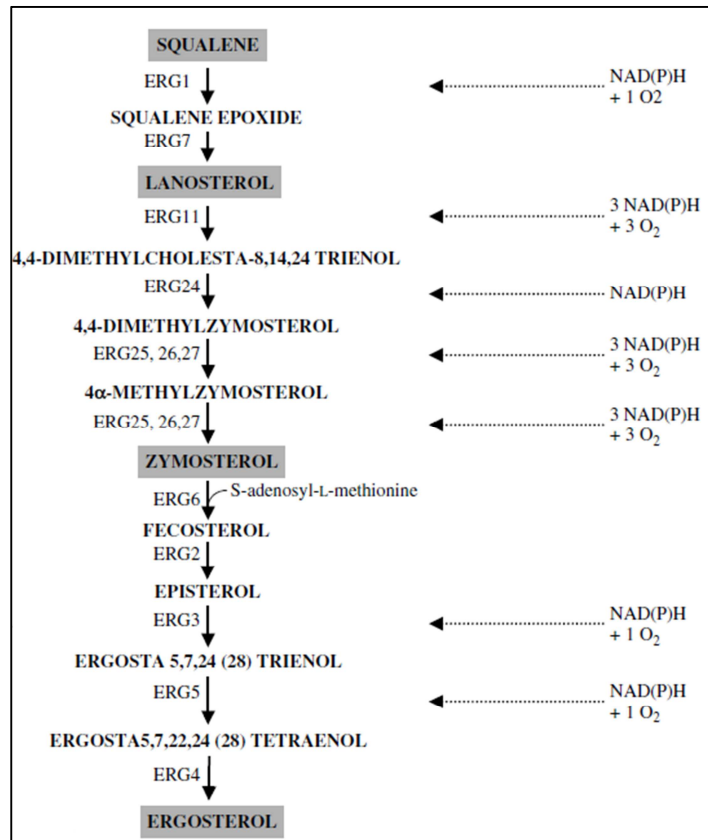


Figure I.2: The oxygen dependent steps of sterol synthesis in *S. cerevisiae*: intermediates and oxygen requirements. Enzymes: Erg1p, squalene epoxidase; Erg7p, lanosterol synthase; Erg11p (Cyp51p), lanosterol C-14 demethylase; Erg24p, sterol C-14 reductase; Erg25p, sterol C-4 methyloxidase; Erg26p, sterol C-3 dehydrogenase (C4-decarboxylase); Erg27p, sterol C-3 ketoreductase; Erg6p, sterol C-24 methyltransferase; Erg2p, sterol C-8 isomerase; Erg3p, sterol C-5 desaturase; Erg5p, sterol C-22 desaturase; Erg4p, sterol C-24 reductase. (Adapted from (Rosenfeld & Beauvoit, 2003)).

Ergosterol and unsaturated fatty acids play a key role in the fluidity of the yeast membrane, which enhances ethanol tolerance (Alexandre et al., 1994). Specifically, the increase of oleic acid (C_{18:1}) (You et al, 2003) and ergosterol (Swan & Watson, 1998) are associated with an enhanced resistance to ethanol. However, yeast cells adapted to high ethanol concentration have a lower content of palmitoleic acid (C_{16:1}) compared to non-adapted yeast cells (Dinh et al 2008), suggesting a consistent role of lipid composition in yeast resistance to stress (Bauer & Pretorius, 2000).

A comprehensive and quantitative approach in wine fermentation conditions could allow a deeper understanding of how oxygen affects wine yeast physiology and the mechanisms that explain the positive effects of oxygen addition in the wine fermentation process. To the best of our knowledge, this comprehensive approach has not been developed yet and is one of the main goals of this thesis.

I.4 Metabolism of *Saccharomyces cerevisiae* in aerobic and anaerobic conditions

The impact of oxygen on the metabolism of *Saccharomyces cerevisiae* has been of great research interest for two main reasons. First, *S. cerevisiae* is one of the few yeasts that can grow fast in anaerobic conditions (Visser et al, 1990). Second, this organism is widely used for the production of ethanol, heterologous proteins, biomass and other biotechnological products (Cot et al., 2007; Kapat et al., 2001; Verduyn, 1991), either in aerobic and anaerobic conditions, as well.

The ability of *S. cerevisiae* to grow in anaerobic and aerobic conditions has been extensively investigated through genetic and physiological studies. Under anaerobic conditions (i.e. fermentative metabolism), the electron surplus generated by the oxidation of carbon sources in the form of NADH is balanced through the generation of ethanol and, to a lesser extent, glycerol. Thus, alcoholic fermentation is a consequence of the redox balance that the yeast must maintain in order to survive (Vargas et al, 2010).

On the other hand, under aerobic conditions (i.e. respiratory metabolism), oxygen can act as an electron sink, through the mitochondrial electron transport chain. The

reduction of oxygen, in this case, allows the reoxidation of NADH and ensures redox balancing (Figure I.3). At high sugar concentrations, the regulation between fermentative and respiratory metabolism in *Saccharomyces cerevisiae* is established by the Crabtree effect. This effect states that, even under aerobic conditions, fermentation predominates over respiration (Walker, 1998).

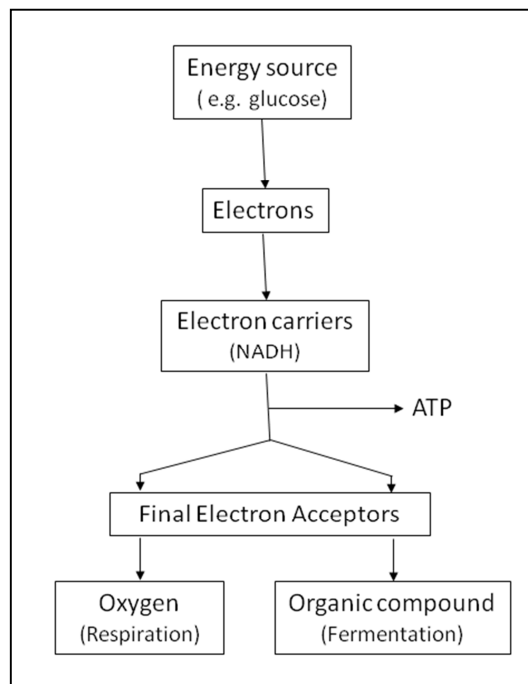


Figure I.3: Electron transfer and energy generation from glucose in aerobic and anaerobic conditions by *S. cerevisiae*. (Adapted from (Walker, 1998))

In the majority of industrial fermentation processes to obtain products such as alcoholic beverages and fuel ethanol, *S. cerevisiae* is introduced into an environment with high sugar concentration and varying oxygen availability (Sánchez & Cardona, 2008). Therefore, it is necessary to understand the regulation of yeast metabolism in response to changes in oxygen availability.

Transcriptomic analyses have been performed using industrial yeasts under conditions relevant to the winemaking process. These include studies of gene expression during fermentation (Marks et al., 2008; Rossignol et al., 2003; Rossouw et al., 2009) and during exposure to a variety of environmental stress conditions such as sub-lethal ethanol concentration (Alexandre et al., 2001), changes in growth temperature (Pizarro et al., 2008), with and without rehydration (Rossignol et al., 2006) and high sugar concentration (Erasmus et al., 2003). The latter, have allowed the identification of stress response mechanisms that are activated by yeast under wine fermentation conditions.

Additionally, studies that combine transcriptomic and proteomic analyses under wine fermentation conditions (Rossouw et al., 2012; Zuzuarregui et al., 2006) have elucidated part of the molecular basis of fermentative behavior between different wine yeast strains such as ethanol production, stress resistance and metabolism of sulfur and nitrogen, which could be related to the production of particular organoleptic compounds. Therefore, these studies provide valuable insight for the understanding of the wine fermentation process.

On the other hand, extensive investigations have been performed to elucidate the mechanism that regulates the transition between fermentative and respiratory metabolism. Several “omics” studies have been carried out using laboratory strains of *S. cerevisiae*, under carbon limited conditions at three levels: metabolomic (Wiebe, et al., 2008), proteomic (de Groot, et al., 2007; Rintala, et al., 2009) and transcriptomic levels (Kwast, et al., 2002; Lai, et al., 2006; Lai et al., 2005; Rintala, et al., 2009; Tai, et al., 2005; ter Linde, et al., 1999; Wiebe, et al., 2008).

Genome wide studies have revealed that a large part of the *S. cerevisiae* transcriptome reacts to dissolved oxygen availability, partly dependent on the carbon source and nutrient limitation. For instance, Piper et al. (2002) identified 877 transcripts differentially expressed between aerobic and anaerobic glucose-limited conditions; and Tai et al. (2005) found that only 155 of these genes responded consistently to anaerobiosis under four different macronutrient limitations. Furthermore, Lai et al. (2005, 2006) monitored the *S. cerevisiae* transcriptome during the transition from aerobic to anaerobic conditions in batch cultivations on glucose and galactose. These studies demonstrated that oxygen availability modifies the transcription of genes which

participate in different biological processes such as mitochondrial respiration, lipids and ergosterol metabolism, oxidative stress response and cell cycle regulation among others.

In addition to transcriptome analyses, a comparison of the transcriptome and proteome revealed the impact of post-transcriptional regulation on different pathways such as glycolysis and amino acid biosynthetic pathways, with respect to oxygen availability (de Groot, et al., 2007). Moreover, Rintala et al. (2009) suggested post transcriptional regulation of the TCA cycle and the electron transport chain under low oxygen levels, after a similar study.

Nevertheless, none of these previously mentioned studies combine both oxygen availability and winemaking conditions. Therefore, we propose the first comprehensive study regarding the effect of oxygen on the physiology of a wine yeast strain under enological conditions (i.e. acidic pH, nitrogen limited and carbon sufficient culture conditions).

I.5 Oxygen regulatory effects on the physiology of *S. cerevisiae*

I.5.1 Gene expression regulated by oxygen

In addition to the oxygen effects on yeast physiology previously mentioned, oxygen also exerts regulatory effects on yeast gene expression at transcriptional level (Zitomer & Lowry, 1992). Oxygen-regulated genes can be divided in two categories: aerobic and hypoxic genes. Aerobic genes are transcribed optimally under normoxic conditions; while hypoxic genes are transcribed under hypoxic and anoxic conditions (Poyton, 1999).

One of the main and best studied mechanisms through which oxygen regulates gene expression in yeast, is the system in which hemes play a central role. Hemes are prosthetic groups of cytochromes and oxygen binding proteins such as catalases. Hemes have some characteristics that convert them in an ideal oxygen effector molecule. First, their biosynthesis is fully oxygen dependent. Second, the enzymes responsible for heme synthesis are present even in anaerobic-grown cells and are controlled at post-

translational level by oxygen. Therefore, the induction of heme biosynthesis begins immediately upon transition from anaerobic to aerobic conditions (Kwast et al., 1998; Rosenfeld & Beauvoit, 2003). Consequently, a simple explicative model of heme dependent regulation of aerobic genes has been established on the assumption that heme levels may increase during oxygenation of anaerobic cultures and decrease as oxygen becomes limiting (Rosenfeld & Beauvoit, 2003; Zitomer & Lowry, 1992).

Furthermore, it has been suggested that the heme redox state, in addition to heme intracellular concentration, is involved in the regulation of gene expression through oxygen (Figure I.4) (Bunn & Poyton, 1996; Rosenfeld & Beauvoit, 2003). The latter is supported by the evidence that some genes that are transcribed optimally under normoxic conditions (e.g. *cytochrome c* and *cytochrome oxidase*) are not regulated collectively at a single oxygen concentration and have different thresholds for activation (Burke et al., 1997).

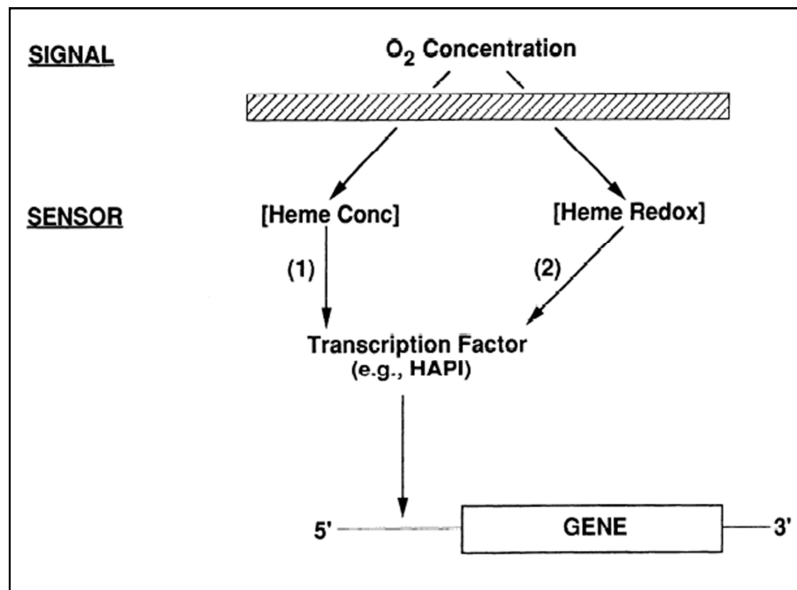


Figure I.4: Diagram showing two mechanisms in which heme may mediate oxygen control of transcription in *S. cerevisiae*. In the first case (1), heme serves as a ligand for a transcription factor and heme concentration regulates transcription. In the second case (2), heme is a prosthetic group of a transcription factor and up- or down regulates transcription in response to changes in its redox state. (Adapted from (Bunn & Poyton, 1996)).

Several heme-dependent transcription regulators exist, e.g. transcription factor Hap1p (heme activated protein), which activates the transcription of several aerobic genes and some hypoxic genes; the transcription factor Hap2/3/4/5p, which activates transcription of many aerobic genes and it is also regulated by kind of carbon substrate; Rox1p (regulation by oxygen), the repressor of hypoxic genes under aerobic conditions (Figure I.5) (Plakunov & Shelemekh, 2009; Zitomer & Lowry, 1992).

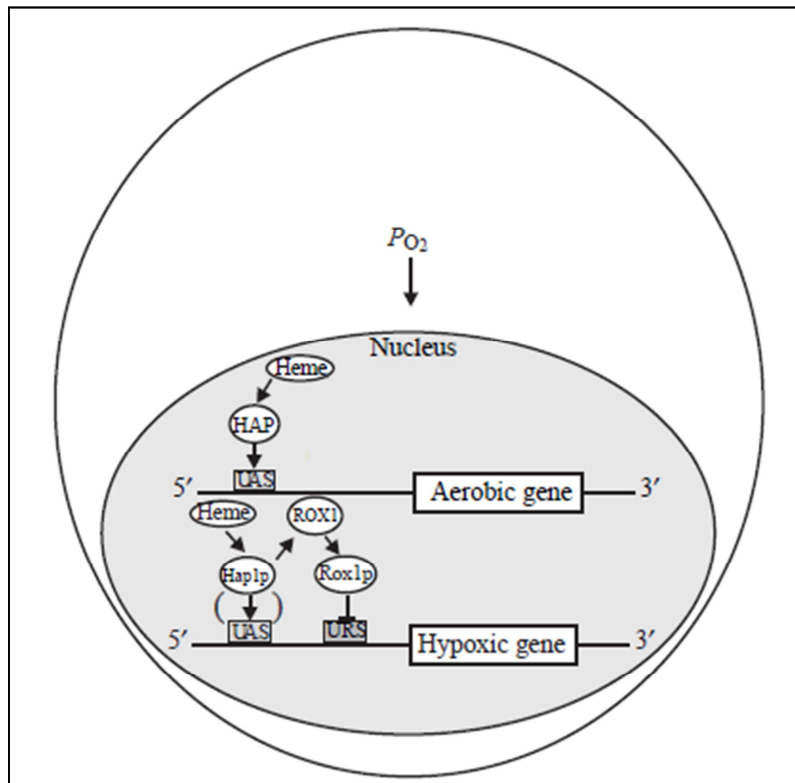


Figure I.5: Hap1p and Hap2/3/4/5p (represented by HAP) interacts with upstream activator sites (UAS) to activate the transcription of aerobic genes. Furthermore, Hap1p also activates transcription of some hypoxic genes. Rox1p represses the transcription of hypoxic genes interacting with upstream repressor sites (URS). (Adapted from (Kwast et al., 1998)).

The transcription factor Hap1p is synthesized independently of the oxygen concentration in the medium; however, in absence of heme, it is transcriptionally inactive. The activity of Hap1p and the expression level of Hap1p-regulated genes are proportional to the oxygen concentration. The oxygen threshold for Hap1p activity is between 0.5 and 1 μM of oxygen. Below this threshold, an abrupt decrease in Hap1p activity is observed and above it, Hap1p activity increases gradually until oxygen concentration reaches 200 μM (Hon, et al., 2003). The latter may explain the dose-

dependent effect of oxygen on the expression of Hap1p-regulated aerobic genes, as observed, for example, with *CYC1* and *TIF51a* (Burke et al., 1997; Kwast et al., 1998).

On the other hand, Hap1p could play a role as transcriptional repressor. Indeed, Hap1p is able to repress the transcription of its own gene (Hon et al., 2005). Furthermore, during hypoxic growth, Hap1p represses the transcription of genes involved in ergosterol synthesis such as *ERG2*, *ERG5* and *ERG11* (Hickman & Winston, 2007).

The other main transcriptional activator of oxygen responsive genes in yeast is the highly conserved heteromeric complex Hap2/3/4/5p. This heteromer activates genes transcription primarily in response to oxygen via heme and/or growth on non-fermentable substrates (e.g. lactate, glycerol). The heterotrimer Hap2/3/5p is involved in binding to DNA, whereas Hap4p is a regulatory subunit necessary for complex activation (Kwast et al., 1998). The Hap2/3/4/5p transcription factor binds to DNA in a heme-independent fashion and the role of heme in the activation of Hap2/3/4/5p complex is unknown. Genes that are upregulated under aerobiosis in a heme-dependent fashion through this complex are mainly involved in mitochondrial respiration (e.g. *COX4*, *COX5a*, *COX6* and *AAC2*) (Plakunov & Shelemekh, 2009).

The counterpart of the transcriptional activators mentioned above, is the transcriptional repressor Rox1p. Rox1p causes most of the transcriptional repression of hypoxic genes in aerobic conditions. Such genes include *COX5b* (anaerobic isoform of the Vb subunit of cytochrome c oxidase), *ANB1* (anaerobic isoform of the transcription initiation factor eIF-5a) and *AAC3* (anaerobic isoform of mitochondrial adenine translocase). The repressor effect of Rox1p is oxygen independent, but the transcription of its gene is activated by the heme-dependent factor Hap1p and requires the presence of heme (Zitomer, et al., 1997). Under aerobic conditions (i.e. in the presence of heme) *ROX1* gene is transcribed to repress its target genes. Whereas in anaerobic conditions, *ROX1* transcription is repressed and the Rox1p level gradually decreases, resulting in activation of hypoxic genes, as mentioned above.

Ergosterol biosynthesis, much like heme biosynthesis, requires the presence of oxygen. This sterol also plays a significant role in oxygen transcriptional regulation in yeast. For example, in *S. cerevisiae*, about one third of the hypoxic genes are presumed

to be regulated by ergosterol through negative feedback (i.e. expression inversely related with ergosterol concentration) (Kwast et al., 2002). In *S. cerevisiae*, the expression of *ERG* genes, encoding for ergosterol biosynthetic enzymes, is regulated by the sterol dependent transcription factors Upc2p and Ecm22p. Upc2p also activates the expression of hypoxic genes such as those encoding proteins transporting sterols into the yeast (e.g. *PDR11*, *AUS1*), as well as the *DAN/TIR* genes involved in mannoprotein synthesis. Activation of these genes, occurs as a response to both a decrease in sterol or heme concentrations (Davies & Rine, 2006).

Despite these previous considerations, it is not yet clear the way how these regulatory networks contribute to the observed effects of oxygen over industrial yeast physiology in wine making conditions. Furthermore, all the above mentioned studies were carried out with laboratory yeast strains, which are significantly different from industrial wine yeast strains (Novo et al., 2009; Rossouw et al., 2012).

1.5.2 Crabtree effect and cytosol-mitochondria redox shuttles

Among all the environmental factors that regulate respiration and fermentation in yeast cells, the availability of glucose and oxygen have been extensively studied. Under enological conditions, i.e. high sugar concentrations, *S. cerevisiae* metabolizes glucose mainly via fermentative metabolism, even when oxygen is available. This phenomenon is known as the Crabtree effect (De Deken, 1966; Walker, 1998). It is only at low sugar concentration and low specific growth rates, that *S. cerevisiae* can exhibit complete respiratory metabolism in the presence of oxygen (Larsson et al., 1993).

Several hypotheses have been suggested to explain the Crabtree effect, such as catabolic repression of respiratory enzymes (Gancedo, 1998), bottleneck of the carbon flux towards the TCA cycle (Pronk et al., 1996) and a limitation of the yeast respiratory enzymes to reoxidize the NADH produced by glycolysis (Vemuri et al., 2007). These hypotheses will be explained below.

Glucose catabolic repression occurs mainly at the transcriptional level of those genes that encode for the enzymes required for the utilization of alternative carbon sources in the presence of glucose or fructose. Furthermore, several genes involved in

respiratory chain, such as *CYC1*, *COX5b* and *COX6* among others, are repressed by glucose (Gancedo, 1998).

Another approach suggested that the inhibition of the activity of the respiratory enzymes, instead of their transcriptional repression, is responsible for the Crabtree effect. Overexpression of a mitochondrial heterologous NADH dehydrogenase in *S. cerevisiae* caused a decrease in ethanol production (i.e. fermentative metabolism) in aerobic and elevated glucose conditions. The latter suggests that there would be an increased carbon flow to respiratory pathways despite the high sugar concentration of the culture medium (Vemuri, et al., 2007), which strongly suggests that respiratory enzymes do not have the capacity to metabolize all the carbon and balance the electrons that arise from upstream glycolytic flow.

How mitochondrial respiratory enzymes oxidize the reduced coenzymes (NADH) produced in glycolysis? The yeast *S. cerevisiae* lacks transhydrogenase activity ($\text{NADH} + \text{NADP}^+ \leftrightarrow \text{NAD}^+ + \text{NADPH}$) and the mitochondrial inner membrane is virtually impermeable to pyridine nucleotide coenzymes (van Dijken et al., 1986; von Jagow et al., 1970). As a consequence, redox balances must be established in each compartment, that is to say the NADH must be reoxidized in the compartment where they are generated (cytosol or mitochondrial matrix) (Rigoulet, et al., 2004). However, redox-shuttle mechanisms could lead to a redox couple between mitochondrial and cytoplasmatic redox equivalents, employing metabolites that are transported, or diffuse freely, across biological membranes.

Three main redox-shuttle mechanisms have been proposed to work in *S. cerevisiae* mitochondria: 1) the glycerol-3-phosphate shuttle (Gut2p), 2) the external NADH dehydrogenase (Nde1p) shuttle and 3) the mitochondrial alcohol dehydrogenase (Adh3p) shuttle (Figure I.6) (Bakker et al., 2001; Murray et al., 2011). The Adh3p reaction consumes the ethanol that diffuses from the cytoplasm and produces acetaldehyde and NADH in the mitochondrial matrix. Acetaldehyde can diffuse back to the cytoplasm, while NADH is reoxidized by oxygen in the electron transport chain. The ethanol-acetaldehyde conversion is potentially reversible ($\Delta G = 33.5 \text{ J/mol}$ at pH 5, 25°C and 0.25 M of ionic strength) (Alberty, 2006). On the other hand, the Nde1p

reaction directly couples cytosolic NADH oxidation to the respiratory chain. This is similar to the functioning of Gut2p, which shuttles electrons from glycerol 3-phosphate oxidation to the mitochondrial quinone pool. Bakker et al. (2000) and Rigoulet et al. (2004) supported the idea of the preeminence of the Adh3p and Nde1p shuttles, respectively. While there is only one study on the function of these shuttles under nitrogen-limited conditions (Pahlman et al., 2001), most authors have accepted Adh3p as the main redox shuttle in anaerobic conditions (Bakker, et al., 2000; Murray, et al., 2011).

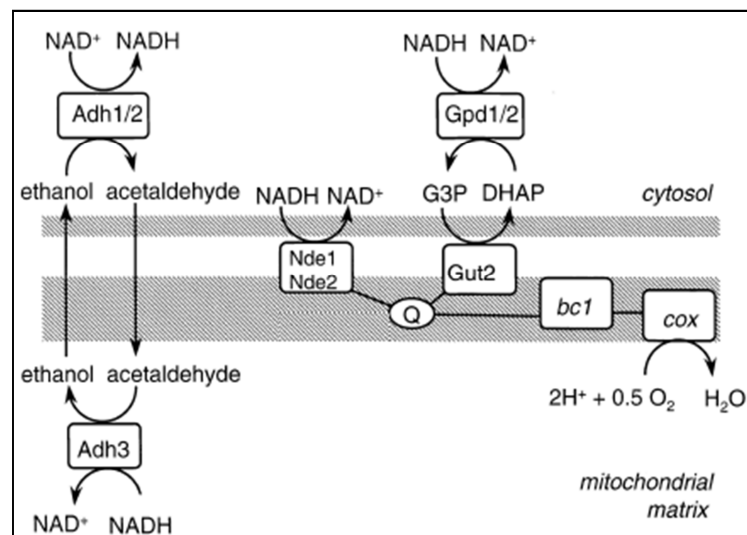


Figure I.6: Three main redox shuttles that have been proposed to work in *S. cerevisiae* 1) the glycerol-3-phosphate shuttle (Gut2p), 2) the external NADH dehydrogenase (Nde1p) shuttle and 3) the mitochondrial alcohol dehydrogenase (Adh3p) shuttle. (Adapted from (Bakker, et al., 2001)).

I.5.3 Effect of oxygen availability on tricarboxylic acid (TCA) cycle

The tricarboxylic acid (TCA) pathway plays a central role in oxidative growth of *S. cerevisiae*. It also plays an important role in biosynthetic processes, especially those generating amino acids. In aerobic conditions, this pathway functions effectively as a

cycle and produces reducing equivalents (NADH and FADH₂) used by the respiratory chain to produce energy in the form of ATP.

In contrast, in anaerobic, carbon-limited conditions, the cycle is interrupted at the level of succinate dehydrogenase (Camarasa et al., 2003). Thus, under fermentation conditions, there is an “oxidative branch” and a “reductive branch” of the cycle (Figure I.7).

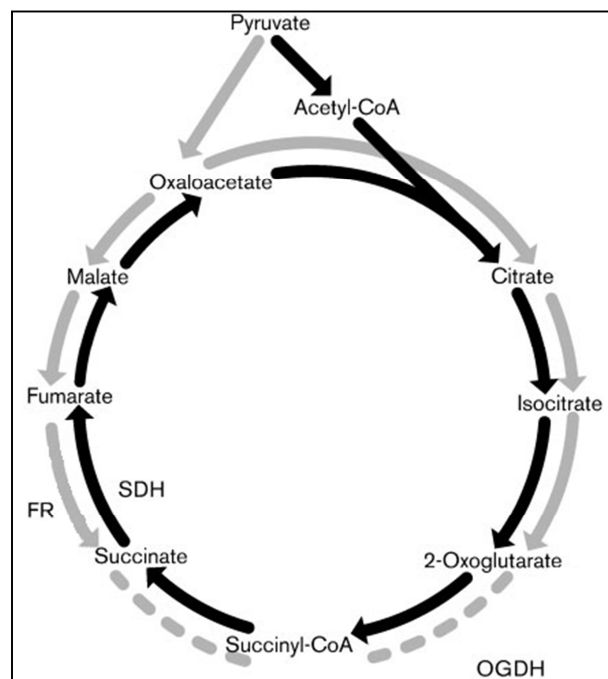


Figure I.7: TCA pathways during respiration and fermentation. Black arrows, the TCA pathway functions as a cycle during respiration. Grey arrows, the TCA pathway operates as an oxidative branch and a reductive branch during fermentative metabolism. FR, fumarate reductase; SDH, Succinate dehydrogenase complex; OGDH, Oxoglutarate dehydrogenase complex. (Taken from (Camarasa, et al., 2003)).

This prediction was first calculated as thermodynamically feasible and has been proposed to operate in *S. cerevisiae* (Lupiañez et al., 1974). Later, the prediction was achieved using Metabolic Flux Analysis (MFA). By measuring the consumption and

production rates of extracellular metabolites and applying those to a stoichiometry-based metabolic model, the need of a reductive branch under anaerobic growth was proposed (Gombert et al., 2001; Nissen et al., 1997). These predictions were confirmed few years later by Camarasa et al. (2003) using NMR isotopic filtration of ^{13}C - glucose to study the redistribution of the ^{13}C -label in anaerobic conditions. The reductive branch of the cycle has an unusual feature; every reaction goes in the opposite direction compared to the normal behavior in respiratory conditions. This is an important issue in the case of succinate dehydrogenase, because this enzyme is strongly repressed by sugar, and is part of both the electron transport chain and the TCA cycle. The reductive branch then bypasses this enzyme and utilizes fumarate reductase, a completely different enzyme that employs FADH_2 as a cofactor to transform fumarate to succinate. This is important since it is this pathway that allows for the regeneration of soluble FAD in the cell (Vargas et al., 2010). However, this FAD cannot fully replace the FAD regenerated by respiration, because some reactions, such as the reaction of proline assimilation by Put1p, depend on FADH_2 oxidation by oxygen, via the mitochondrial respiratory chain (Wanduragala et al., 2010). However, so far there is no assessment of the operation of the TCA cycle in wine making conditions according to oxygen availability.

I.6 Continuous cultures as a tool for conducting physiological studies.

“Omic” studies require cultivation of cells under controlled, well-defined and reproducible conditions. Therefore, batch cultures are not appropriate, because it is known that culture conditions, e.g. nutrient concentrations, change continuously and simultaneously with time. On the other hand, steady-state continuous cultures, offer the unique possibility to minimize the variations of environmental conditions, as well as those related to the specific growth rate (μ), by controlling the dilution rate (D [h^{-1}]), under narrowly defined nutritional conditions (Hoskisson & Hobbs, 2005).

Continuous cultivation is an open system in which liquid medium from the feed reservoir is supplied to the culture at a constant rate (Figure I.8). At the same time,

medium with cells is removed to the same rate to maintain a constant culture volume in the bioreactor (Acevedo et al., 2004). When the output variables are constant in time, the culture reaches steady state conditions.

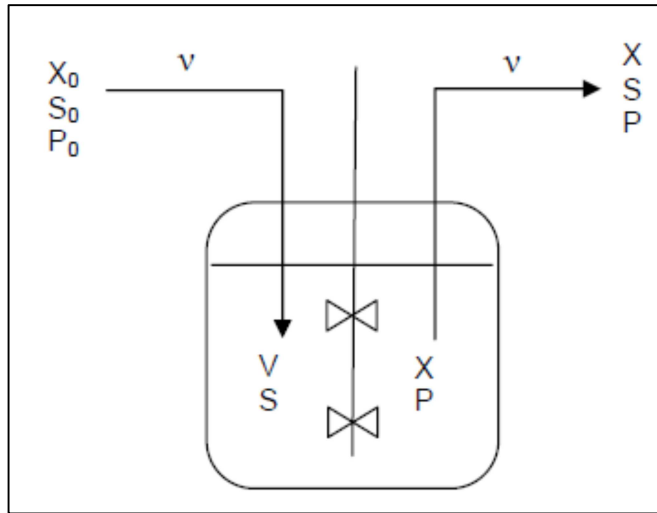


Figure I.8: Representation of a continuous culture in a stirred tank bioreactor. The liquid medium from the feed reservoir, containing known concentrations of substrates (S_0), biomass (X_0 , commonly $=0$), and products (P_0), is pumped into the bioreactor at a flow rate v . Gaseous feed can also be used (not shown). The concentrations of biomass (X), substrates (S) and products (P) inside the bioreactor are equal to those in the effluent. The effluent is pumped out at the same rate as the feed rate, v . The volume of medium in the bioreactor, V , is constant. The dilution rate D is defined as v/V (Adapted from (Acevedo, et al., 2004)).

All continuous systems are set up initially as a batch culture (Hoskisson & Hobbs, 2005). The feeding from a feed reservoir is turned on preferentially during the exponential phase of microbial growth and lasts until the culture reaches steady state conditions predicted for the continuous culture.

The criterion used to control the feed rate determines the continuous culture type (Villadsen et al., 2011). In chemostats, the usually carbon-limited culture medium is

delivered at a constant rate, which determines the cell growth rate and parameters at the steady state. In turbidostats, fresh medium is delivered when the cell density increases above a predetermined value, with all nutrients in excess. In pH-auxostats, feed is controlled to keep a constant pH.

An essential parameter in continuous culture is the dilution rate (h^{-1}), which is defined as:

$$D = \frac{v}{V}$$

where v is the feed rate, in $L \cdot h^{-1}$, and V is the medium volume in the bioreactor, in L . Because v and V are kept constant in continuous cultures, D is also constant.

The inverse of the dilution rate is the residence time (h):

$$t = \frac{1}{D}$$

Generally, steady state is reached after three to five residence times have elapsed since feeding was started.

Using mass balances, it can be easily demonstrated that at the steady state the specific growth rate, μ , is equal to the dilution rate, D (Acevedo, et al., 2004; Hoskisson & Hobbs, 2005; Villadsen, et al., 2011). This is a major advantage of this culture system as it allows control of the cell growth rate and enables to work at constant growth rate values. Therefore, in steady state, the growth rate can be manipulated as a function of the dilution rate, provided that the growth rate is below the critical dilution rate (D_c), the rate at which the steady-state biomass concentration is zero. That is, D_c is higher than the maximum specific growth rate (μ_{max}) of the organism under the given conditions, and the culture washes out of the vessel (Hoskisson & Hobbs, 2005; Villadsen, et al., 2011)

Volumetric and specific rates can be determined easily from continuous culture experimental data (Villadsen, et al., 2011). The volumetric production rate, q_i , is defined as the mass of compound i produced per volume of reactor and per unit of time. The specific production rate, r_i , refers to the mass of compound i produced per unit weight of cell per unit of time. The specific production rate can be calculated from the volumetric production rate:

$$r_i = \frac{q_i}{x}$$

where x is the biomass in unit weight of cell per volume of reactor. The production rates of products are positive, while consumption rates of substrates are negative.

Additionally, the specific growth rate is equal to μ and corresponds to:

$$r_x = \frac{q_x}{x}$$

Yield coefficients are useful parameters for comparison, design and optimization of culture processes (Villadsen, et al., 2011). They are calculated by scaling two production rates, according to the definition:

$$Y_{ij} \equiv \frac{|r_j|}{|r_i|} = \frac{|q_j|}{|q_i|}$$

where the first index i indicates the reference rate. Yield coefficients are always positive. They can be expressed in $\text{g} \cdot \text{g}^{-1}$, $\text{mole} \cdot \text{mole}^{-1}$, or $\text{C-mole} \cdot \text{C-mole}^{-1}$.

In chemostat based studies, it has been demonstrated that growth rate can drastically affect the *S. cerevisiae* transcriptome, proteome and metabolome (Castrillo, et al., 2007; Regenber, et al., 2006). Furthermore, when comparing the transcriptome of a wild-type and a slow-growing *S. cerevisiae* mutant grown in batch cultures, several genes appeared to change their expression. However, when these cells were grown in continuous culture, at the same specific growth rate, only a few genes were expressed differentially (Hayes et al., 2002).

Chemostat cultures are more appropriate than batch cultures for tightly controlled, physiological studies of -omics because they allow discrimination between the direct effects of the tested conditions (in this case, the variations in dissolved oxygen concentration) and the indirect ones, that are dependent on growth rate variations (Boer et al., 2007; Castrillo et al., 2007; Hayes et al., 2002; Knijnenburg et al., 2009). Furthermore, since specific growth rate and other culture parameters are kept constant in a chemostat continuous culture, this system constitutes a useful tool for the calculation

of cellular physiological parameters, conversion rates, and for genome-wide transcription studies.

On the other hand, prolonged chemostat cultivation (100 generations or more) can lead to evolutionary adaptation of cells to the culture conditions (Mashego, et al., 2005), to avoid this drawback we carried out the experiments approximately until 7 generations (equivalent to five residence times), sufficient to reach steady-state conditions and avoid the adaptation of yeast cells. Furthermore, given the nature of steady-state chemostat cultures it is clear that it is not possible to mimic the dynamic conditions characteristics of a batch winemaking process (such as variable glucose and ethanol concentration), nevertheless our culture conditions corresponds to the late exponential cell growth phase of a batch winemaking process, in which the effect of the discrete oxygen additions on the fermentation kinetics are more important (Sablayrolles, et al., 1996).

Therefore, chemostat continuous cultures were selected in this thesis as the most appropriate conditions to understand the molecular and metabolic effects of oxygen on the wine yeast physiology under enological conditions; despite the dynamic nature of winemaking process at industrial scale.

I.7 Dynamic response of *Saccharomyces cerevisiae* physiology to environmental perturbations

The ability of *Saccharomyces cerevisiae* to adapt to changes in its nutritional environment and other environmental changes has been subjected to considerable attention due to its crucial importance for survival. For instance, there are a substantial number of genes whose modification in their expression patterns are shared by most of the environmental changes as a part of a common environmental response. Additionally, unique gene expression patterns have been found for different environmental perturbations such as temperature, oxidative stress and different nutrient limitation (Causton, et al., 2001; Gasch, et al., 2000). These studies contributed considerably

towards the understanding of the molecular mechanisms utilized by yeast to adapt and survive under different environmental conditions.

Changes in glucose concentration (Dikicioglu et al., 2011; Kresnowati et al., 2006; van den Brink et al., 2008) and oxygen availability (Lai et al., 2005; Lai et al., 2006; van den Brink et al., 2008) are among the most studied environmental perturbations - and resulting physiological effects - on yeast cells. From these studies, part of the regulatory network that modulates gene expression in each case has been deciphered.

Furthermore, the dynamic analysis of the transcriptome allowed to divide the transcriptional response into two main phases, both shared by glucose and oxygen perturbations: a primary, acute and transient transcriptional response that allows yeast cells to adapt to the new conditions; and a secondary, delayed transcriptional response, explained by the long term effects of the environmental perturbation on yeast metabolism. Unfortunately, all of these studies have been carried out using laboratory yeast strains under conditions that are far from those found in winemaking (i.e. nitrogen limited, carbon sufficient cultures, with variable dissolved oxygen availability).

On the other hand, during the industrial winemaking process, air is discretely added to avoid detrimental effects of elevated oxygen concentrations on the final product and to maximize the beneficial effects of oxygen. Therefore, in order to mimic more faithfully the effects of oxygen on wine yeast physiology in an enological context, it is necessary to evaluate the response of wine yeast metabolism under a transient increase of oxygen concentration under wine fermentation conditions. The latter is the second specific objective of this thesis.

I.8 Metabolic flux analysis (MFA) as a tool for research

To understand and describe cell metabolism from a global, systemic perspective, it is necessary to know both the metabolic fluxes and the intracellular concentrations of metabolites involved. Nevertheless, it is quite difficult to determine a large number of intracellular metabolite concentrations, due to the multiple steps involved in their

determination and the protocols specificity required for the different intracellular metabolites (Villas-Bôas et al, 2005).

Metabolic fluxes are the rates at which a metabolite is processed by the cell. These rates constitute a fundamental determinant of cell physiology, primarily because they provide a measure of the degree of participation of various pathways in overall cellular functions and metabolic processes (Stephanopoulos et al., 1998).

A powerful method for the determination of fluxes across metabolic pathways is Metabolic Flux Analysis (MFA), in which intracellular fluxes are calculated by using a stoichiometric model that includes the most important intracellular reactions and by applying mass balances over each intracellular metabolite. Therefore, enzymatic kinetics and regulatory information, which are difficult to obtain, are not required for analyzing the behavior of metabolic networks (Varma & Palsson, 1994)

A set of measured extracellular fluxes, typically consisting of specific substrate uptake rates and specific product secretion rates is used as input for calculations. The final outcome of flux calculations is a metabolic flux map showing a diagram of the biochemical reactions included in the calculations along with an estimate of the steady state rate (i.e. the flux) at which each reaction in the diagram occurs (Stephanopoulos et al., 1998; Villadsen et al, 2011).

In a metabolic network, metabolite concentrations, reaction fluxes and stoichiometric coefficients are related by the following dynamic mass balance:

$$\frac{dX_{met}}{dt} = M * v$$

In this equation, X_{met} is a $m \times 1$ concentration vector for the intracellular metabolites; M is the $m \times r$ stoichiometric matrix, in which the element of the i th row and j th column is the stoichiometric coefficient of metabolite i in reaction j ; and v is a $r \times 1$ reaction rate vector. As a result of the very high turnover of the pool of most intracellular metabolites, the concentration of the different metabolite pools rapidly adjust to new levels, even after the cells have experienced large environmental perturbations (Stephanopoulos, et al., 1998). Therefore, a pseudo-steady state of the

system is assumed, implying that there is no metabolite accumulation, i.e. $\frac{dx_{met}}{dt} = 0$, then

$$0 = M * v$$

This equation forms the basis of the metabolic flux analysis (i.e. the determination of the unknown pathway fluxes in the intracellular rate vector v). Each column in M corresponds to a reaction and each row in M corresponds to a metabolite in the network. Each row in v corresponds to the flux through the previously mentioned reaction. This vector equation represents K linear algebraic balances for the K metabolites with J unknown pathway fluxes. Because the number of reactions (J) is always greater than the number of metabolites (K) in the metabolic network, there is a certain number of degrees of freedom in the set of algebraic equations given by $F = J - K$. Therefore, some reaction rates (or elements of v) have to be able to determine the remaining rates.

When solving for a metabolic model, three different situations can occur:

- If exactly F fluxes (or reaction rates) in v are measured, the system becomes *determined* and there is a single solution that is simple to obtain.
- If less than F fluxes are measured, the system is *underdetermined* and the unknown fluxes can be determined only if additional constraints are introduced or if an overall optimization criterion is imposed (e.g. cellular growth or production of particular metabolite), subject to the constraints of metabolic balancing.
- Finally, if more than F fluxes are measured, the system of flux balance equations is *overdetermined*, and the redundant fluxes (or equations) can be used to calculate better estimates of measured and non-measured fluxes. (Wang & Stephanopoulos, 1983).

Metabolic flux analysis has been used successfully to evaluate changes in *S. cerevisiae* metabolism under different conditions (Jouhten et al., 2008; Nissen et al., 1997; Pizarro et al., 2007; Varela et al., 2004). Nissen et al. (1997) predicted several important features of the yeast metabolism in anaerobic conditions, most remarkably the

first indication that the TCA cycle operated in two branches, later experimentally confirmed by Camarasa et al. (2003).

To the best of our knowledge, fluxes redistributions of wine yeast metabolism grown in enological conditions due to changes in dissolved oxygen availability have not been evaluated yet. Therefore, Metabolic Flux Analysis was employed to evaluate changes in *S. cerevisiae* physiology, under different steady state dissolved oxygen levels, in wine fermentation conditions.

I.9 Yeast oxygen consumption under winemaking conditions

Oxygen consumption by *Saccharomyces cerevisiae* under enological conditions has been extensively studied due to its relevance at industrial level. The addition of oxygen during winemaking is essential to reach wine dryness (i.e. residual sugar below 2 g·L⁻¹) (Sablayrolles, et al., 1996), and to avoid sluggish and stuck fermentations (Blateyron & Sablayrolles, 2001). Research on oxygen consumption by yeast cells under enological conditions has focused on the impact of oxygen on fermentation kinetics, yeast viability and biomass production (Fornairon-Bonnefond et al., 2002; Julien et al., 2000; Rosenfeld et al., 2003).

The contribution of different pathways to the overall oxygen consumption in wine fermentation conditions has also been evaluated through the use of respiratory deficient mutants, electron transport chain inhibitors and blockers of lipid synthesis (Rosenfeld et al., 2002; Salmon et al., 1998). These studies showed that several metabolic pathways are involved in oxygen consumption under enological conditions. Furthermore, they have allowed to quantitate oxygen consumption by these different pathways; for example, sterol biosynthesis during enological fermentation required between 0.3 and 1.5 mg of dissolved oxygen per gram of biomass, whereas only a negligible amount was required for unsaturated fatty acids (UFA) biosynthesis (Rosenfeld et al., 2003; Salmon et al., 1998).

Rosenfeld et al. (2002, 2003) calculated that the sterol biosynthetic pathway was responsible for 30% to 75% of the total oxygen consumed by yeast cells under

enological conditions. Unfortunately, these results were obtained using specific inhibitors of lipids and sterol biosynthesis in concentrations that might be toxic for yeast cells. Furthermore, in vitro studies suggest that uncoupling cytochrome P450 oxidases involved in sterol biosynthesis can consume oxygen, generating reactive oxygen species (ROS). The latter, explain part of yeast oxygen consumption under enological conditions (Rosenfeld et al., 2002; Salmon, 2006).

According to these authors, oxidative phosphorylation, i.e. aerobic respiratory metabolism, does not occur under alcoholic fermentation conditions (Salmon, 2006). This hypothesis was supported by the low level of respiratory enzymes and mitochondrial cytochromes determined during the wine fermentation process (Salmon et al., 1998). Furthermore, promitochondria only slightly contribute to the overall oxygen consumption capacity by yeast cells growing under high glucose concentrations (Rosenfeld et al., 2004). Salmon (2006) proposed an overall distribution of oxygen consumption among the previously mentioned metabolic pathways under wine fermentation conditions. However, 46% of the total oxygen consumption by yeast cells could not be explained by the considered metabolic pathways.

Oxygen is also essential for proline consumption under enological conditions (Ingledeew & Magnus, 1987). Additionally, a functional respiratory chain is necessary for the utilization of proline as nitrogen source by *S. cerevisiae* (Wang & Brandriss, 1987). Indeed, the enzyme proline oxidase directly transfers electrons to ubiquinone in the mitochondrial membrane, allowing the metabolism of proline in yeast (Wanduragala, et al., 2010).

As a whole, the above mentioned evidences do not support the hypothesis that the mitochondrial respiratory chain is not functional under enological conditions and, together with proline consumption, could explain why Salmon and coworkers could not achieve a total oxygen balance.

In this work, we have re-evaluated the fate of oxygen during enological fermentations taking advantage of an integrated, more comprehensive approach to better understand the impact of oxygen metabolism on wine yeast physiology. For this purpose, we carried out fluxomic, transcriptomic and metabolic analyses, under dynamic

and steady-state continuous culture conditions at increasing dissolved oxygen concentration.

I.10 Working hypotheses

The way in which oxygen impacts *S. cerevisiae* physiology at metabolic and transcriptional levels has been thoroughly discussed above. However, some questions about potential metabolic pathways involved in oxygen consumption by industrial wine yeasts under enological - i.e. nitrogen limited and carbon sufficient – culture conditions remain to be elucidated, considering that:

- Quantitative and qualitative re-evaluation of the different pathways involved in oxygen consumption, using an industrial strain of *S. cerevisiae*, under the same culture conditions is required.
- Some of the evidence previously presented here has been obtained through the use of respiratory chain or lipid synthesis inhibitors. These compounds were utilized at high concentrations (Rosenfeld, et al., 2002). The latter could have been toxic for yeast cells and led to incorrect conclusions.
- Evidence on proline consumption by *Saccharomyces cerevisiae* when a small amount of oxygen is supplied under these culture conditions casts doubt about nonfunctional mitochondrial respiratory chain under enological conditions.

Thus, we suggest that pathways involved in oxygen metabolism under enological culture conditions are still not well understood and need to be revisited employing state-of-the-art system biology tools.

Moreover, the hypothesis of this thesis is that the respiratory chain is triggered at a low oxygen threshold, and increases its activity when oxygen concentration increases. This also results in the canonical operation of the TCA cycle.

A systemic analysis of oxygen fate on wine yeast physiology under enological conditions, will allow a better understanding of wine yeast metabolism and its potential impact in wine quality.

I.11 Objectives

The general objective of this work was to evaluate the impact of oxygen on wine yeast physiology through the analysis of the main pathways involved in oxygen consumption by wine yeast, under enological conditions.

The following specific objectives were developed:

- i. To quantify the long-term impact of different levels of dissolved oxygen on wine yeast physiology, at metabolic, transcriptomic and fluxomic levels, under enological culture conditions.
- ii. To evaluate the transient effect of oxygen on wine yeast physiology, in anaerobic conditions using an impulse of oxygen, at transcriptomic and metabolic levels, under enological conditions.

I.12 Approach

In the first part of this study, the long-term effects of oxygen on wine yeast physiology were evaluated using nitrogen-limited continuous cultures with five different steady-state dissolved oxygen concentrations. These studies were carried out under tightly controlled conditions that reproduce winemaking process at laboratory scale (objective i.). Metabolic Flux Analysis (MFA) was used to determine intracellular flux redistribution in wine yeast, using the five dissolved oxygen levels evaluated in this study. Furthermore, Affymetrix microarray technologies were employed to evaluate the differential gene expression of wine yeast cells at the different dissolved oxygen levels.

These results are presented in the section III.1. The results, derived from the completion of Objective i., are contained in the article “Oxygen response of the wine yeast *Saccharomyces cerevisiae* EC1118 strain grown under carbon-sufficient, nitrogen-limited oenological conditions.”, published in Applied and Environmental Microbiology, in December 2012.

In the second part of this study, the transient (i.e. short-term) effects of oxygen on the physiology of wine yeast cells were evaluated during and after an oxygen impulse, under the same culture conditions of the first part of this study. In this case, Affymetrix microarray technologies were employed to evaluate the differential transcriptome expression of wine yeast cells before and after the oxygen impulse. These results are presented in the section III.2. The results, derived from the completion of Objective ii., are contained in the article “Metabolic and transcriptomic response of the wine yeast *Saccharomyces cerevisiae* strain EC1118 after an oxygen impulse under carbon sufficient, nitrogen-limited fermentative conditions.”, submitted to FEMS Yeast Research, in September 2013.

II. MATERIALS AND METHODS

II.1 Yeast strain and culture conditions

Saccharomyces cerevisiae EC1118 (Lalvin, Switzerland), an industrial strain used worldwide by the wine industry, was employed throughout this study. Dried yeasts were rehydrated as specified by the supplier and stored as frozen stocks with 15% glycerol, at -80°C. From these stocks, 50-100 µL of cell suspension were inoculated into 50 mL of YPD medium (1% yeast extract, 2% peptone and 2% glucose) at 28 °C in aerobic conditions until mid – logarithmic growth phase, prior to bioreactor cultures.

For bioreactor cultivation, 2 L BIOSTAT B bioreactor (Sartorius Biotech, Germany) with a working volume of 1.5 L was inoculated with enough volume of the previously mentioned microbial broth, to obtain an initial cell density of 10^6 cells· mL⁻¹ determined using a Neubauer chamber (Hausser Scientific, Blue bell, PA). The culture was allowed to grow in batch mode until reaching early-to-mid exponential growth. Constant feeding was then initiated at a dilution rate (D) of 0.1 h⁻¹. Temperature was set to 20°C to simulate white wine fermentation and pH was automatically kept at 3.5 using NaOH 5N.

II.2 Culture media

A defined medium simulating standard white grape juice was used in the bioreactor fermentations. Residual glucose concentration in the chemostat outlet was targeted to 40 g·L⁻¹ to sustain glucose repression at the same level in all experiments. In order to achieve this, glucose feed concentration were modified according dissolved oxygen concentration, glucose feed concentrations were 80 g·L⁻¹ for the cells grown anaerobically, with 1.2 µM and with 21 µM of dissolved oxygen. For cells grown at 2.7

μM and $5 \mu\text{M}$ of dissolved oxygen $85 \text{ g}\cdot\text{L}^{-1}$ and $95 \text{ g}\cdot\text{L}^{-1}$ were used, respectively. On the other hand, in oxygen impulse experiments, the glucose feed concentrations were $80 \text{ g}\cdot\text{L}^{-1}$. Fructose was not included in the formulation in all cases. The composition for other nutrients was based on the MS300 medium described by Salmon and Barre (Salmon & Barre, 1998). Since MS300 was designed for batch fermentations and its use in chemostats resulted in $100 \text{ mg}\cdot\text{L}^{-1}$ of residual nitrogen (data not shown), it was modified to run continuous cultures limited in nitrogen. The modified medium, called cMS300 was different from MS300 in phosphate, sulfate and biotin content. cMS300 contained : $3 \text{ g}\cdot\text{L}^{-1}$ of KH_2PO_4 , $5.75 \text{ g}\cdot\text{L}^{-1}$ of K_2SO_4 , $500 \text{ mg}\cdot\text{L}^{-1}$ of $\text{MgSO}_4\cdot 7\text{H}_2\text{O}$ and $0.05 \text{ mg}\cdot\text{L}^{-1}$ of biotin, following the mineral medium used by Pizarro et al. (Pizarro et al., 2008). Other vitamins and micronutrients were the same as MS300. Yeast Assimilable Nitrogen (YAN) corresponded to $380 \text{ mg}\cdot\text{L}^{-1}$ for all culture conditions. However, in anaerobic conditions, the YAN corresponded to $300 \text{ mg}\cdot\text{L}^{-1}$, since proline is not assimilable by yeast under anaerobic growth conditions (Ingledew et al., 1987). The nitrogen sources employed were (% w/w): 18.6% ammonium chloride (NH_4Cl), 20.5%; l-proline, 16.9%; l-glutamine, 1.25%; l-arginine, 6%; l-tryptophan, 4.9%; l-alanine, 4%; l-glutamic acid, 2.6%; l-serine, 2.6%; l-threonine, 1.6%; l-leucine, 1.5%; l-aspartic acid, 1.5%; l-valine, 1.3%; l-phenylalanine, 1.1%; l-isoleucine, 1.1%; l-histidine, 1.1%; l-methionine, 0.6%; l-tyrosine, 0.6%; l-glycine, 0.6%; l-lysine and l-cysteine, 0.4% (Salmon & Barre, 1998).

The biomass yields of both ergosterol and oleic acid of the *S. cerevisiae* EC1118 strain in chemostats was determined, as described by Mateles (Mateles & Battat, 1975). The resulting Y_{Xerg} and Y_{Xoleic} under anaerobic conditions were 0.9 and 3.45 mg of substrate $(\text{g biomass})^{-1}$, respectively. Ergosterol and oleic acid concentration in the final culture medium were set three-fold above their biomass yields to ensure excess but still being less than the original anaerobic factors formulation ($15 \text{ mg}\cdot\text{L}^{-1}$ ergosterol and $90 \text{ mg}\cdot\text{L}^{-1}$ oleic acid). Accordingly, culture media were supplemented with $10 \text{ mg}\cdot\text{L}^{-1}$ of ergosterol and $30 \text{ mg}\cdot\text{L}^{-1}$ of oleic acid, in the form of Tween 80, for all experiments carried out. Ergosterol and oleic acid excess was confirmed by detecting these anaerobic

factors in the supernatant of all cultures at steady state, i.e. continuous cultures were limited only in nitrogen.

II.3 Gas measurement and control

The gas flow was controlled by an Aalborg GFC Mass Flow meter (Aalborg, USA). Polyurethane tubing and butyl rubber septa were used to minimize oxygen diffusion into the anaerobic cultures. The gas entered through a 0.2 μm filter to maintain sterility. The dissolved oxygen concentration was measured online with an InPro 6950 probe (Mettler Toledo, USA). This probe has a detection limit of 0.03 μM and an accuracy of 1%. Gaseous carbon dioxide and gaseous oxygen were measured on-line with gas analyzers Gascard NG (Edinburgh Instruments, UK) and Parox 1000 (Messtechnik Engineering, Switzerland), respectively. Afterwards, a condenser connected to a cryostat set at 2°C cooled the off-gas. The entire system was monitored and controlled online by a SIEMENS PCS7 computer server.

II.3.1 Dissolved oxygen levels

To achieve different levels of dissolved oxygen, the cultures were sparged, with different oxygen/nitrogen gas mixtures at a flow rate of 0.25 $\text{L}\cdot\text{min}^{-1}$. For anaerobic experiments, ultrapure nitrogen (certified 99.999% N_2 , INDURA, Chile) was passed through an HPIOT3-2 oxygen trap (Agilent, USA) to reduce residual oxygen levels to less than 15 ppb. Other oxygen levels were achieved by sparging 1%, 5% and 21% oxygen/nitrogen mixtures (INDURA, Chile) directly into the culture, reaching 1.2 μM , 2.7 μM and 5 μM dissolved oxygen (20°C) at steady state, respectively (Table II.1). For the last oxygen condition, gaseous flow rate with the 21% mixture was increased from 0.25 to 1 $\text{L}\cdot\text{min}^{-1}$. At this point, stirring was increased from 200 to 400 rpm, reaching 21 μM dissolved oxygen (20°C) at a steady state. All dissolved oxygen conditions were performed by triplicate. In all cases, steady state was reached within 5 residence times (60 hours) and kept for at least 1.5 more residence times.

Table II.1: Conditions used to generate the steady state dissolved oxygen levels evaluated in this study.

Gas feed composition	Feed rate (liter min ⁻¹)	Agitation (RPM) ^b	Dissolved oxygen concentration (μM) ^a
Nitrogen	0.25	200	0 ± 0.00
1% oxygen	0.25	200	1.2± 0.06
5% oxygen	0.25	200	2.7± 0.28
21% oxygen	0.25	200	5.0± 0.02
21% oxygen	1.00	400	21.0± 1.1

^a The data are the averages ± standard deviations for three independent chemostat steady states.

^b RPM: Revolutions per minute.

II.3.2 Oxygen impulses generation and sampling time

Aerated pump over, a typical enological operation for oxygen addition, was simulated by adding an impulse of oxygen under the same culture conditions described above. In order to achieve this, triplicate anaerobic continuous cultures ($D=0.1 \text{ h}^{-1}$, 20°C), were sparged with ultrapure nitrogen (certified 99.999% N₂, INDURA, Chile) at 0.25 L·min⁻¹ gas flow rate. The stirrer speed was set to 300 rpm. Steady state anaerobic conditions were reached within six residence times (60 h). At this point, the nitrogen gas feed was substituted with pure oxygen (INDURA, Chile). After 30 seconds of sparging oxygen, the nitrogen gas feed was restored. Control experiments were carried out to discard that dissolved oxygen consumption could be attributed to stripping by the restoration of nitrogen gas feeding after oxygen addition (Supplementary Figure 1, annexes D). The dissolved oxygen concentration was monitored using a high accuracy optical sensor 3 LCD-trace Fibox v7 (PreSens®, Regensburg, Germany). This sensor was calibrated according to manufacturer instructions. A maximum of 125-156 μM (4-5 ppm) of dissolved oxygen were generally obtained with this protocol. Samples were taken after 0 min, 4 min, 10 min, 20 min, 30 min, 45 min, 1 hour, 5 hours and 10 hours

(equivalent to one residence time) following the oxygen impulse and used for further analyses.

II.4 Bioreactor sampling

Steady-state culture samples were taken after at least six residence times using an ice-cold, sterile 50 mL, plastic syringe plugged into the sampling device of the bioreactor. The samples were immediately transferred into a 50 mL sterile plastic tube, from which 10 mL of culture were either employed for dry weight determination or transferred to 2.0 EppendorfTM tubes. Afterwards, samples were centrifuged at 10.000 x g for 3 min. and 1 mL supernatant aliquots were transferred to clean tubes and stored at -80°C until further chemical analyses. Alternatively, for RNA isolation, 20 mL culture samples were collected as fast as possible into a FalconTM tube filled with 35 to 40 mL of crushed ice (Pizarro et al., 2008). From this tube, 1 mL of sample was transferred to a 1.5 ml EppendorfTM tube. After centrifuging at 10000 x g for 3 min, the supernatant was removed and the pellet was directly frozen in liquid nitrogen and stored at -80°C until RNA isolation.

II.5 Analytical techniques

II.5.1 High pressure liquid chromatography (HPLC)

Extracellular metabolites were determined as follows: 20 µL of the supernatant samples were injected automatically in a LaChrom L-7000 HPLC system (Hitachi, Japan). Organic acids, alcohols and sugars were separated using an Aminex HPX-87H anionic exchange column (Bio-Rad, USA), with H₂SO₄ 5mM as the mobile phase. Each run lasted 30 min per sample. Organic acids (citric, malic, succinic and acetic acid) were detected by a LaChrom L-7450A diode array detector (Hitachi, Japan) at 210 nm. Sugars (glucose, fructose and trehalose) and alcohols (glycerol and ethanol) were detected by LaChrom L-7490 refraction index detector (Hitachi, Japan). Each compound

was quantified automatically by the equipment operating software, using a calibration curve made with known concentration standards for each compound quantified.

II.5.2 Dry cell weight determination

Dry cell weight (DCW) was determined by filtering 10 mL of culture samples through 0.2 μm acetate ester filters (Whatman). The filters were dried to a constant weight before use. After filtering the sample, the filter was washed twice with 10 mL MiliQ water, and then removed and dried again to a constant weight at 65°C in an infrared dryer-equipped balance (Precisa, Switzerland).

II.5.3 Assimilable nitrogen and proline determination

Residual assimilable nitrogen in the cultures was determined using the σ -phthalaldehyde/N-acetyl-L-cysteine spectrophotometric assay (NOPA) procedure (Dukes & Butzke, 1998) using an UV/Visible spectrophotometer UV-150 (Shimadzu, Japan) at 335 nm. On the other hand, proline was determined by HPLC performed after derivatization of amino acids with 6-aminoquinolyl-N-hydroxysuccinimidyl carbamate to detect it by fluorescence (Liu et al., 1998). This measurement was subcontracted (IADET Ltda., Chile).

II.5.4 Ergosterol extraction and determination

From the bioreactor sampling device, 50 mL of sample was collected. The cells were centrifuged at 5000 rpm for 5 min. The supernatant was discarded, and the cells were frozen in liquid nitrogen. The pellet was kept at -80°C until used. Ergosterol was extracted with ethyl ether, using a method based in the method previously described by Nylund (Nylund & Wallander, 1992). Briefly, the cells were mixed with 8M KOH for saponification. A 10% of ethanol was added to improve cell disaggregation. The mixture was boiled in reflux for 3 hours and was then extracted 4 times with 100 mL ethyl ether. The organic phase was washed 2 times with 100 mL MiliQ water and the remaining humidity was removed by filtering in anhydrous sodium sulfate. The organic phase was

then evaporated in a rotary evaporator at 60°C, obtaining yellow oil that was dissolved in methanol up to 5 mL. 1 mL of this extract was then used for HPLC analysis (Salmanowicz et al., 1990). A C-18 column was used with pure methanol for the mobile phase. Ergosterol peak appeared at 4 min under these conditions, and was detected at 280 nm with a diode array detector. Ergosterol concentration was determined by interpolation of a standard curve ranging between 2 and 50 mg·L⁻¹

II.5.5 Biomass components determination

Biomass samples were treated as the samples for RNA described later. DNA extraction was performed using the Wizard SV Genomic DNA extraction kit (Promega, USA). Total lipids were determined gravimetrically, and saturated and unsaturated fatty acids measured by gas chromatography by an external service (ANALAB Ltda., Chile). Total carbohydrates were determined using the phenol method (Varela et al, 2004). Proteins were determined using the BCA assay (Santa Cruz Biotech, USA). The RNA amount was determined from the extractions described later. All the determinations were normalized to the biomass dry weight of the corresponding samples.

II.6 RNA extraction and quantification

Before RNA isolation, all water-based reagents were DEPC-treated. RNA was extracted from frozen cell pellets obtained as previously described using the AxyPrep Multisource RNA kit (Axygen Biosciences, USA), modified for use with glass beads for cell lysis. Briefly, the cell pellet was re-suspended in the R-I kit buffer and put into a screw-cap tube containing 250 µL of acid-washed glass beads (500 µm diameter) (Sigma, USA). These tubes were stirred in three cycles of 45 seconds in a Mini Bead BeaterTM (Biospec, USA), left for an equivalent time in ice between cycles. The lysate was centrifuged at 10.000 x g, and the supernatant was transferred to a tube with 250 µL of isopropanol. After this point, kit manufacturer instructions were followed. RNA was checked for integrity in a 1.3% agarose gel, prepared in a buffer with 20mM MOPS, 5mM sodium acetate and 1mM EDTA. After heating, 2 % v/v formaldehyde was added.

This was also used as the electrophoresis running buffer. RNA was quantified in a NanoDrop (Thermo Scientific, USA) and samples with absorbance ratios of 260nm/280nm and 260nm/230nm > 1.8 were used for further processing.

II.7 Transcriptome analysis

II.7.1 Microarray analysis of dissolved oxygen levels

The Yeast Genome 2.0 chips from Affymetrix were used for microarray experiments. Triplicate arrays for each one of the five dissolved oxygen conditions were performed. 5 µg of total RNA for chips hybridization was prepared according to manufacturer instructions using GeneChip® 3' IVT Express Kit (Affymetrix). Microarray hybridization, staining and scanning were performed according to manufacturer instructions (Affymetrix, 2009). Gene expression data was imported from the CEL files into R and the quality was assessed using the tools in the simpleaffy package from Bioconductor (Gentleman, et al., 2004). After the quality check step, data was normalized in R using robust multiarray analysis (RMA) from the affy package from Bioconductor (Gentleman, et al., 2004). Differential expression analyses between the different conditions were carried out using the Rank Products algorithm (Breitling et al., 2004) with a false discovery rate cut-off of 0.1. Hierarchical clustering on the data was also performed as detailed below. Calculations were performed using the R statistical software (R Development Core, 2006). The resulting lists of genes from differential expression analyses were then submitted to the AmiGO term enrichment analysis (Carbon, et al., 2009) to find out which Gene Ontology (GO) annotations, and functions, were overrepresented among the genes regulated by oxygen levels. Full gene annotation was then extracted from Saccharomyces Genome Database (Christie, et al., 2004). The raw microarray data was submitted to Gene Expression Omnibus (GEO, <http://www.ncbi.nlm.nih.gov/geo/>), where it is available under the code GSE34964.

II.7.2 Data clustering analysis of dissolved oxygen levels

A hierarchical clustering of gene expression levels was performed using Euclidean distance to measure differences between expression vectors and group average clustering algorithm. This clustering method was selected because exhibited the highest cophenetic correlation coefficient (CCC=0.61) compared to single linkage (CCC=0.41), Complete Linkage (CCC=0.58) and Ward's method (CCC=0.55). The CCC values were calculated as previously described (Sokal & Rohlf, 1962) . A distance cut-off value of 2.25 was selected to make the partition of the clustered data into 56 groups with different gene expression patterns upon the tested conditions. The specific clustering algorithm and distance cut off value were defined after a partition-based cluster structure consistency analysis using the Silhouette measure (Pearson et al, 2004). Briefly, all possible values of cut off distance to split the clustered data into k different groups were tested and the Silhouette associated values for each partition were calculated. According to this analysis, the maximum average value of 0.30 for Silhouette measure was obtained when using the group average clustering algorithm and a distance cut off value of 2.25, thus producing 56 independent gene groups. The resulting partition was then visually inspected for consistency in the dendrogram with the associated heat maps of the clustered genes in each group. The dendrogram with the heat maps for each gene was built using the iTOL webserver (Letunic & Bork, 2007). A color-coded strip illustrating the independent gene clusters was added to the dendrogram to facilitate the mapping and analysis of individual genes. A Gene Ontology enrichment analysis was then carried out independently for each of the 56 groups obtained with the partition-based clustering methodology described above. Blast2GO software (Conesa, et al., 2005) was used to perform the Gene Ontology enrichment analysis. This software has integrated the Gossip package for statistical assessment, which uses the Fisher's exact test and corrects for multiple testing to find enriched GO terms between two sets of sequences (Blüthgen, et al., 2005). The complete set of annotated genes for *Saccharomyces cerevisiae* was used as reference control group with a false positive discovery rate value of 0.05.

II.7.3 Microarray analysis through dissolved oxygen impulse

The Yeast Genome 2.0 chips from Affymetrix were used for microarray experiments, as described previously. RNA samples of two independent experiments taken at 0 min, 4min, 10 min, 1 hour, 5 hours and 10 hours following the oxygen impulse were used for transcriptome analysis. 5 µg of total RNA was prepared for chips hybridization was prepared according to manufacturer instructions using GeneChip® 3' IVT Express Kit (Affymetrix). Microarray hybridization, staining and scanning were carried out according to manufacturer instructions (Affymetrix, 2009). Gene expression data was imported from the CEL files into R and the quality was assessed using the tools in the simpleaffy package from Bioconductor (Gentleman, et al., 2004). After the quality check step, data was normalized in R using robust multiarray analysis (RMA) from the affy package from Bioconductor (Gentleman, et al., 2004). Differential expression analyses between the points over time were carried out using the Rank Products algorithm (Breitling et al., 2004) with a false discovery rate cut-off of 0.1. We analyzed differential expression comparing all time points to the zero time point, and we also compared each point to the one that immediately followed. Hierarchical clustering using Pearson correlation on the data was also performed as detailed below. Calculations were performed using the R statistical software (R Development Core, 2006). Full gene annotation was then extracted from Saccharomyces Genome Database (Christie, et al., 2004).

II.7.4 Data clustering analysis for dissolved oxygen impulse

A hierarchical clustering of gene expression levels was performed using Pearson correlation to measure differences between expression vectors and group average clustering algorithm. This clustering method was selected because exhibited the highest cophenetic correlation coefficient (CCC=0.651) compared to single linkage (CCC=0.455), Complete Linkage (CCC=0.571) and Ward's method (CCC=0.524). The CCC values were calculated as previously described (Sokal & Rohlf, 1962) . A distance cut-off value of 0.656 was selected to make the partition of the clustered data into 6 groups with different gene expression patterns upon the tested conditions. The specific

clustering algorithm and distance cut off value were defined after a partition-based cluster structure consistency analysis using the Silhouette measure (Pearson et al, 2004). Briefly, all possible values of cut off distance to split the clustered data into k different groups were tested and the Silhouette associated values for each partition were calculated. According to this analysis, the maximum average value of 0.624 for Silhouette measure was obtained when using the group average clustering algorithm and a distance cut off value of 0.656, thus producing 6 independent gene groups. The resulting partition was then visually inspected for consistency in the dendrogram. The dendrogram was built using the iTOL webserver (Letunic & Bork, 2007). A color-coded strip illustrating the independent gene clusters was added to the dendrogram to facilitate the mapping and analysis of individual genes (Supplementary figure 2, annexes D). A Gene Ontology (GO) enrichment analysis was then carried out independently for each of the 6 groups obtained with the partition-based clustering methodology described above. Blast2GO software (Conesa, et al., 2005) was used to perform the Gene Ontology enrichment analysis. This software has integrated the Gossip package for statistical assessment, which uses the Fisher's exact test and corrects for multiple testing to find enriched GO terms between two sets of sequences (Blüthgen, et al., 2005). The complete set of annotated genes for *Saccharomyces cerevisiae* was used as reference control group with a false positive discovery rate value of 0.1.

II.7.5 Transcriptional network analysis

We mapped each gene present in the different clusters to its potential transcriptional regulators. We searched for this in the YEASTRAC (Teixeira, et al., 2006) and TRANSFAC (Matys, et al., 2003) databases, and built a consensus list from the information from both databases. Then, using the Cytoscape software (Smoot et al., 2011), we mapped each of the transcription factors onto a previously published regulatory network (Jothi, et al., 2009) and obtained the sub-networks for each transcription factor. Then we identified the target genes for each cluster. As a result, we obtained a regulatory module, related to a specific transcription factor and a specific gene cluster.

I.8 Metabolic flux analysis

The Metabolic Flux Analysis (MFA) model was built with the intention to describe yeast metabolism under fermentative conditions and how it is affected by the addition of oxygen. We sought to solve the mass balance equation:

$$M * v = 0$$

Where “M” is a stoichiometric matrix and “v” is the vector of fluxes through the intracellular reactions. This equation assumes that intracellular metabolites are at a steady state; hence the rate of accumulation of intracellular metabolites is 0. This makes the equation solvable for “v”.

II.8.1 Stoichiometric matrix

Stoichiometric matrix was built based on the model developed by Varela (Varela, et al., 2004). This matrix includes glycolysis, TCA cycle, fermentative and anaplerotic reactions, as well as essential anabolic pathways. The following oxygen-related reactions were added to this matrix: proline consumption, NADH- and FADH₂ - dependent respiration pathways (each one lumped in one reaction), ergosterol and unsaturated fatty acid synthesis. These reactions were extracted from YeastCyc database. The approach of Nissen (Nissen, et al., 1997) was used for the biomass equation, leaving every biomass component (protein, DNA, RNA, carbohydrate and lipids) as individual products. Moreover, the lipids were separated into sterols, unsaturated and saturated fatty acids, in order to have a better description of the oxygen-dependent pathways. The resulting matrix, which has 47 reactions and 44 metabolites, is detailed in Annexes A. The condition number of the matrix was 44, indicating that the model is numerically robust (Villadsen, et al., 2011).

II.8.2 Flux estimation

Since the model has three degrees of freedom (number of reactions minus number of metabolites) the system becomes over-determined if more than three extracellular rates are measured. The inputs was evaluated including all of the possible combinations of rates (from 3 to 15), were selected from the following set of experimentally measured extracellular rates of substrate uptake or metabolic production: glucose, ethanol, glycerol, succinate, acetate, CO₂, oxygen, proline, biomass components (carbohydrates, DNA, RNA, proteins) and the three classes of lipids mentioned above. The procedures for measuring biomass components have been previously stated. Since the resulting matrix is not square, a “pseudo-inverse” operation was carried out (Stephanopoulos et al, 1998) to solve the mass balance equation and estimate the flux vector, including the unselected rates. Evaluation of the rate combinations indicated that the more rates selected for input, the more accurate the estimations of the model. This prompted us to use 13 extracellular rates as an input, leaving ethanol and CO₂ as calculated rates. This was validated by sensitivity analysis as described below. Redistribution of intracellular fluxes under different oxygen conditions was assessed by determining the flux vector for the three individual replicates for each condition, and comparing resulting fluxes to each other using a t test.

II.8.3 Consistency and sensibility analysis

Data consistency was checked using the method described by Wang and Stephanopoulos (Wang & Stephanopoulos, 1983). After confirming the absence of gross measurement errors, a custom-sensitivity analysis was performed, based on the normalized error distribution, which was calculated as the differences between the estimated fluxes and the fluxes calculated using modified rates (specific rates plus - minus experimental error). Afterwards, the square root of the square sum of these differences was calculated, in order to obtain the error value. Finally, the errors were normalized by the value of the corresponding flux calculated with the unmodified rates. The specific rates were modified by the experimental error one at a time and the sum of the errors on all the fluxes of the stoichiometric matrix was calculated. The errors in ethanol and CO₂ rates were ones that contributed the most to the overall flux error of the

model. Therefore, we used 13 rates as input and estimated the specific rates of ethanol and CO₂ to validate the model. These estimations had less than 11% error (Table II.2). All the preceding calculations were carried out using custom scripts in R computer language.

Table II.2: Estimation of ethanol and CO₂ specific production rates by the MFA model.

Estimated specific rates ^a	Dissolved oxygen (μM)				
	0	1.2	2.7	5	21
Ethanol	26.44	26.67	21.44	18.35	10.9
error (%)	-4.27	5.64	-8.99	2.68	-11.4
CO₂	13.59	15.05	11.46	13.77	10.2
error (%)	1.29	8.3	-5.58	-3.88	-8.0

^a Data in C-mmol (gDCW·h)⁻¹

III. RESULTS

III.1 Long-term impact of increasing concentrations of dissolved oxygen on wine yeast physiology under enological conditions

III.1.1 Simulation of dissolved oxygen concentrations and oxygen uptake rates under enological conditions

The oxygen uptake capabilities of *S. cerevisiae* EC 1118 from a synthetic must was evaluated in continuous cultures (Figure III.1). An increase in specific oxygen uptake rate (OUR) was found with dissolved oxygen up to 21 μM . From this critical value on, the specific OUR remained constant at $3.9 \text{ mmol} \cdot (\text{g DCW h})^{-1}$. This empirical critical value was close to the value previously reported for the OUR under fully aerobic, nitrogen-limited continuous cultures ($3.5 \text{ mmol} \cdot (\text{g DCW h})^{-1}$) (Larsson, et al., 1993). Thus, five different levels of dissolved oxygen were selected to cover the complete range from anaerobic to the maximum specific OUR (Figure III.1 and Table III.1). These concentrations covered the entire dissolved oxygen range for the yeast cells under enological conditions (Saa et al., 2012).

Table III.1: Dissolved oxygen concentrations and specific oxygen uptake rate of *S. cerevisiae* EC 1118 grown under different oxygen levels.

Dissolved oxygen concentration (μM) ^a	OUR ^{a,b} ($\text{mmol O}_2 \text{ gDCW}^{-1} \text{ h}^{-1}$)
0 ± 0.00	NA
1.2 ± 0.06	-0.1 ± 0.0
2.7 ± 0.28	-0.7 ± 0.3
5.0 ± 0.02	-2.3 ± 0.3
21.0 ± 1.1	-3.9 ± 0.1

^a The data are the averages \pm standard deviations for three independent chemostat steady states.

^b OUR: Specific Oxygen Uptake Rate.

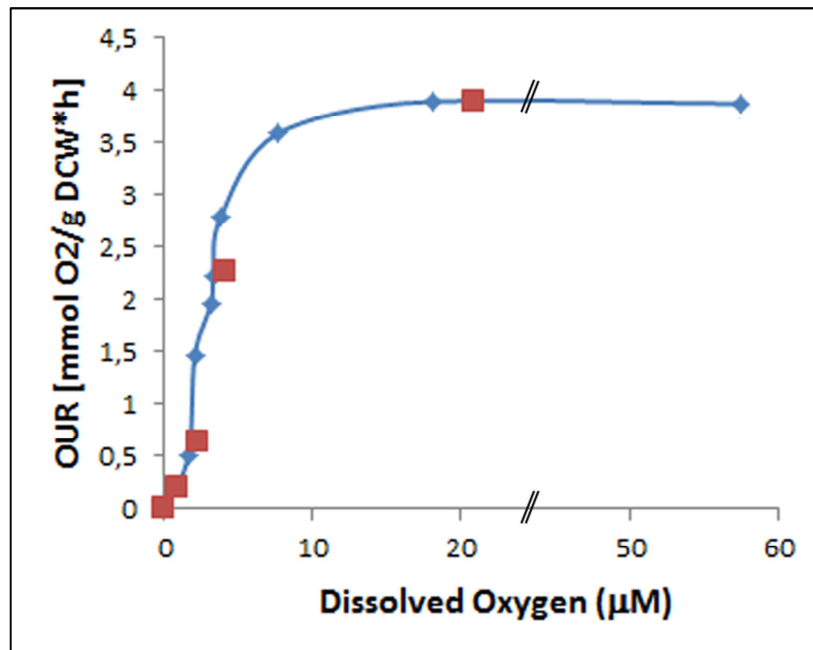


Figure III.1: Relationship between dissolved oxygen concentration and specific oxygen uptake rate (OUR) of *Saccharomyces cerevisiae* strain EC1118. Blue symbols correspond to steady state nitrogen limited continuous cultures with increasing dissolved oxygen concentrations. The corresponding OURs were determined in the same cultures. Brown squares represent the five dissolved oxygen conditions evaluated in this research.

III.1.2 Carbon balances at different dissolved oxygen concentration

Accounting for all the carbon inputs and outputs to and from the culture (i.e. the carbon balance) is a requirement for a quantitative assessment of metabolic physiology. Sugar and oxygen uptakes were measured, as well as the accumulation of several organic compounds. Carbon balances, calculated through the yields on glucose (in Cmol per Cmol of glucose consumed), close near to one (Table III.2), indicating that no major product or substrate had been left out. Analyzing the carbon balances more in depth, it was found that at highest dissolved oxygen concentration the biomass yield on glucose (Y_{gx}) increased, while ethanol and glycerol yields on glucose decreased when dissolved oxygen increases. (Table III.2).

Table III.2: Dissolved oxygen concentration and glucose yields in different oxygen feeding conditions^a.

Dissolved Oxygen (μM)	Y _{gx} C-mol biomass (C-mol glucose) ⁻¹	Y _{gly} C-mol glycerol (C-mol glucose) ⁻¹	Y _{ge} C-mol ethanol (C-mol glucose) ⁻¹	Y _{gc} C-mol CO ₂ (C-mol glucose) ⁻¹	Carbon recovery (%)
0 ± 0.00	0.094 ± 0.01	0.03 ± 0.01	0.60 ± 0.02	0.32 ± 0.03	107 ± 2.6
1.2 ± 0.06	0.094 ± 0.005	0.03 ± 0.002	0.57 ± 0.02	0.27 ± 0.02	97 ± 3.6
2.7 ± 0.28	0.108 ± 0.002	0.037 ± 0.001	0.61 ± 0.08	0.29 ± 0.015	107 ± 7.2
5 ± 0.02	0.12 ± 0.007	0.027 ± 0.008	0.55 ± 0.08	0.38 ± 0.02	108 ± 10.3
21 ± 1.1	0.18 ± 0.01	0.018 ± 0.004	0.52 ± 0.07	0.33 ± 0.04	106 ± 5.9

^aThe data are average ± standard deviations for three independent chemostat steady states.

III.1.3 Relationship between biomass increase and proline consumption in the presence of oxygen

Biomass concentration significantly increased with the availability of dissolved oxygen, almost doubling at 5 μM dissolved oxygen, compared to anaerobic conditions (Table III.3). This also correlated with an increase in proline consumption, which concurs with the limitation of all other nitrogen sources (Ingledeew & Magnus, 1987). Proline consumption and biomass increase matched each other, up to 2.7 μM dissolved oxygen, according to the biomass yield on nitrogen for this strain in anaerobic conditions (Pizarro et al. (2008) and Table III.3). This correspondence did not occur for higher dissolved oxygen concentrations, most likely because the biomass yield on nitrogen under aerobic conditions is different that the yield calculated for anaerobic conditions (12.1 g biomass (g Nitrogen)⁻¹). Consistent with the biomass increase, the glucose consumption volumetric rate increased with increasing dissolved oxygen levels (from 141 to 197 C-mmol glucose·(L h)⁻¹ for 0 to 5 μM dissolved oxygen, respectively). Nevertheless, increasing the dissolved oxygen further, resulted only in a modest increase in biomass and a decrease of the glucose consumption volumetric rate (to 125 C-mmol glucose·(L h)⁻¹).

Table III.3: Proline consumption and nitrogen yields.

Dissolved oxygen (μM) ^a	Biomass ($\text{g}\cdot\text{L}^{-1}$) ^a	Proline consumed ($\text{mg}\cdot\text{L}^{-1}$) ^a	Nitrogen consumed as proline ($\text{mg}\cdot\text{L}^{-1}$)	Total nitrogen consumed ($\text{mg}\cdot\text{L}^{-1}$)
0 ± 0.00	3.1 ± 0.2	0 ± 0.0	0	300.0
1.2 ± 0.06	3.7 ± 0.05	90 ± 1.8	21.9	321.9
2.7 ± 0.28	4.2 ± 0.1	239 ± 4.8	58.3	358.9
5.0 ± 0.02	5.6 ± 0.3	318 ± 6.3	77.4	377.4
21.0 ± 1.1	5.8 ± 0.2	438 ± 8.8	106.6	406.6

^aThe data are the average \pm standard deviations for three independent chemostat steady states.

III.1.4 Impact of dissolved oxygen concentration on specific rates and respiratory quotient (RQ)

The impact of oxygen on cell physiology was more evident when analyzing specific rates (Table III.4a). An inverse relationship with dissolved oxygen was observed for glucose consumption and ethanol and glycerol specific production rates. However, in all cases, significant ethanol production was found (Table III.4b), consistent with the presence of the Crabtree effect. Accordingly, the respiratory quotient (RQ) were all larger than 1 for all oxygenated conditions (Table III.4a). Organic acid production was also affected by oxygen availability. For instance, acetic acid was produced only under strict anaerobiosis ($0.3 \text{ C}\cdot\text{mmol}\cdot(\text{gDCW h})^{-1}$). On the other hand, a striking and significant ($p < 0.01$) increase in succinic acid production occurred between 1.2 and $2.7\mu\text{M}$ dissolved oxygen conditions (from 0.02 to $0.27 \text{ C}\cdot\text{mmol}\cdot(\text{gDCW h})^{-1}$). This increase was unexpected, as there is no known mechanism of succinic acid export in yeast, though succinic acid production has been consistently reported in previous studies (Pizarro et al., 2007; Pizarro et al., 2008).

Table III.4: a) Specific consumption and production rates and b) Steady-state metabolite concentration in *S. cerevisiae* EC 1118 grown under increasing dissolved oxygen culture conditions.

Dissolved oxygen concentration (μM)	Specific consumption and production rates ^a ($\text{C}\cdot\text{mmol}\cdot(\text{gDCW h}^{-1})$)					RQ ^b
	Glucose	Ethanol	Glycerol	Succinic Acid	CO ₂	
0.0 ± 0.00	-43.6 ± 5.5	27.7 ± 4.0	1.5 ± 0.6	0.06 ± 0.02	13.8 ± 1.8	NA
1.2 ± 0.06	-43.9 ± 2.6	25.2 ± 0.6	1.4 ± 0.2	0.02 ± 0.04	12.0 ± 1.2	241
2.7 ± 0.28	-37.5 ± 0.0	25.4 ± 1.2	1.4 ± 0.0	0.27 ± 0.05	11.5 ± 0.2	17
5.0 ± 0.02	-37.4 ± 1.0	18.0 ± 2.3	1.0 ± 0.3	0.22 ± 0.00	13.3 ± 0.1	6
21.0 ± 1.1	-21.6 ± 0.2	12.3 ± 0.2	0.4 ± 0.0	0.15 ± 0.01	11.0 ± 0.2	2.8

^aThe data are the average ± standard deviations for three independent chemostat steady states.

^bRQ: Respiratory Quotient, NA: Not applicable.

Dissolved oxygen concentration (μM)	Steady state metabolite concentration (g L^{-1})		
	Biomass	Glucose	Ethanol
0.0 ± 0.00	3.1 ± 0.2	42.1 ± 1.8	20.3 ± 2.4
1.2 ± 0.06	3.7 ± 0.05	40.5 ± 5.4	21.1 ± 0.5
2.7 ± 0.28	4.2 ± 0.1	40.7 ± 3.0	23.5 ± 2.8
5.0 ± 0.02	5.6 ± 0.3	37.5 ± 3.0	24.2 ± 2.8
21.0 ± 1.1	5.8 ± 0.2	41.7 ± 1.4	16.2 ± 0.8

^aThe data are the average ± standard deviations for three independent chemostat steady states.

III.1.5 Metabolic flux analysis

The redistribution of intracellular carbon fluxes in the central metabolic pathways of *Saccharomyces cerevisiae* occurring in response to increasing availability

of dissolved oxygen under enological conditions was determined using a stoichiometric model specially developed for this work (see Annexes A). The carbon flux towards fermentation progressively decreased, with a concomitant increase of the flux through the TCA cycle as the dissolved oxygen content increased (Figure III.2). Furthermore, the TCA cycle under anaerobic conditions was not functional and operated in two branches, as previously suggested for anaerobic, carbon-limited conditions (Camarasa, et al., 2003; Nissen, et al., 1997). A similar situation was observed with 1.2 μM dissolved oxygen level. However, with 2.7 μM and higher dissolved oxygen concentrations, the TCA cycle followed its canonical direction, with a large increase in carbon flux circulation through it ($p < 0.05$) (Figure III.2). Another remarkable feature was the increase of the flux towards carbohydrate synthesis in conditions with 21 μM dissolved oxygen, increasing more than 60% compared to the other conditions (Figure III.2). This was supported by experimental data (Table III.5).

Table III.5: Specific production rates of major biomass components at different dissolved oxygen concentration^a.

Component rates ^b	Dissolved oxygen concentration (μM).				
	0	1.2	2.7	5	21
Carbohydrates	0.915 \pm 0.039	0.951 \pm 0.041	1.070 \pm 0.048	1.020 \pm 0.045	2.588 \pm 0.129
DNA	0.006 \pm 0.000	0.007 \pm 0.000	0.006 \pm 0.000	0.0063 \pm 0.000	0.006 \pm 0.000
Proteins	0.864 \pm 0.056	0.874 \pm 0.060	0.836 \pm 0.054	0.877 \pm 0.061	0.865 \pm 0.051
RNA	0.062 \pm 0.006	0.059 \pm 0.005	0.044 \pm 0.004	0.054 \pm 0.005	0.061 \pm 0.006
Ergosterol	2.13E-9 \pm 0.0	0.009 \pm 0.000	0.022 \pm 0.001	0.018 \pm 0.001	0.004 \pm 0.000
Proline ^c	0 \pm 0.000	- 0.108 \pm 0.003	- 0.244 \pm 0.005	- 0.242 \pm 0.005	- 0.322 \pm 0.007

^aThe data are the averages \pm standard deviations for three independent chemostat steady states.

^bRates in (C-mmol (gDCW h)⁻¹)

^cspecific rate of proline consumption.

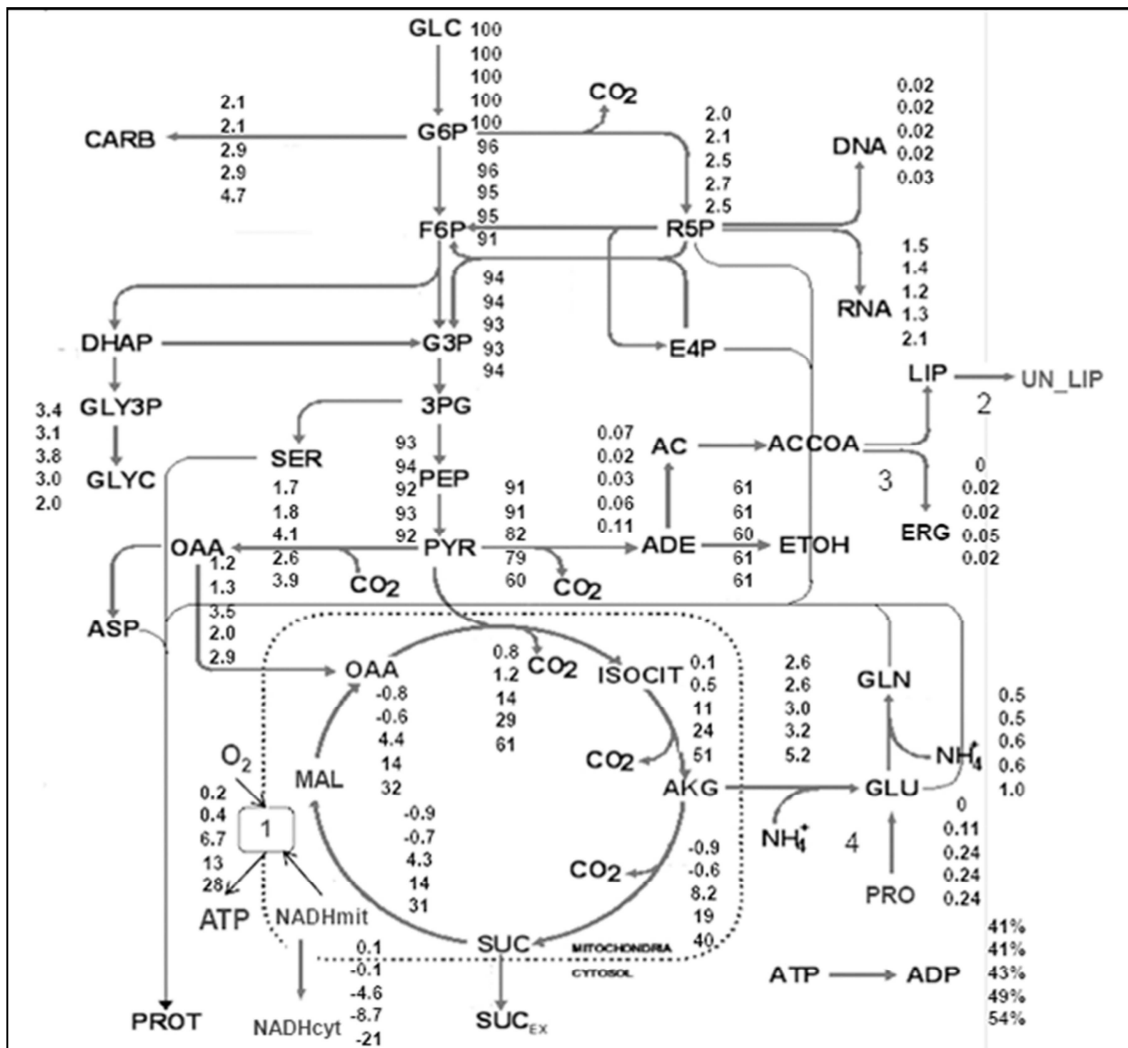


Figure III.2: Flux distributions in *S. cerevisiae* EC1118 strain grown in nitrogen limited chemostats at $D = 0.1 \text{ h}^{-1}$ from anaerobic (top) to $21 \mu\text{M}$ (bottom) dissolved oxygen concentrations. Numbers indicate specific reactions related with oxygen consumption: 1) Respiration, 2) Unsaturated lipid synthesis, 3) Ergosterol synthesis, 4) Proline uptake. The fluxes are expressed as percentage of the total carbon uptake. Negative numbers indicate flux in the reverse direction. The flux for maintenance is expressed as a percentage of the total ATP produced. CARB, carbohydrates; GLC, glucose; FRUC, fructose; F6P, fructose 6-phosphate; R5P, ribose 5-phosphate; DHAP, dihydroxyacetone phosphate; G3P, glyceraldehyde 3-phosphate; E4P, erythrose 4-phosphate; GLY3P,

glycerol 3-phosphate; 3PG, 3-phosphoglycerate; GLYC, glycerol; SER, serine; PEP, phosphoenolpyruvate; AC, acetate; ACCoA, acetyl coenzyme A; LIP, lipids; OAA, oxaloacetate; PYR, pyruvate; ADE, acetaldehyde; ETOH, ethanol; ASP, aspartate; ISOCIT, isocitrate; GLN, glutamine; FUM, fumarate; AKG, α -ketoglutarate; GLU, glutamic acid; PROT, protein; SUC, succinate; SUCEX, extracellular succinate; mATP, maintenance ATP; PRO, proline; NADH_{mit}, mitochondrial NADH; NADH_{cyt}, cytosolic NADH; ERG, ergosterol; UN_LIP, unsaturated lipids.

III.1.5.1. Sources and sinks of NADH and NADPH

Metabolic Flux Analysis showed that mitochondria played an increasingly important role in NADH and ATP turnover above 2.7 μ M dissolved oxygen. Fluxes through respiration, as well as cytosol to mitochondria NADH exchange, increased significantly as dissolved oxygen rose (Figure III.2). Mitochondrial NADH production and utilization significantly increased with oxygen ($p < 0.05$), rising from 25% to 60% of the total NADH production in the cell, when increasing from 2.7 to 21 μ M dissolved oxygen levels, respectively. Analyses of NADH reoxidation pathways showed that ethanol production was still the dominating form for reoxidizing cytosolic NADH produced by glycolysis under all the conditions tested (Table III.6). Below 2.7 μ M dissolved oxygen, glycerol is the only other electron sink, albeit a minor one (~ 4% of NADH reoxidation). Above 2.7 μ M dissolved oxygen in the culture, reoxidation of cytosolic NADH through the mitochondrial redox shuttle significantly exceeds its reoxidation by glycerol synthesis (t test, $p < 0.05$); moreover, glycerol synthesis showed almost no contribution at the 21 μ M dissolved oxygen condition.

NADPH metabolism was slightly affected by oxygen levels. The most remarkable change occurred in the aldehyde dehydrogenase reaction. NADPH production by this reaction decreased from 4% to 1% when the available oxygen increased from 0 μ M to 1.2 μ M dissolved oxygen. The rest of the NADPH was produced through the pentose phosphate pathway, a flux that slightly increased when comparing the anaerobic condition to the rest of the conditions. However, the flux

through this pathway represents only 2% of the carbon in all conditions (Supplementary Table 1, see Annexes B), confirming previous results reported by Varela et al. (2004).

III.1.5.2 Sources and sinks of ATP

Oxygen also increased mitochondrial contribution to ATP production. Under anaerobic conditions, ATP was produced through glycolysis by substrate-level phosphorylation. On the other hand, ATP produced by oxidative phosphorylation had a noticeable contribution, rising from 5.7% to 21% of total ATP when dissolved oxygen increased from 2.7 μM to 21 μM , respectively. Furthermore, at a dissolved oxygen concentration of 21 μM , the glycolytic pathway was still the main contributor to ATP production, producing more than 70% of the total ATP (Table III.6). Nevertheless, at the highest dissolved oxygen level, the amount of ATP produced by any means is significantly reduced - decreasing by approx. 30%-. This was also associated with an increase of the fraction of ATP used in maintenance, which increased from 43% to 54% in the 2.7 μM and 21 μM dissolved oxygen conditions, respectively.

Table III.6: Contribution to NADH and ATP turnover of different metabolic pathways in *S. cerevisiae* EC1118 grown under different dissolved oxygen culture conditions.

Process	Dissolved oxygen concentration ^a (μM)				
	0	1.2	2.7	5	21
<i>Total NADH synthesis</i> (mmol (gDCW h) ⁻¹)					
Cytosolic	13.7± 1.7	13.8 ± 0.8	11.6 ± 0.1	11.1 ± 0.5	6.7 ± 0.5
Mitochondrial	0.1 ± 0.2	0.2 ± 0.1	3.4 ± 0.0	7.1 ± 0.2	9.5 ± 0.2
<i>Cytosolic NADH consumed (%) for:</i>					
Ethanol production	96.0 ±1.7	96.0 ± 0.8	89.6 ± 0.0	85.0 ± 0.5	73.5 ± 0.5
Glycerol production	4.0 ± 0.2	4.0 ± 0.1	3.4 ± 0.0	3.0 ± 0.1	1.2 ± 0.1
Mitochondrial shuttle	0.0	0.0	7.0 ± 0.0	12.0 ± 0.0	25.3 ± 0.1
<i>Total ATP produced</i> (mmol (gDCW h) ⁻¹)					
Glycolysis	27.2 ±3.4	27.5 ±1.60	23.1 ±0.00	22.0 ±0.90	13.20 ±0.90
TCA cycle	0.0	0.00	0.61 ±0.06	1.32 ±0.06	1.70 ± 0.17
Oxidative phosphorylation	0.0	0.05 ±0.05	1.45 ±0.34	2.85 ±0.07	3.20 ± 0.40

^aThe data are the average ± standard deviations for three independent experiments.

III.1.6 Gene expression analysis of dissolved oxygen levels

To complement the metabolic flux data, global gene expression of *S. cerevisiae* EC 1118 for the five dissolved oxygen culture conditions, was determined. As a whole, the effect of oxygen on the transcriptome was limited, since only 8.8% of the transcripts (507 genes) were affected by oxygen availability. This percentage was calculated taking into account the differentially expressed genes in all the possible comparisons between the different oxygen conditions. The comparison between the anaerobic and the highest dissolved oxygen conditions (21 μM) yielded 313 differentially expressed genes. This data was consistent with previous reports (Tai, et al., 2005), in which 371 genes were differentially expressed between anaerobic and aerobic conditions in nitrogen-limited, continuous cultures.

III.1.6.1 Analysis of oxygen level transitions

To simulate the oxygen consumption kinetics of yeast cells after an oxygen impulse during wine-making aeration operations a pseudo-dynamic setting was simulated by comparing the data of one condition with the next higher dissolved oxygen condition (Table III.7). The largest effect with 200 differentially expressed genes, occurred upon the onset of oxygen addition (i.e. between 0 and 1.2 μM dissolved oxygen). The transition between 5 μM and 21 μM had an equivalent impact, causing differential changes in 195 genes. Remarkably, this was the transition between oxygen-limited and oxygen-saturated conditions (Figure III.1). The effect was much lower when comparing the intermediate transitions (1.2 μM with 2.7 μM , and 2.7 μM with 5 μM), affecting the expression of 25 and 19 genes, respectively.

III.1.6.1.1 Genes differentially expressed between 0 and 1.2 μM dissolved oxygen

These genes can be classified into two groups. The first group consisted of six genes annotated as “siderophore transport”, which participate in iron uptake. The putative increase in iron uptake could be related to the overexpression of haemoprotein-related genes, such as cytochromes. The second group comprised nine genes annotated as “aminoacid transport”, including the proline transporter *PUT4*. This highlights both the induction of respiratory genes and the impact of oxygen in regulating the nutrient uptake of yeast.

III.1.6.1.2 Genes differentially expressed between 1.2 μM and 2.7 μM dissolved oxygen

Between 1.2 μM and 2.7 μM dissolved oxygen, key mitochondrial genes, such as *CYCI* (cytochrome c) and *NDE1* (external NADH dehydrogenase), were induced. Nde1p is responsible for the shuttling of cytosolic redox equivalents directly into the respiratory chain. *GUT2*, another gene responsible for a shuttle mechanism (Rigoulet, et al., 2004) was also induced between 0 μM and 2.7 μM dissolved oxygen. Among repressed genes, two members of the *TIR* genes and the *HPF1* gene – all encoding for

the synthesis of cell wall mannoproteins - were found. It is worthy to note that the repression of mannoproteins could have several consequences on wine quality, modulating astringency and other organoleptic properties (Gonzalez-Ramos et al., 2008). The *AUS1* gene involved in fatty acids and sterol uptake was also repressed.

III.1.6.1.3 Genes differentially expressed between 5 and 21 μ M dissolved oxygen

This transition consolidated the trend in induction of respiratory genes. Induced genes included more respiratory genes, such as *CYC1* and *COX7* (subunit of Complex IV), supporting the idea of active respiration, even under these high-glucose conditions. Other induced genes were stress response genes, such as *CTT1* (catalase), *HSP12* (membrane heat-shock protein) and *GRX4* (glutaredoxin) hinting to a potential oxidative stress occurring at highest dissolved oxygen condition. The repressed genes at this transition included genes involved in iron metabolism, as well as those involved in sulfate and phosphate ion transport (Table III.7).

III.1.6.1.4 Other gene expression changes

The genes annotated to the “TCA cycle” Gene Ontology (GO) term showed no differential expression in the analyzed transitions. However, when comparing anaerobic and 21 μ M dissolved oxygen conditions, the TCA cycle term was statistically enriched among the induced genes ($p < 0.01$), including *ACO1* (aconitase) and *CIT1* (citrate synthase). On the other hand, *FRD1* was significantly repressed when comparing anaerobic with 5 μ M dissolved oxygen conditions. *FRD1* encodes a soluble fumarate reductase that is responsible for the operation of the reductive branch of the TCA cycle. This observation is consistent with the redistribution of metabolic carbon fluxes observed by MFA with increasing dissolved oxygen concentrations: increase of TCA fluxes and the disappearance of the anaerobic, two-branch operation of the TCA cycle.

Table III.7: Characterization of differentially expressed genes across the different oxygen levels.

Transition of oxygen concentration. (μM) (gene expression effect)	Differentially expressed genes (FDR < 0.1) ^a	Enriched GO Biological Process terms ($p < 0.01$) ^b (GO term frequency) ^c	Highlighted genes
0 - 1.2 (induced)	39	Siderophore transport (10.3/0.2) Amino acid transport (12.8/1.0)	<i>FRE3</i> (ferric reductase) <i>ENB2</i> (enterobactin) <i>PUT4</i> (proline transporter)
0 - 1.2 (repressed)	161	NF ^d	NF ^d
1.2 – 2.7 (induced)	11	Mitochondrial intermembrane space (27.3/0.8) Inorganic anion transmembrane transporter activity (18.2/0.3)	<i>NDE1</i> (external NADH dehydrogenase) <i>CYC1</i> (cytochrome c) <i>SUL1</i> (high affinity sulfate transporter) <i>PHO84</i> (phosphate transporter).
1.2 – 2.7 (repressed)	14	Cell wall (18.9/1.8) Sterol transport (13.5/0.9)	<i>HPF1</i> (haze-protective mannoprotein) <i>TIR2</i> (cell wall mannoprotein) <i>UPC2</i> (sterol regulatory element binding protein) <i>AUS1</i> (ABC-type sterol transporter)
2.7 – 5.0 (induced)	3	NF ^d	NF ^d
2.7 – 5.0 (repressed)	16	NF ^d	NF ^d
5.0 – 21.0 (induced)	100	Respiratory chain (7/0.5)	<i>CYC1</i> (cytochrome c, isoform 1) <i>COX7</i> (subunit VII of cytochrome c oxidase)
5.0– 21.0 (repressed)	95	Iron ion homeostasis (23.2/0.9) Transport (45.3/19.6)	<i>FRE3</i> (ferric reductase) <i>ENB2</i> (enterobactin) <i>PHO84</i> (phosphate transporter) <i>SUL1</i> (high affinity sulfate transporter)

^a FDR, false discovery rate, as determined by the Rank Products method

^b As determined by the GO Term Enrichment tool at AmiGO (Carbon, et al., 2009)

^c Data between parenthesis: (frequency of the term among the differentially expressed genes/ frequency among the whole transcriptome of *S. cerevisiae*).

^d NF: No significant GO term.

III.1.6.2 Clustering analysis

Genes that responded to oxygen in at least one condition were classified into 56 clusters (Figure III.3), by means of hierarchical clustering. We classified the clusters according to their major tendencies with regard to the dissolved oxygen concentration. We analyzed the 12 clusters that showed at least one enriched GO term according to the GO term enrichment analysis (Table III.8). We classified the clusters according to their general trends in relation to the dissolved oxygen concentration. We found four broad categories: First, clusters with genes down-regulated at 21 μM dissolved oxygen. Second, clusters with genes down-regulated with 1.2 μM dissolved oxygen. Third, genes negatively correlated with dissolved oxygen. Fourth, genes positively correlated with dissolved oxygen. We describe the genes that belong to each cluster below.

III.1.6.2.1 Genes down-regulated at 21 μM dissolved oxygen

Several gene clusters displayed this behavior. Four clusters (2, 8, 26 and 52) related to iron metabolism were repressed under 21 μM dissolved oxygen. From these, clusters 2, 26 and 52 were induced with 1.2 μM dissolved oxygen. This confirms the induction of iron uptake at low oxygen levels a trend that is reversed at high oxygen concentrations. Besides genes related to iron metabolism, several genes involved in ergosterol metabolism were down-regulated at high oxygen levels. This suggests a possible product repression, when enough oxygen is present to synthesize these compounds (Davies & Rine, 2006).

III.1.6.2.2 Genes down-regulated with 1.2 μM dissolved oxygen

Several clusters show a common negative response to low levels of oxygen. Gene expression in clusters 25 and 29 dropped significantly at 1.2 μM dissolved oxygen, although it increased concomitantly with oxygen concentration for the higher oxygen levels (Figure III.3). Several transcription factors belong to these clusters, most notably two positive regulators of nitrogen catabolism, *DAL81* and *GZF3* (Georis et al, 2009). Other genes, such as those from cluster 37, displayed a very low expression. This is characteristic of silenced transposable elements, which are further lowered with oxygen

increase. Cluster 43 also shows this pattern. This cluster includes *FRD1*, the fumarate reductase gene, confirming the two-branch TCA transition; as well as *SLC1*, a key enzyme involved in phospholipid metabolism (Athenstaedt & Daum, 1997).

III.1.6.2.3 Genes negatively correlated with dissolved oxygen

The family of *TIR* genes appeared both in cluster 53 and the 1.2 - 2.7 μM oxygen transition, showing a dose-dependent response to oxygen (Figure III.3). These results suggest that cell wall remodeling is taking place when oxygen increases, which could be also linked to the increasing ergosterol production (Table III.5). Consistently, the *UPC2* transcription factor, which regulates ergosterol biosynthesis and *TIR* genes (Davies & Rine, 2006), was also repressed as the oxygen level increased (Cluster 13).

III.1.6.2.4 Genes positively correlated with dissolved oxygen

Supporting the idea of a respiratory metabolism under these conditions, several genes related to the complex IV of the respiratory chain were jointly induced with dissolved oxygen, and they were grouped in cluster 32 (Figure III.3).

Despite these findings, some metabolic pathways, such as acetate production showed phenotypic changes that were not reflected by gene expression. For instance, we observed that the *ALD* genes, coding for aldehyde dehydrogenases responsible for acetate production (Boubekeur et al, 2001), were not affected by oxygen levels, despite acetate was only detected in anaerobic cultures.

Table III.8: Functional terms enrichment for the genes in each cluster

Cluster number ^a	Number of genes	Representative enriched GO terms (FDR < 0.05)	Highlight genes ^b
2	5	Iron ion transport	<i>FRE2, FRE3</i> (Ferric and cupric reductase), <i>ENB2</i> (Enterobactin)
8	23	Iron ion homeostasis	<i>FRE1, FRE6</i> (Ferric and cupric reductase)
13	18	-	<i>UPC2</i> (sterol regulatory element binding protein)
16	13	Response to zinc ion	<i>EEB1</i> (acyl CoA-ethanol O-acyltransferase)
25	60	Transcription, DNA-dependent	<i>DAL 81, GZF3</i> (nitrogen metabolism regulators)
26	3	Iron ion transport	<i>FET3</i> (ferrous ion transport)
29	16	Oxoacid metabolic process	-
32	10	Mitochondrial respiratory chain complex IV	<i>COX4, COX5A, COX13</i> (cytochrome c oxidase subunits)
37	5	DNA integration	-
43	23	1-acylglycerol -3-phosphate O-acyltransferase activity	<i>FRD1</i> (fumarate reductase) <i>SLC1</i> (1-acylglycerol-3-phosphate O-acyltransferase) <i>ERG1, ERG2, ERG3</i>
51	5	Cellular alcohol biosynthetic process	(ergosterol biosynthetic process) <i>OLE1</i> (fatty acid desaturase)
52	4	Iron ion transmembrane transport	<i>SIT1</i> (siderophore iron transport)
53	2	Structural constituent of cell wall	<i>TIR1, TIR2</i> (cell wall mannoproteins)

^a Clusters not described in the table did not show any enriched GO terms.

^b Annotations extracted from SGD

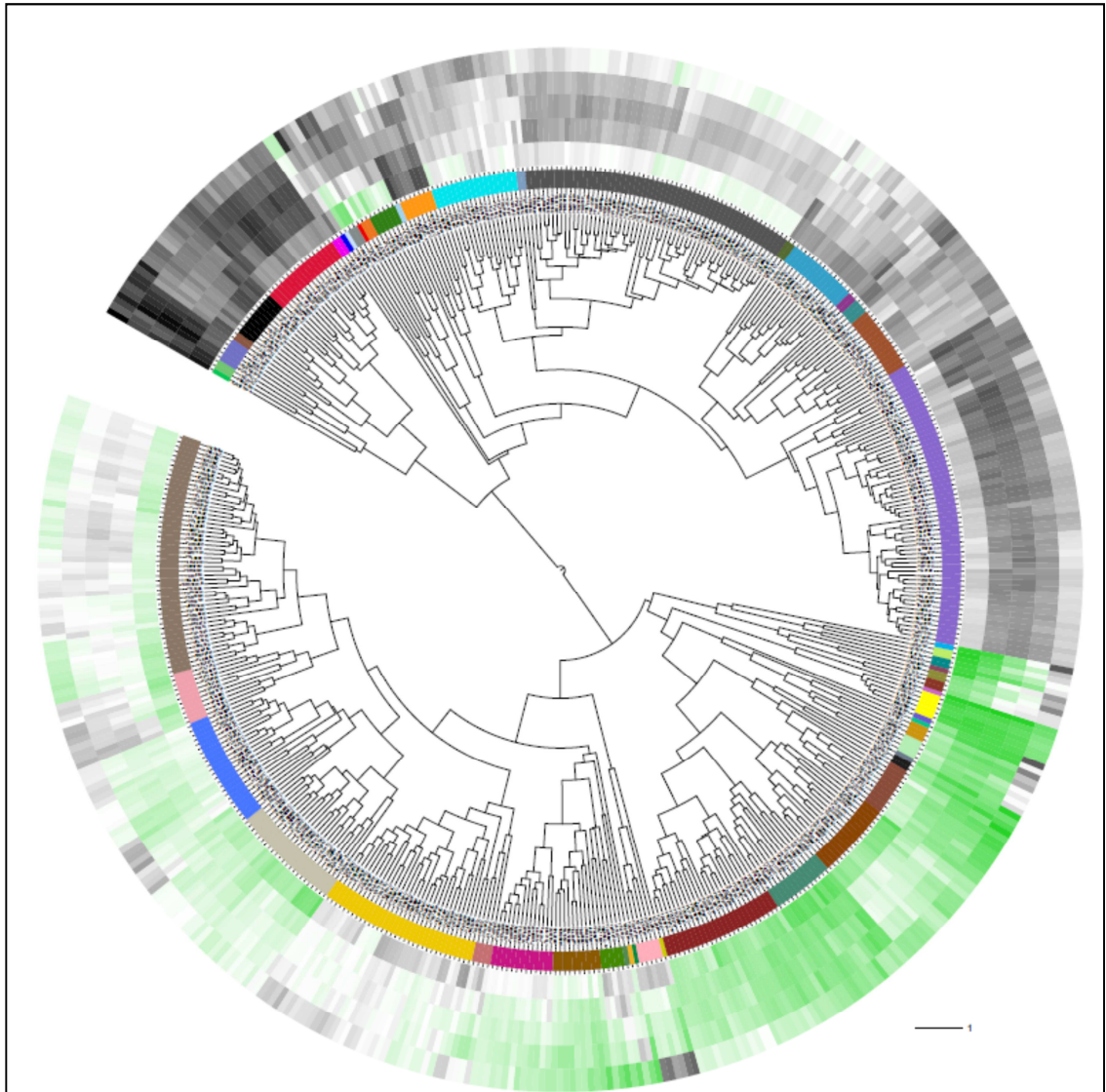


Figure III.3: Hierarchical clustering of the *S. cerevisiae* transcriptome data obtained for the five dissolved oxygen conditions. From center to outside, the dendrogram depicts: 1) Hierarchical clustering tree; 2) Color ribbons indicate each of the 56 clusters; 3) Heatmaps of gene expression values, where black and green represent low and high gene expression levels, respectively. Increasing dissolved oxygen concentrations, from 0 (most internal) to 21 μM (most external), are shown. The scale of the calculated distances in the dendrogram is also illustrated.

III.2 Transient effect of oxygen on wine yeast physiology, in anaerobic conditions using an impulse of oxygen

III.2.1 Dissolved oxygen dynamics under wine fermentation conditions at laboratory scale.

We mimic the industrial discrete oxygen additions carried out during enological fermentations, perturbing anaerobic chemostat cultures ($D = 0.1 \text{ h}^{-1}$), with pure oxygen for 30 seconds. The dynamics of dissolved oxygen was characterized by a sudden increase of dissolved oxygen concentration from 0.03 mg L^{-1} ($0.94 \text{ }\mu\text{M}$) till 4.2 mg L^{-1} ($131.2 \text{ }\mu\text{M}$), followed by consumption within the next 4 minutes from the beginning of the oxygen impulse (Figure III.4a). The maximum value of dissolved oxygen reached under these conditions was almost 1.5 times the maximum value of dissolved oxygen determined after a pump over during Cabernet Sauvignon wine fermentation at industrial scale (Moenne et al, in preparation). Furthermore, the specific oxygen uptake rate (OUR) estimated throughout a model recently developed by our group (Saa, et al., 2012) was $1.28 \text{ mmol (g DCW h)}^{-1}$. This value was within the range of the previously reported values under our culture conditions (Aceituno, et al., 2012).

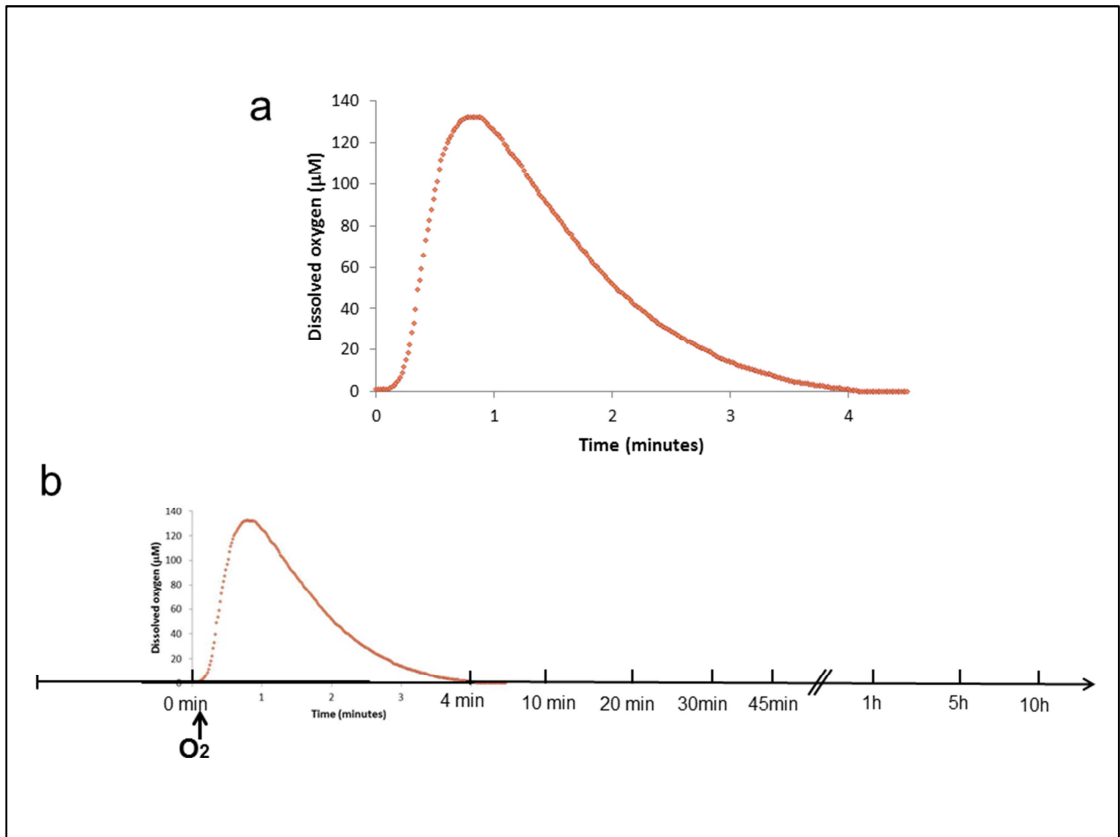


Figure III.4: a) Dissolved oxygen dynamics during dissolved oxygen impulse. Time zero corresponds to anaerobic, steady state anaerobic conditions. The curve is the dissolved oxygen average value of three independent experiments. b) Sampling points before and after oxygen impulse.

III.2.2 Metabolic dynamics of the yeast cells throughout the oxygen impulse

The transient modification of dissolved oxygen availability under these culture conditions did not show significant short-term effects on the major specific rates of substrates and products (glucose, ethanol, glycerol and carbon dioxide), nor in biomass concentration (Figure III.5). These results illustrate that the steady-state fermentative metabolism was not modified by the transient addition of dissolved oxygen under our culture conditions, in contrast to the transition between fermentative and respiro-

fermentative metabolism that occurred under continuous, increasing dissolved oxygen concentration (Aceituno, et al., 2012).

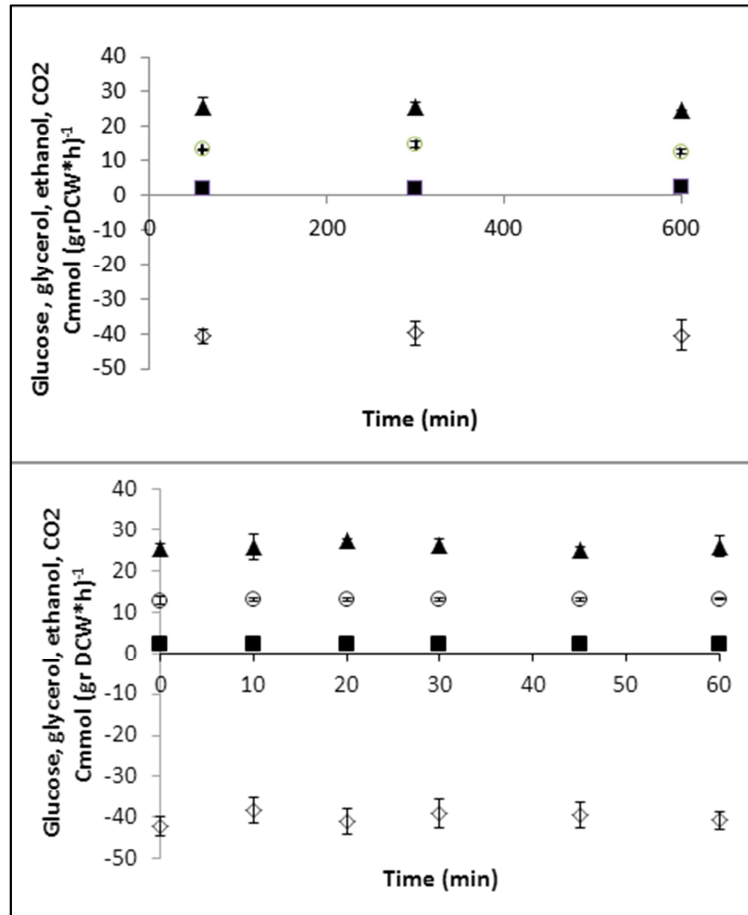


Figure III.5: Metabolic dynamics of wine yeast throughout a dissolved oxygen impulse within the first hour (upper panel) and within the first residence time (bottom panel). Specific rates of glucose consumption (open diamond), glycerol production (close square), ethanol production (close triangle) and CO₂ production (open circle) are indicated. Each point represents the average value of three independent experiments during the time course (0 (steady state), 10 min, 20 min, 30 min, 45 min, 60 min, 300 min and 600 min (one residence time)).

III.2.3. Transcriptomic dynamics of the yeast cells before and after the oxygen impulse

III.2.3.1 Characterization of yeast transcriptome after the oxygen impulse

The analysis of the transcriptional dynamics of *S. cerevisiae* strain EC1118 in response to oxygen impulse yielded a total of 104 genes differentially expressed (FDR < 0.1, according to rank products analysis (Breitling, et al., 2004)). Hierarchical clustering and partition of these genes resulted in 6 clusters (Figure III.6 and supplementary Figure 2, annexes D). Clusters 1, 3 and 5 contain genes that are transiently induced after the oxygen impulse; and clusters 2, 4 and 6, group those genes that are transiently repressed after the impulse (Figure III.6).

We classified the clusters in three categories according to their temporal response after the oxygen impulse. The first group corresponds to genes of immediate response to oxygen, whose peak of expression was 10 minutes after impulse (cluster 1 induced and cluster 2 repressed). The second group corresponds to genes of delayed response to oxygen, whose peak of expression was 1 hour after the dissolved oxygen impulse (cluster 3 induced and cluster 4 repressed). Finally, the third group corresponds to genes of over-delayed response to oxygen, whose expression peak was reached 5 hours after the oxygen impulse (cluster 5 induced and cluster 6 repressed) (Figure III.6). The following is a description of the genes that belong to these clusters.

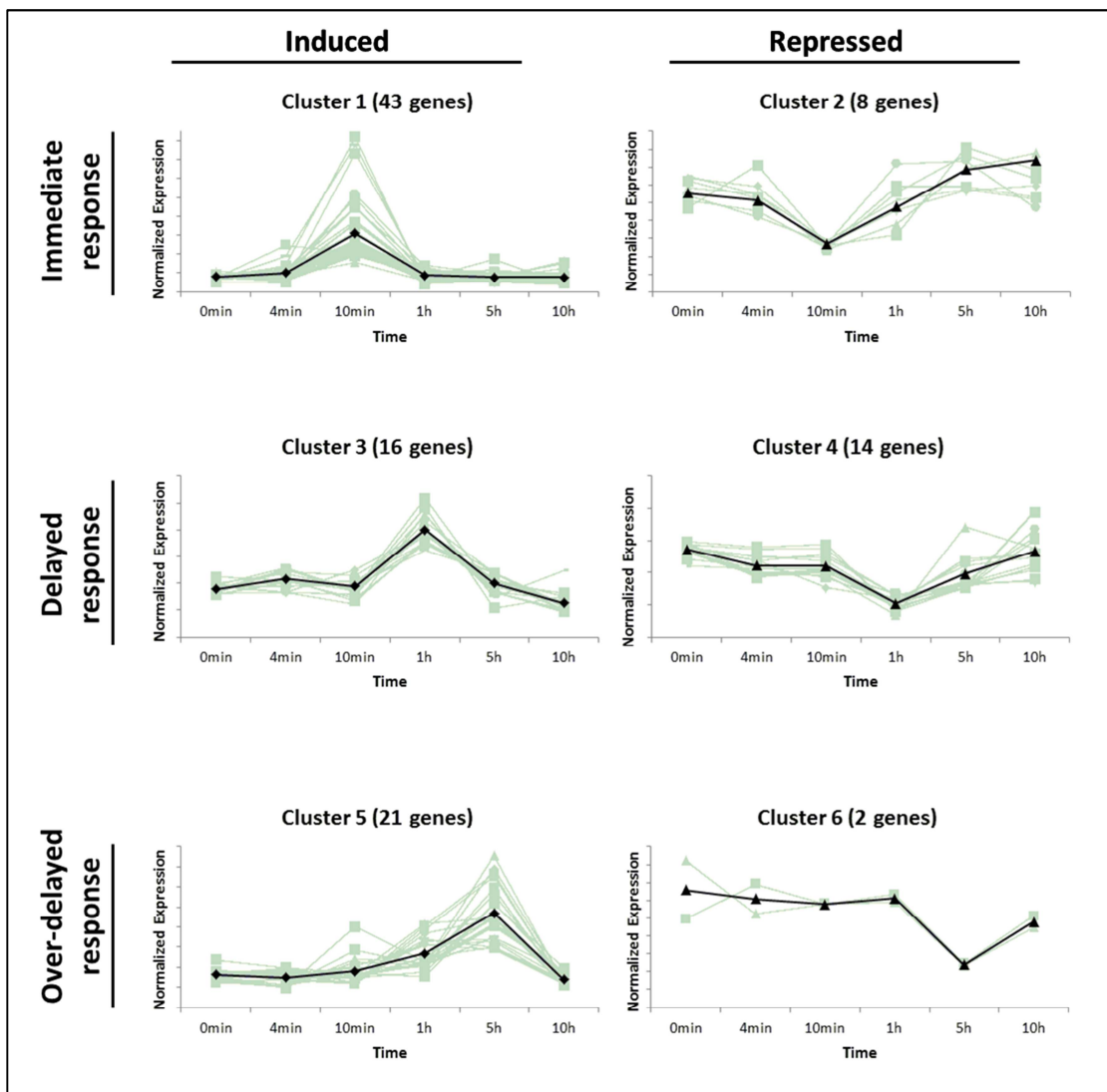


Figure III.6: Mean time-dependent profiles of clustered genes. Differentially expressed genes through dissolved oxygen pulse were clustered in six groups according to their time dependent expression profiles. Grey lines represent the expression level of each gene in that cluster during the time course. Black line represents the average expression level of all genes in that cluster during the time course (0 (steady state), 4 min, 10 min, 1 hour, 5 hours and 10 hours). Absolute intensity values were mean normalized for each gene and for each time-point.

III.2.3.1.1 Genes of immediate response to oxygen

Among the 43 genes that were induced 10 minutes after oxygen impulse (cluster 1), it is worthy to mention the presence of genes encoding components of the mitochondrial respiratory chain, such as *CYCI* (aerobic isoform of cytochrome c) and *RIP1* (component of the mitochondrial cytochrome bc1 complex). *HMG1*, *ERG5* and *CYB5*, which are involved in sterol synthesis and *SOD2* which participates in oxidative stress response, were also induced 10 minutes after impulse. Furthermore, genes that encode transcription factors such as *ROX1* and *MOT3* also belong to cluster 1. Concomitantly, 8 genes were repressed after this period (cluster 2). Among these, *WSC4* is part of a family of proteins that look after cell wall integrity (Levin, 2011; Zu, et al., 2001). Another 6 genes of unknown function are part of this cluster; among them, *YML083C* was repressed under aerobic conditions by an heme dependent mechanism (Ter Linde, et al., 2003), which is consistent with our results.

III.2.3.1.2 Genes of delayed response to oxygen

Among the 16 genes induced an hour after the dissolved oxygen impulse (cluster 3), there are genes related to stress response such as *HOR7* whose over expression increases yeast resistance to high salt concentration (Lisman, et al., 2004) and *TSL1* who is involved in trehalose biosynthesis (Bell, et al., 1998). Trehalose is accumulated in yeast under stress conditions (Li, et al., 2009). Moreover, the genes *ZEO1*, which regulates the activity of the cell wall integrity pathway (Green, et al., 2003) and *CWPI* (cell wall protein 1), whose expression is regulated by this pathway (Klis, et al., 2006), were both induced. On the other hand, among the 14 genes repressed an hour after the dissolved oxygen impulse (cluster 4); we found a large group of *PAU* genes encoding members of the seripauperin family of proteins. The repression of these proteins by aerobiosis, similarly to the DAN/TIR family of mannoproteins (Luo & van Vuuren, 2009), has been already reported (Luo & van Vuuren, 2009; Rachidi, et al., 2000). *HEM13* involved in heme synthesis and *AUS1*, which encodes for an ABC transporter responsible for sterol uptake, were also repressed 1 hour after the oxygen impulse. The repression of *HEM13* is intriguing, but it could be a delayed response caused by heme excess after the sudden increase of oxygen (Keng, 1992). Interestingly, genes that supply

nucleotides for DNA synthesis, such as *RNR3* (Yao, et al., 2003), also belong to cluster 4.

III.2.3.1.3 Genes of over-delayed response to oxygen

Among the 21 over-delayed oxygen response genes whose peak of induction was 5 hours after the oxygen impulse (cluster 5), there are several genes involved in stress response by different environmental stimuli, such as: *HSP12* (encoding a heat-shock protein induced by oxidative stress), *CTTI* (catalase 1), *GRE1* (stress response gene), *DDR2* (multi-stress response protein induced by environmental stresses) (Kobayashi, et al., 1996) and *SIP18* (induced by osmotic stress) (Singh, et al., 2005). Additionally, the induction of the proline transporter *PUT4* is in line with the oxygen requirement for proline assimilation in yeast (Ingledeu, et al., 1987). On the other hand, the glutamine transporter *AGPI* was repressed 5 hours after the oxygen impulse (cluster 6).

III.2.3.2 Gene ontology analysis

Gene ontology enrichment analysis of each cluster showed that only clusters 1 (induction at 10 min) and 4 (repression at 1 hour) have significantly enriched functional terms (Table III.9). For cluster 1, processes related to ergosterol synthesis, electron transport chain and iron and heme metabolism were enriched. For cluster 4, only the term “response to stress” is enriched (Table III.9), due to the presence of the large group of *PAU* genes encoding members of the seripauperin family of proteins. Seripauperins have been implicated in enological fermentation stress response (Marks, et al., 2008), and are known to be induced by anaerobiosis and repressed in aerobiosis. This pattern is coherent with the observed delayed repression after the oxygen impulse (Figure III.6, cluster 4).

Table III.9: Functional terms enrichment for the genes in each cluster

Cluster number	Number of genes	Representative enriched GO terms (FDR < 0.1)	Highlight genes ^a
1	43	Sterol metabolic process Electron transport chain Heme binding	<i>ARE2</i> (Acyl-CoA:sterol acyltransferase), <i>ERG5</i> , <i>HMG1</i> , <i>CYC1</i> , <i>CYB5</i> (cytochrome b5) <i>RIP1</i> (Ubiquinol-cytochrome-c reductase) <i>CYC1</i> , <i>CYB5</i> , <i>ERG5</i>
2	8	NF	NF
3	16	NF	NF
4	14	Response to stress	<i>PAU3-4-7-8-17-18-23</i> (seripauperin family)
5	21	NF	NF
6	2	NF	NF

^a Annotations extracted from SGD
NF: no significant GO term.

III.2.3.3 Transcriptional networks controlling the oxygen response

III.2.3.3.1 Master transcriptional regulators

The regulatory mechanism(s) responsible for the different transcriptional profiles obtained in response to the oxygen impulse were investigated. We searched for the transcription factors controlling the genes in these clusters and extracted the specific regulatory networks corresponding to those transcription factors from the global network (Jothi, et al., 2009). The latter included 80 out of the 104 differentially expressed genes. We found several overlapping transcriptional modules that controlled several genes across the different clusters; but not a single individual transcription factor network was found to be responsible for a single cluster. Nevertheless, shared upstream regulators for the different transcription factor networks, such as Hap1p and Skn7p, were identified. These are shared by more than six different sub-networks, which are described below.

III.2.3.3.2 Hap1p regulatory network

The genes belonging to the Hap1p regulatory networks are a significant part of the genes in four of the different clusters (cluster 1 = 49%, cluster 4 = 33%, cluster 3 = 31% and cluster 5 = 48 %). In absolute terms, Hap1p is mainly involved in the regulatory networks of cluster 1 genes (21 out of 41 genes). In fact, a GO term enrichment analysis of the complete list of differentially expressed genes related to Hap1p is partially coincident with the GO terms of cluster 1 (related with the electron transport chain and sterol metabolism).

A closer analysis, however, reveals that Hap1p exerts its action in two ways. One direction involves the direct regulation by Hap1p of target genes, such as those of iron metabolism (*FRE1/4*), proline uptake (*PUT4*), sterol metabolism (*HMG1*) and respiratory chain components (*CYCI/7*) (Hickman & Winston, 2007; Ter Linde & Steensma, 2002) (Figure III.7c). Alternatively, Hap1p regulates intermediate transcription factors that control different branches of the oxygen response. One of these intermediates is Msn2p (Figure III.7b), a transcription factor involved in oxidative stress response (Chen, et al., 2009). Msn2p directly modulates the expression of *UBX6*, which belongs to cluster 1, and participates in protein degradation (Decottignies, et al., 2004). Moreover, Msn2p controls the expression of transcription factors such as Yap1p, which was also a direct target of Hap1p (Figure III.7b). Additionally, Msn2p together with Yap1p, control several genes related to oxidative stress that are members of either cluster 1 (*SOD2*) or cluster 5 (*CTT1*, *HSP12*).

Another target of Yap1p - and intermediate of the Hap1p network - is Rox1p (Figure III.7a), a transcription factor known to repress the so-called hypoxic genes (Plakunov & Shelemekh, 2009). The induction of *ROX1*, occurring 10 minutes after the dissolved oxygen impulse (cluster 1), is consistent with the subsequent repression of its target genes, *HEM13* and *AAC3* (Kwast, et al., 2002), 1 hour after the oxygen impulse (cluster 4).

Therefore, the transcriptional cascades Hap1p-Rox1p, and Hap1p-Msn2p –both modulated by Yap1p– strongly suggest that there are overlapping functions between the oxygen and oxidative stress transcriptional networks.

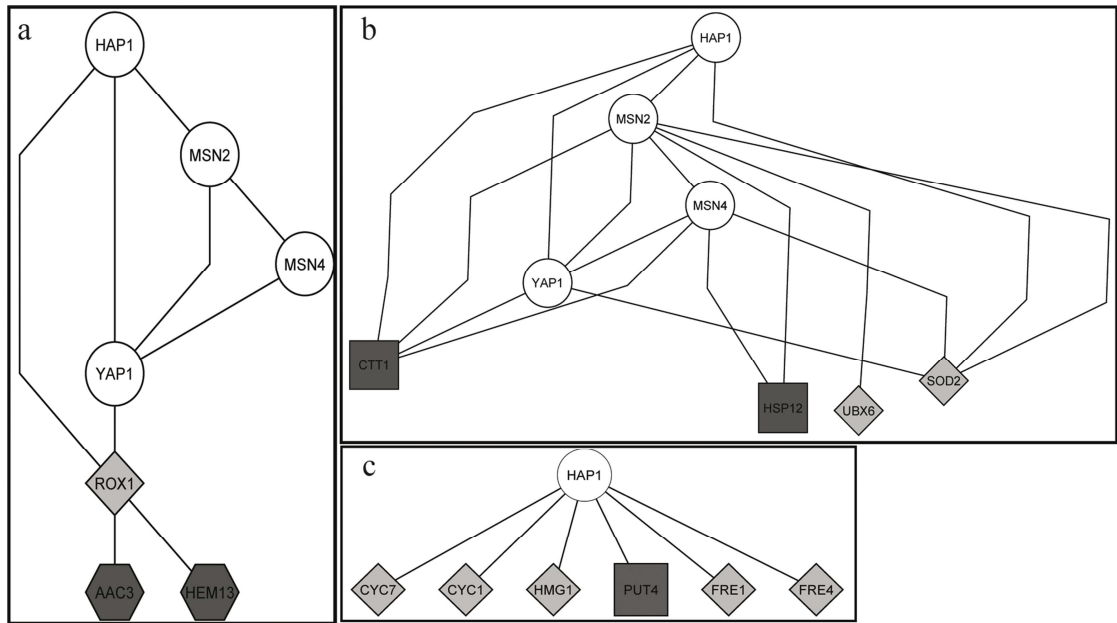


Figure III.7: Genes regulated by Hap1p. Master transcription factor and target genes are illustrated from the top to the bottom of the figure. Nodes were identified according to the cluster to which they belong: Cluster 1 (light diamond), Cluster 4 (grey hexagon) and Cluster 5 (grey square). a) Genes directly regulated by Hap1p, b) Genes regulated by Hap1p through transcription factors related to stress and c) Genes regulated by Hap1p through Yap1p/Rox1p.

III.2.3.3.3 Skn7p regulatory network

Most of the networks described above are also dependent on Skn7p, a transcription factor that has homology with two-component bacterial transcription factors, and is involved in the induction of heat shock and oxidative stress response transcription factors (Morgan, et al., 1997; Raitt, et al., 2000). For instance, transcription factors such as Yap1p and Msn2p are targeted by both Skn7p (Figure III.8a) and Hap1p (Figure III.7b), as described above. Another example of overlapping functions between Skn7p and Hap1p regulatory networks is the transcriptional regulation of *PUT4*. This

gene is directly targeted by both master regulators Skn7p and Hap1p (Figures III.8a and III.7c respectively).

Overlapping between Hap1p and Skn7p is not complete; Skn7p is an upstream regulator of the Mot3p transcription factor, which is part of cluster 1. Thus, it appears to be responsible for the subsequent transcriptional repression of cluster 4 gene members, such as *PAU5* (Figure III.8b). Additionally, Skn7p directly regulates the expression of *PAU23* (also known as *DAN2*). Therefore, the main functional module of cluster 4 (repressed 1 hour after the oxygen impulse) is regulated through this pathway (Figure III.8b). On the other hand, Skn7p modulates the transcription of *MGA1* (Figure III.8b), a regulator of pseudohyphal differentiation (Lorenz & Heitman, 1998).

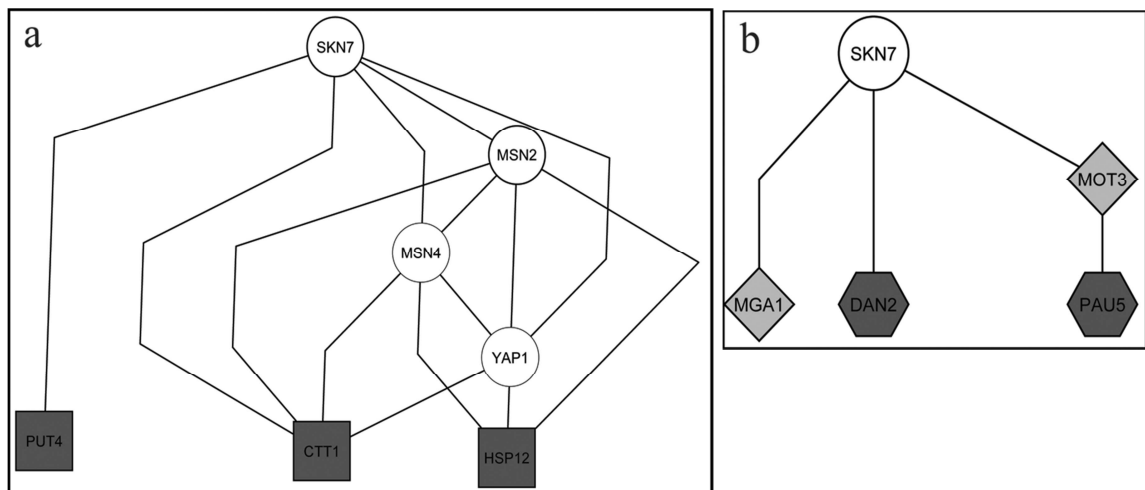


Figure III.8: Genes regulated by Skn7p. Master transcription factor and target genes are illustrated from the top to the bottom of the figure. Nodes were identified according to the cluster they belong: Cluster 1 (light diamond), Cluster 4 (grey hexagon) and Cluster 5 (grey square). a) Skn7p regulatory network and b) Genes regulated by Skn7p and Hap1p.

IV. DISCUSSION

This research addresses the impact of oxygen on the physiology of an industrial strain of *Saccharomyces cerevisiae* under enological (i.e. carbon-sufficient, nitrogen-limited) conditions. In the first part, we experimentally captured a subset of dissolved oxygen concentrations aiming to represent the oxygen-limiting range of dissolved oxygen concentrations found in the discrete enological aeration operations (Saa, et al., 2012). In the second part, we utilized an impulse of oxygen in anaerobic conditions, in order to represent the dynamic of dissolved oxygen after an oxygen impulse during industrial winemaking aeration operations (Moenne and Agosin, unpublished data).

IV.1 Impact of different oxygen levels in wine yeast extracellular metabolism.

Oxygen levels had major metabolic effects, reflected by changes in the production of several extracellular compounds and metabolic flux redistribution within the cell. For instance, ethanol and glycerol specific production rates decreased with oxygen along with the respiratory quotient. This is an indication of a transition from fermentative to mixed respiro-fermentative metabolism. Nevertheless, the respiratory quotient values indicate that full respiratory metabolism was never achieved. Although this has been already reported for laboratory strains under nitrogen-limited conditions (Tai, et al., 2005), the evidence of an active respiratory metabolism under enological conditions is striking since there is a general belief that respiration is under catabolic repression under these conditions (Gancedo, 1998; Rosenfeld et al., 2002; Salmon, 2006).

The exportation of acetic acid also shows an interesting trend being present only in strict anaerobic conditions. Even with a low dissolved oxygen level (1.2 μM), acetic acid production could not be measured. This correlates with decrease of the flux through the aldehyde dehydrogenase reaction and a slight increase of flux through the pentose phosphate pathway. Therefore, it is likely that acetate production in anaerobiosis is

necessary to provide NADPH to the cell, a function that is taken over by the pentose phosphate pathway when oxygen is available. In fact, both pathways are complementary and, together, they are the only source of NADPH in glucose-containing media (Grabowska & Chelstowska, 2003). While the mechanism for the coordination of these two pathways is unclear, the lack of change in the expression of *ALD6* gene (encoding aldehyde dehydrogenase) in response to oxygen suggests a non-transcriptional mechanism. Ald6p involvement in a calcium/calmodulin-dependent signaling pathway supports this hypothesis (Butcher & Schreiber, 2004).

IV.2 Effect of different oxygen concentration in the transition between fermentative and respiro-fermentative metabolism

The respiratory quotient showed a large decrease between 1.2 and 2.7 μM of dissolved oxygen. Consistently, Metabolic Flux Analysis predicts two very different metabolic configurations depending on the concentration of dissolved oxygen: fully fermentative (including 0 and 1.2 μM dissolved oxygen conditions) and mixed respiro-fermentative metabolism (from 2.7 μM and higher dissolved oxygen content).

Fully fermentative conditions featured low carbon fluxes and a two-branch operation of the TCA cycle, with ethanol and glycerol as the only redox sinks and glycolysis as the major source for ATP and NADH. The two-branch TCA cycle operation for anaerobic conditions was initially suggested by MFA (Nissen, et al., 1997) and later proven by ^{13}C based metabolomic analysis (Camarasa, et al., 2003) under carbon-limited conditions. To the best of our knowledge, this is the first report of a two-branch TCA cycle operation under carbon sufficient, nitrogen-limited conditions.

Cultures with more than 2.7 μM of dissolved oxygen showed a mixed respiro-fermentative metabolism despite the high external sugar concentration (40 $\text{g}\cdot\text{L}^{-1}$). It is worth noting that the model assumes that respiration is working under these conditions. Under this assumption, the estimations of ethanol and CO_2 production were reliable (Table II.2), providing further support for a functional and active respiratory pathway under these culture conditions.

The main features of the putative mixed respiro-fermentative metabolic configuration were: significant respiratory activity, TCA cycle operation in its canonical direction, increased succinic acid production, and mitochondrial redox shuttle working as a significant cytosolic NADH sink. This effect of oxygen on yeast metabolism is mirrored by gene expression, e.g. induction of *COX* and *CYCI* genes (respiration), the repression of fumarate reductase gene (reductive branch of the TCA cycle) and the induction of the *NDE1* and *GUT2* genes (mitochondrial electron shuttles). Moreover, TCA genes such as *ACO1* (aconitase) and *CIT1* (citrate synthase) are induced at the highest concentration of oxygen evaluated. Altogether, the data confirmed the occurrence of a respiratory metabolism. Nevertheless, ATP and NADH were still mainly produced by glycolysis, confirming that this is the major pathway regarding carbon flow operating in these conditions.

IV.3 Succinic acid transport under different dissolved oxygen levels

One of the hallmarks of mixed respiro-fermentative metabolism was the large increase (approx. 10 fold) of succinic acid production between 1.2 and 2.7 μM of dissolved oxygen. This most likely resulted from the much larger flux towards the TCA cycle, as compared to the two-branch TCA cycle operation, since this was not observed above 1.2 μM of dissolved oxygen. Nevertheless, how succinic acid is exported remains unclear. Several succinic acid transporters of the mitochondrial membrane are known and could account for exportation out of this organelle (Palmieri et al, 2000). However, no transporter for succinic acid has been identified at the plasma membrane yet. Therefore, succinic acid could be exported either by diffusion and/or active transport. However, the diffusion mechanism implicates a production rate that is six fold higher than the one observed (see Annexes C). Preliminary experiments argued in favor of an active transport mechanism, since batch cultures of *Saccharomyces cerevisiae* EC1118 with approx. 2.7 μM of dissolved oxygen were able to export succinic acid, despite being supplemented with exogenous succinic acid.

IV.4 Role of cytosol-mitochondria redox shuttles in respiro-fermentative metabolism

Another feature of the mixed respiro-fermentative metabolism under the culture conditions of this study was the increase of shuttling redox equivalents from the cytoplasm to the mitochondria. MFA analysis suggested that the functioning of Adh3p shuttle is necessary to explain the ethanol reduction under the 21 μ M of dissolved oxygen condition. However, the function of neither Nde1p nor Gut2p can be ruled out in respiro-fermentative metabolism, since replacing Adh3p with Nde1p does not change model estimations. Moreover, inclusion of the Gut2p shuttle in the MFA model yielded good estimations for all aerobic conditions (data not shown). Experimental evidence for Nde1p and Gut2p suggests that both mechanisms are active as enzymatic activity for both was detected under aerobic, nitrogen-limited conditions (Pahlman, et al., 2001). Moreover, at the oxygen metabolic threshold (between 1.2 and 2.7 μ M dissolved oxygen), we found an induction of the Nde1p gene at the transcriptional level. Gut2p gene was also gradually induced by oxygen, contradicting previous studies where this gene was reported to be catabolically repressed (Rigoulet, et al., 2004) . Therefore, the increased mitochondrial capacity for cytosolic NADH reoxidization could be attributed to the presence of these shuttles, as well as of the Adh3p shuttle, which showed a constant and significant gene expression regardless of the oxygen level.

Despite the increase in mitochondrial shuttle activity, the mitochondria showed a limited reoxidization capacity, as reflected by the large contribution of the ethanol production pathway to NADH reoxidization, even when the yeast was under the highest dissolved oxygen concentration (Table III.6). This limited capacity, instead of catabolic repression, was the most likely cause of the Crabtree effect (Vemuri, et al., 2007) and, overall, of the inability of *Saccharomyces cerevisiae* to develop a full respiratory metabolism under nitrogen limitation. Whether this limitation occurs at the shuttle level or at the activity of the respiratory enzymes level is unclear from our experiments. Nevertheless, the shuttle hypothesis is in line with recent reports that have proposed that mitochondrial membrane surface availability is crucial in regulating the respiro-

fermentative transition (Zhuang et al, 2011). Therefore, focusing on the shuttles can be a valuable and novel approach to shift yeast metabolism to a more oxidative state. This could be useful, for example, to lower ethanol production in enological fermentation, an active area of research in metabolic engineering (see, for example, Ehsani et al., (2009)).

IV.5 Respiratory related genes are expressed under steady state oxygen levels despite high sugar concentrations

The hypothesis of a limited mitochondrial reoxidization as the major cause of the Crabtree effect was reinforced by gene expression analyses. We found little evidence of glucose catabolic repression of respiratory enzymes, as the *COX*, cytochromes b and c (*CYB2* and *CYCI*) genes are responsive to oxygen despite high external sugar concentration. This was also observed by Tai et al (Tai, et al., 2005). Even under anaerobic conditions, expression of these genes was higher than the average (Figure III. 3), which discards any repressive effect from the high external glucose concentration. The data also suggests that oxygen was able to override glucose catabolic repression, as the expression of many responsive genes (such as *COX*) was positively correlated with dissolved oxygen concentrations (Figure III.3). Therefore, heme-dependent oxygen induction, through the HAP transcription factor (Plakunov & Shelemekh, 2009), could be able to by-pass catabolic repression. However, it was not possible to detect significant changes in transcription factor activities using Network Component Analysis (Liao, et al., 2003), suggesting that the mechanisms involved in this phenomenon are too elaborated to be inferred only from gene expression profiles. This regulatory landscape appears to encompass all conditions in the presence of oxygen.

IV.6 Physiological response of wine yeast at the highest dissolved oxygen concentration.

The physiological response of wine yeast at the highest dissolved oxygen level (21 μM), has several unique features. For instance, a puzzling gene expression scheme occurred. Respiratory genes were induced, but those encoding for ion transporters, such as those for iron and copper, were repressed. This is the opposite of what occurs upon oxygen exposure where both, iron transport and respiratory genes are induced coordinately, since iron is required for building the essential hemoproteins of the respiratory chain.

The situation at 21 μM could be a major physiological reconfiguration when maximum OUR capacity of yeast cells is reached (Figure III.1). One component of this reconfiguration could be oxidative stress, which would also explain the iron uptake restriction, seeing that an excess of iron generates more free radicals into the cell (Eide, 1998). Furthermore, some oxidative stress marker genes, such as *GRX4* are induced. Grx4p negatively regulates the activity of Aft1p (Pujol-Carrion et al, 2006), the master transcriptional factor regulating iron metabolism. The latter provides a mechanism to explain iron transporter repression. Aft1p could also influence nitrogen metabolism (Shakoury-Elizeh, et al., 2004) which is indeed the case under high oxygen conditions. For instance, *DAL81*, (regulator of allantoin utilization), a transcription factor that positively regulates the utilization of alternative nitrogen sources, shows the highest expression at anaerobic condition and 21 μM dissolved oxygen, both conditions in which nitrogen is effectively unavailable. Aft1p could influence other nutrients metabolism (Shakoury-Elizeh, et al., 2004), for which we also found transporter repression (Table III.7).

The repression of the nutrient transporters could explain the modest biomass increase when comparing 21 μM with 5 μM dissolved oxygen conditions. Also, limited nutrient availability could play a role in establishing OUR saturation at 21 μM dissolved oxygen (Figure III.1), since nutrient limitation can impair the yeast capacity to build more respiratory complexes and/or mitochondria. This is supported by the fact that the

critical OUR is much higher in carbon-limited cultures (Larsson, et al., 1993), indicating that the catalytic capacity of the respiratory chain can sustain a higher OUR. Therefore, the low critical OUR under nitrogen-limited culture conditions is more likely related to the total respiratory complexes available.

The evidence presented here suggests some degree of both oxidative and nutritional stress in the oxygen-saturated conditions (21 μM). Consistently, we have observed that with dissolved oxygen higher than 21 μM (Figure III.1), biomass can drop as low as 4 $\text{g}\cdot\text{L}^{-1}$ (data not shown), suggesting that at 21 μM dissolved oxygen yeast cells are at the limit of its biomass producing capacities. Additionally, in this condition there is a strong increase in carbohydrate synthesis (Table III.5), which is a landmark of physiological stress responses in microorganisms (Li, et al., 2009). Altogether, this data suggests that yeasts are possibly under multi-factorial stress under nitrogen-limited conditions at the OUR saturation regime. Increased carbohydrate synthesis also explains the simultaneous increase of biomass/glucose yield and decrease of ethanol and CO_2 /glucose yields, another puzzling feature of the 21 μM dissolved oxygen condition (Table III.2).

IV.7 Yeast cell wall remodeling by different steady state dissolved oxygen concentration

The changes in dissolved oxygen concentrations also impact the cell wall. For instance, *SLC1*, which encodes a key enzyme in phospholipid metabolism, is repressed at 1.2 μM of dissolved oxygen. At the highest oxygen concentration, these changes can be another source of stress. For example, ergosterol and unsaturated lipid biosynthetic gene expression significantly decreased at 21 μM dissolved oxygen. In fact, the ergosterol content and synthesis rate decreased by 77% when comparing 5 μM and 21 μM dissolved oxygen conditions (Table III.5). This ergosterol reduction could also contribute in establishing a stress phenotype, given that ergosterol has been regarded as a protective compound against oxidative stress (Landolfo, et al., 2010). On the other hand, oxygen represses several mannoprotein-encoding genes (*TIR*) in a dose-dependent

fashion This could be caused by Upc2p, an inducer of the ergosterol biosynthesis and *TIR* genes (Davies & Rine, 2006). Upc2p decreases at high dissolved oxygen levels (Table III.8) by a yet unknown mechanism. Moreover, oxygen represses another cell wall-related gene, *MUC1*, (also called *FLO11*), which is involved in flocculation of non-industrial yeast strains (Bayly, et al., 2005).

IV.8 Dissolved oxygen levels impact for winemaking process.

From a wine making perspective, metabolic flux analysis and gene expression data suggest that elevated dissolved oxygen concentrations could affect yeast performance during and after fermentation. During fermentation, reaching oxygen levels above 2.7 μM would reduce the ethanol yield (Table III.2); and reaching 21 μM or higher would induce a severe stress on the yeast cell, further decreasing its fermentative capacity. These oxygen levels are easily achieved in the industrial wine making practice (Moenne et al, unpublished data). Therefore, these results indicate that it is advisable not to keep wine yeast cells at these oxygen levels for an extended period of time. Furthermore, mannoprotein genes repression by oxygen could also be damaging since their presence in wine has been linked to many beneficial effects, such as increased mouth feel, aroma retention and astringency reduction (Gonzalez-Ramos, et al., 2008). Furthermore, one of these mannoproteins (Hpf1p) is a key contributor to white wine clarification by protein haze removal (Dupin, et al., 2000). Another repressed gene product, Flo1p, is crucial for flocculation. Repression of these proteins could be a novel mechanism of how oxygen can affect wine quality, aside from its known oxidative effect on phenolic compounds (Waterhouse & Laurie, 2006).

On the contrary, low oxygen levels could be beneficial for winemaking. For instance, with 1.2 μM of dissolved oxygen, ethanol production is similar to anaerobiosis, and without acetic acid detection, which is beneficial since acetic acid is a common “off-flavor” in wine when is present in high concentration (Boulton, et al., 1998). Viability and stress resistance of the wine yeast might also increase, as specific content of ergosterol, a protective compound against stresses in wine fermentation (Landolfo, et al.,

2010), increases to its maximum (Orellana, M, Aceituno F.F, & Agosin E., unpublished data). Moreover, nitrogen-deficient musts can be used more efficiently in winemaking since the proline carrier (*PUT4*) is induced (Table III.7) and proline assimilation effectively increased at 1.2 μM of dissolved oxygen (Table III.5), which in turn allows further biomass synthesis. Further research will be aimed to find a trade-off between oxygen addition and limitation under wine making conditions.

IV.9 Physiological response of the wine yeast *S. cerevisiae* EC1118 to an oxygen impulse under enological conditions.

The impact of an oxygen impulse on wine yeast physiology resulted in several unique features. For instance, in terms of dissolved oxygen dynamics, the time during which the dissolved oxygen was consumed was close to four minutes, in agreement with previously published data for transient anoxia (Lai, et al., 2006; van den Brink, et al., 2008). From a physiological perspective, dissolved oxygen is quickly consumed as compared to another nutritional perturbations (such as glucose and ammonia) performed under similar conditions (Dikicioglu, et al., 2011). This results from the fact that, under anaerobic conditions, wine yeast cells actively express several genes involved in pathways and reactions that require oxygen for their function. Therefore, post-transcriptional regulation mechanisms are probably responsible for the regulation of the corresponding proteins, which would allow yeast cells to rapidly respond to changes in dissolved oxygen availability (Rintala, et al., 2009; Varela, et al., 2005).

This hypothesis is reinforced by the limited number of genes whose expression is significantly affected by oxygen impulse (104 genes), as compared with those differentially expressed after glucose (372 genes) or ammonia impulses (369 genes), evaluated under similar culture conditions (Dikicioglu, et al., 2011). The differential expression of 104 genes is small, but coherent with the notion that oxygen is not a powerful stimulus on transcriptional change, as demonstrated by the wine yeast response to increasing long-term dissolved oxygen levels (Aceituno, et al., 2012). The small

number of genes differentially expressed also brings, as a consequence, lack of gene ontology term enrichment in our analysis. This reinforces the notion that oxygen, as a short or long-term transcriptional stimulus, acts only on a few key genes.

It is noteworthy that the specific rates of main carbon compounds (glucose consumption, and ethanol, biomass, glycerol and carbon dioxide production) remained constant throughout the experiment. The latter, could be attributed to the fast oxygen consumption kinetics (4 minutes) that occurred in our experiments (Figure III.4a), in agreement with previously published data for carbon-limited media, either in batch or continuous culture conditions (Lai, *et al.*, 2006, van den Brink, *et al.*, 2008).

IV.10 Gene expression response and regulatory networks throughout dissolved oxygen impulse

The gene expression clusters gathered throughout the oxygen impulse showed a single peak or valley at a certain time, reflecting an uniphasic and, to some extent, simpler response to the oxygen impulse under nitrogen-limited conditions; this was not the case with more complex gene expression patterns previously reported for carbon-limited, dynamic studies evaluated at aerobic/anaerobic transitions or vice versa (Lai, *et al.*, 2006; Lai, *et al.*, 2005; van den Brink, *et al.*, 2008).

IV.11 Master transcription factors controlling the short-term oxygen yeast response.

Integrating gene expression data with existing global transcriptional networks allowed us to find several master transcriptional regulators of the oxygen response in yeast. In particular, Hap1p and Skn7p were the most important, despite not being regulated directly by oxygen itself. These regulators have well-known small metabolite dependent activation mechanisms and, therefore, they could be a likely starting point for the regulatory cascade that results in the observed transcriptome dynamics. For instance,

Hap1p is activated by heme (Kwast, et al., 1998) and Skn7p responds to free radical generating agents, such as hydrogen peroxide (Ng, et al., 2008).

Each of these transcription factors have a major role in different, although related, biological processes that are induced in wine yeast cells due to a sudden increase of dissolved oxygen under enological conditions. Hap1p is the master regulator of the so-called “aerobic genes” (Kwast, et al., 1998); Skn7p is one of the main transcriptional controllers of *S. cerevisiae* oxidative stress response (OSR) (Morano, et al., 2012; Morgan, et al., 1997).

IV.11.1 Beneficial oxygen impulse effects from a winemaking perspective: the role of Hap1p.

The analysis of temporal gene expression of the different clusters shows a trend towards induction of mitochondrial respiratory chain genes, as part of the immediate response to oxygen impulse (cluster 1), supporting our previous findings that mitochondrial respiration could be active under wine fermentation conditions (Aceituno, et al., 2012). This can impact the viability and fermentative rate of yeast after discrete oxygen additions, under enological conditions (Rosenfeld, et al., 2003; Valero, et al., 2001).

On the other hand, the induction of sterol biosynthetic genes, such as *HMG1*, *ERG5* and *CYB5*, 10 minutes after the oxygen impulse (cluster 1), is in line with the absolute requirement of oxygen for the biosynthesis of these compounds (Rosenfeld & Beauvoit, 2003); and also, concurs with the induction of ergosterol synthesis due to oxygen availability, by wine yeast under winemaking conditions (Rosenfeld, et al., 2003). Ergosterol plays a key role in the fluidity of the yeast membrane, allowing to increase ethanol tolerance (Alexandre, et al., 1994), an important attribute of industrial yeast strains. Supporting our findings, the induction of genes involved in sterol homeostasis (*CYB5* and *ERG* gene family, among others) has been previously reported during the transition from anaerobic to aerobic conditions (Lai, et al., 2006). The transient induction of ergosterol biosynthesis is coordinated with the down-regulation of its uptake; this is reflected in the repression of *AUS1*, one hour after the oxygen impulse

(cluster 4). It is remarkable that, for long-term oxygen addition experiments, this coordinated response of the ergosterol-related genes was not detected (Aceituno, et al., 2012), strongly suggesting that the induction of oxygen-dependent ergosterol biosynthesis is a transient phenomenon. The latter, lends support to the enological practice of discrete oxygen additions, since one of the main goals of this operation is to allow ergosterol and unsaturated fatty acid synthesis in the fermenting yeast (Valero, et al., 2001).

Furthermore, the over-delayed induction of proline transporter *PUT4* (cluster 5) reveals that the discrete addition of oxygen under enological conditions also allows nitrogen deficient musts to be more efficiently fermented during winemaking (Aceituno, et al., 2012). The induction of *PUT4* and the repression of glutamine transporter *AGPI* within the same temporal frame (5 hours after oxygen impulse), could represent a coordinated response due to the availability of proline as a nitrogen source. Coherently with this idea, in long-term oxygen additions, *PUT4* is induced even at low oxygen concentration (Aceituno, et al., 2012).

As for the transcriptional regulation of this group of genes all, except *AGPI*, belong to the Hap1p transcriptional network, supporting the hypothesis that Hap1p is the master coordinator of the metabolic changes caused by oxygen addition on wine yeast physiology. Nevertheless, some of these genes are not solely controlled by the Hap1p transcriptional network. For instance, the induction of *PUT4* is also controlled by oxidative stress through Skn7p (Figure III.8a). The latter is supported by the current induction of *PUT4* with *HSP12* and *CTT1* (Figure III.8a), five hours after oxygen impulse (cluster 5). *HSP12* and *CTT1* are known to participate in oxidative stress response (Jamieson, 1998). Indeed, there are several evidences that support the relationship between stress response and *PUT4* induction. For instance, Ni and coworkers (Ni, et al., 2009) demonstrated the direct interaction between Skn7p and *PUT4* promoter through ChIP experiments. Additional evidence supports *PUT4* induction by saline stress (Dhar, et al., 2011; Rep, et al., 2000; Yale & Bohnert, 2001). Therefore, the induction of *PUT4* could also be a nutritional response caused by oxygen availability as part of metabolic changes due to oxidative stress by the sudden increase of dissolved oxygen.

IV.11.2 Other yeast oxidative stress response upon oxygen addition in wine fermentation conditions: the role of Skn7p.

Several evidence support that oxidative stress response of wine yeast cells is induced by a sudden increase of dissolved oxygen; for instance, the induction of both, *CTT1* and *SOD2*, which belong to two of the major antioxidant defense mechanisms in yeast (Jamieson, 1998). These genes are regulated by Yap1p, Msn2p and Msn4p, which in turn are regulated by the master oxidative stress transcription factor Skn7p. The latter is consistent with the known role of Msn2p, Msn4p and Yap1p in the yeast oxidative stress response. Interestingly, *CTT1* and *SOD2* are regulated either directly or indirectly by Hap1p (Jamieson, 1998), supporting the idea that there are overlapping functions between oxygen transcriptional response and oxidative stress response. Moreover, *SOD2* is induced 10 minutes after the oxygen impulse (cluster 1), while *CTT1* is induced 5 hours later (cluster 5). This temporal difference might be explained by the fact that Sod2p is a mitochondrial ROS scavenger, while Ctt1p is a cytosolic. Therefore, the yeast response against ROS caused by the oxygen impulse would be biphasic, composed of: a short-term response, i.e. the control of ROS generation from its mitochondrial source; and a secondary response, minimizing ROS concentration in the cytoplasm.

However, oxidative stress response modifies the expression of genes that do not respond uniquely to oxidative stress, the so-called common stress response (CER) genes (Causton, et al., 2001) or environmental stress response (ESR) genes (Gasch, et al., 2000). For instance, *CTT1* and *HSP12* expression are induced by heat shock and saline stress (Martínez-Pastor, et al., 1996). Additionally, the induction of *TSL1*, an hour after the oxygen impulse (cluster 3), suggests a delayed induction of trehalose biosynthesis due to oxidative stress caused by the sudden increase of dissolved oxygen. This hypothesis is supported by the induction of trehalose synthesis as yeast's response to hydrogen peroxide, an oxidative damaging agent (Estruch, 2000). Nevertheless, the induction of genes that participate in trehalose metabolism is also considered as an environmental stress response (Gasch, et al., 2000), considering the essential role of trehalose in response to thermal, osmotic and ethanol stresses (Pereira, et al., 2001). The induction of the genes mentioned above clearly establishes that the sudden increase of dissolved oxygen concentration represents an environmental stress for the wine yeast.

On the other hand, the involvement of Skn7p in the transcriptional regulation of *PAU* genes (Figure III.8b) was coherent with its known role in oxidative stress just as the cell-wall related Pau proteins are known to respond to stress (Luo & van Vuuren, 2008). This hypothesis is supported by the fact that transcriptional repression of Pau proteins by oxygen is independent of Rox1p and heme (Rachidi, et al., 2000).

IV.12 Other stress related responses and effect of oxygen impulse on the yeast cell wall.

Another effect of oxidative stress on wine yeast physiology is related with cell wall remodeling through the modification in the expression of cell wall mannoprotein genes (Abramova, et al., 2001), as suggested by the repression of *PAU* genes (cluster 4) and the induction of *CWPI* (cluster 3). Moreover, transcription factor analysis suggests that these genes are simultaneously regulated by the Ste12p transcription factor (Supplementary Figure 3, annexes D).

The role of some of the above mentioned genes in wine fermentation sheds some light on the impact of oxygen in winemaking. For example, genes such as *PAU5* are highly up-regulated during early stages of wine fermentation (Rachidi, et al., 2000; Rossignol, et al., 2003). Furthermore, the stability of Pau5p is increased by osmotic and ethanol stresses (Luo & van Vuuren, 2008), reinforcing the idea that oxygen has a deleterious impact on the yeast stress response through, for instance, *PAU5* repression. On the other hand, *PAU* genes behavior coincides with the dose-dependent repression of *TIR* genes with increasing steady-state concentration of dissolved oxygen (Aceituno, et al., 2012). Altogether, these evidence suggests that oxygen affects the mannoprotein composition of yeast cell wall and, consequently, wine organoleptic properties (Caridi, 2006; Gonzalez-Ramos, et al., 2008). Therefore, it seems that excessive oxygen addition could be detrimental for wine yeast stress resistance during winemaking, as well as for resulting wine quality.

V. CONCLUSIONS AND FUTURE DIRECTIONS

During the industrial winemaking process, oxygen additions are a common practice in most wineries because it is beneficial for yeast growth, fermentative rate (Julien, et al., 2000; Rosenfeld, et al., 2003), aromatic diversity and color stability (Pérez-Magariño et al., 2007) among other factors. Furthermore, oxygen is an efficient tool in order to avoid sluggish and stuck fermentations, a mayor problem for winemaking industry (Bisson & Butzke, 2000; Blateyron & Sablayrolles, 2001).

Nonetheless, oxygen could have also detrimental effects when added at the wrong moment or in too high concentrations, resulting in wine oxidation, color degradation and off-flavors synthesis (Toit et al., 2006). Therefore, to facilitate the development of oxygen addition strategies that maximize yeast performance in industrial fermentations and, to avoid the detrimental effects of oxygen on winemaking process, improved knowledge about how oxygen modifies wine yeast physiology under enological conditions is fundamental.

In this study, we present the first quantitative and systemic assessment of the impact of dissolved oxygen on wine yeast physiology, under winemaking (i.e. nitrogen limited and carbon sufficient) conditions.

In the first part of this study, we found that, under a nitrogen-limited setting, dissolved oxygen levels exert a large metabolic effect mainly on wine yeast mitochondria. Furthermore, there is a threshold that separates fermentative and respiro-fermentative metabolism. This is related to the expression of some key genes, such as *COX*, *NDE1* and *GUT2* and *FRD1*. Changes in the expression of these genes could explain most of the flux changes estimated in relation to respiration, cytosolic NADH shuttling to the mitochondria and the change in TCA cycle operation when dissolved oxygen increases.

Additionally, gene induction casts doubts on the operation of glucose catabolic repression under nitrogen-limited conditions, since it can be overridden by oxygen. Indeed, the significative gene inductions of some key mitochondrial respiratory enzymes (Supplementary table 2, annexes B) do not support the hypothesis of catabolic repression

as the principal cause of Crabtree effect. Furthermore, Metabolic Flux Analysis suggests that the Crabtree effect could be explained by the limited capacity of yeast mitochondria to reoxidize cytosolic NADH under winemaking conditions.

On the other hand, the physiological response of wine yeast at its fastest OUR presents two main features: the nutritional restriction reflected by the repression of genes encoding ion transporters, such as iron and copper and the stress responses of wine yeast due to high oxygen concentration. The nutritional restriction in these conditions, could explain both, the modest biomass increase when comparing 21 μM with the 5 μM dissolved oxygen condition and the fact that the critical OUR is higher under carbon-limited conditions. This could be related with the reduced availability of respiratory complexes under nitrogen limited conditions.

The stress phenotype of wine yeast at its fastest OUR is configured by the strong increase in carbohydrate synthesis, which is a landmark of stress responses in microorganisms (Li, et al., 2009). Additionally, the reduction of ergosterol content could also contribute in establishing a stress phenotype since ergosterol is necessary to mitigate oxidative stress and oxidative damage in *S. cerevisiae* wine yeast strains during growth under unfavorable conditions (Landolfo, et al., 2010).

From a winemaking perspective, the results suggest that high dissolved oxygen levels, could affect yeast performance throughout the fermentation process. For instance, reaching dissolved oxygen levels above 2.7 μM would reduce the ethanol yield on glucose (Table III.2), which is beneficial if the objective is to reduce the final ethanol content in wine. Additionally, dissolved oxygen level of 21 μM would produce severe stress phenotype on wine yeast, further decreasing its fermentative capacity. This is reflected in the reduction of the specific ethanol production rate (Table III.4a), at the highest dissolved oxygen concentration.

Nonetheless, low oxygen levels could be beneficial for winemaking. For instance, with 1.2 μM dissolved oxygen, ethanol production is similar to anaerobiosis (Table III.4b), and without acetic acid production, which is beneficial since acetic acid is a common “off-flavor” in wine when its produced at high concentration (Boulton, et al., 1998). Moreover, nitrogen-deficient musts can be used more efficiently in winemaking

since the proline carrier (*PUT4*) is induced under transient or steady-state addition of oxygen. Indeed, proline assimilation effectively increased at 1.2 μ M oxygen (Table III.5), which in turn, increases the biomass synthesis. Additionally, the induction of genes coding for ergosterol pathway by the transient addition of dissolved oxygen supports this enological practice, since one of the main goals of discrete oxygen additions during winemaking process, is allowing ergosterol and unsaturated fatty acid synthesis in the fermenting yeast (Valero, et al., 2001)

Other genes affected by an oxygen impulse and steady-state dissolved oxygen levels were mannoprotein-encoding genes, which were repressed as part of the global remodeling of the cell wall. This repression could have negative consequences in wine quality, considering the positive impact of yeast mannoproteins for wine aroma, color and astringency, among others (Caridi, 2006).

The induction of mitochondrial respiratory genes by means of oxygen, despite high sugar concentrations, supports the hypothesis of an active respiration under winemaking conditions. Furthermore, Metabolic Flux Analysis assumes that respiration works in presence of oxygen. Under this assumption, the estimations of ethanol and CO₂ production were reliable (Table II.2), providing further support for a functional and active respiratory pathway under our culture conditions.

These evidence mentioned above, contradicts the general belief that mitochondrial respiratory enzymes are subjected to catabolic repression (Gancedo, 1998) due to high sugar concentrations under winemaking conditions (Salmon, 2006). Nonetheless, the inclusion of an active respiratory pathway under winemaking conditions could explain an important part of the 46% of overall yeast oxygen consumption, which is not explained by several oxygen consumption pathways evaluated in a recent study (Salmon, 2006).

In the second part of this study, we assessed the impact of transient oxygen addition on the yeast transcriptome in nitrogen-limited conditions. The impact of the transient oxygen addition was related to the induction of mitochondrial respiratory chain components, proline transport and sterol biosynthetic pathways -which might have a positive impact on the wine fermentation progress- and repression of mannoprotein coding genes, which could have detrimental effects for wine quality. However, we did

not find an alteration on the dynamics of extracellular metabolites, because the oxygen added is quickly consumed under our culture conditions. Nevertheless, data on short-term transcriptomic dynamics were informative since they differ to long-term oxygen responses in the induction of sterol biosynthetic pathways, oxidative stress response and other stress-associated responses. Furthermore, several transcription factors were identified such as Hap1p and Skn7p among the most relevant. These transcription factors control the expression of the majority of the genes directly involved in the physiological oxygen response in wine yeast. Thus, they represent attractive targets for fine-tuning expression, with the aim of enhancing the beneficial effects of oxygen on wine quality and/or improving the wine yeast stress resistance under winemaking conditions.

Therefore, in order to validate our evidence that strongly suggest that respiratory pathway is active under winemaking conditions, we are currently working on measuring oxygen consumption by mitochondria extracted from wine yeasts that were grown under the same conditions employed in our experiments, (i.e. nitrogen limited and carbon sufficient) mimicking winemaking conditions.

This study is a contribution to the understanding of how oxygen modifies yeast physiology, metabolism and gene expression during winemaking. The effect of different dissolved oxygen concentrations, using different oxygen addition strategies, on wine yeast physiology has been highlighted. Progress in this research area will make it possible to develop oxygen addition strategies, which maximize wine yeast performance in industrial fermentations, and minimize the detrimental effects of oxygen on wine yeast metabolism and wine quality, while considering the dual role of oxygen in “making or breaking wines.”

VI. ANNEXES

Annexes A. Reactions included in the MFA model

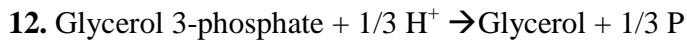
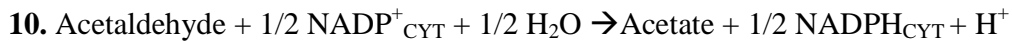
In the following biochemical reactions the subscripts CYT, MIT, and EX indicate cytosolic, mitochondrial, and extracellular metabolites, respectively; AICAR refers to 5-phosphoriboxyl-5-aminoimidazole-4-carboxamide; THF refers to tetrahydrofolate.

Glycolysis

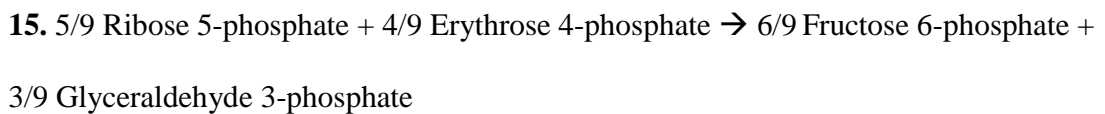
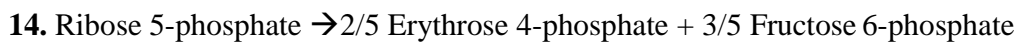
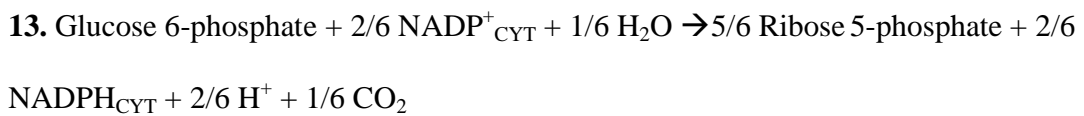
1. $\text{Glucose} + 1/6 \text{ ATP} \rightarrow \text{Glucose 6-phosphate} + 1/6 \text{ ADP} + 1/6 \text{ H}^+$
2. $\text{Glucose 6-phosphate} \rightarrow \text{Fructose 6-phosphate}$
3. $\text{Fructose 6-phosphate} + 1/6 \text{ ATP} \rightarrow 3/6 \text{ Glyceraldehyde 3-phosphate} + 3/6 \text{ Dihydroxyacetone phosphate} + 1/6 \text{ ADP} + 1/6 \text{ H}^+$
4. $\text{Dihydroxyacetone phosphate} \rightarrow \text{Glyceraldehyde 3-phosphate}$
5. $\text{Glyceraldehyde 3-phosphate} + 1/3 \text{ NAD}^+_{\text{CYT}} + 1/3 \text{ ADP} + 1/3 \text{ P} + 1/3 \text{ H}_2\text{O} \rightarrow 3\text{-Phosphoglycerate} + 1/3 \text{ ATP} + 1/3 \text{ NADH}_{\text{CYT}} + 2/3 \text{ H}^+$
6. $3\text{-Phosphoglycerate} \rightarrow \text{Phosphoenolpyruvate} + 1/3 \text{ H}_2\text{O}$
7. $\text{Phosphoenolpyruvate} + 1/3 \text{ ADP} + 1/3 \text{ H}^+ \rightarrow \text{Pyruvate} + 1/3 \text{ ATP}$

Ethanol, glycerol, and acetate synthesis

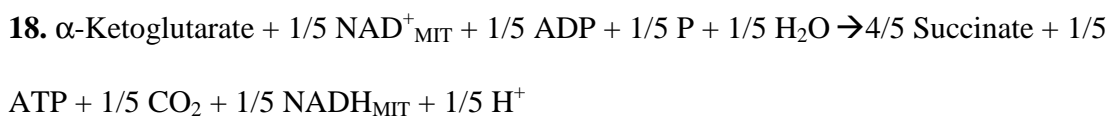
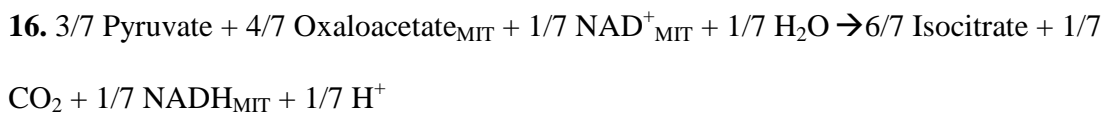
8. $\text{Pyruvate} + 1/3 \text{ H}^+ \rightarrow 2/3 \text{ Acetaldehyde} + 1/3 \text{ CO}_2$
9. $\text{Acetaldehyde} + 1/2 \text{ NADH}_{\text{CYT}} + 1/2 \text{ H}^+ \rightarrow \text{Ethanol} + 1/2 \text{ NAD}^+_{\text{CYT}}$

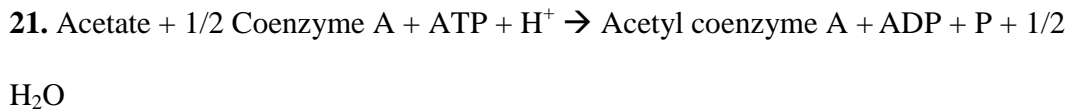


Pentose phosphate pathway



Tricarboxylic acid cycle

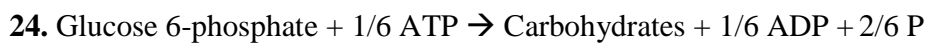




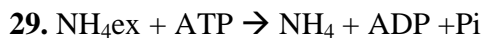
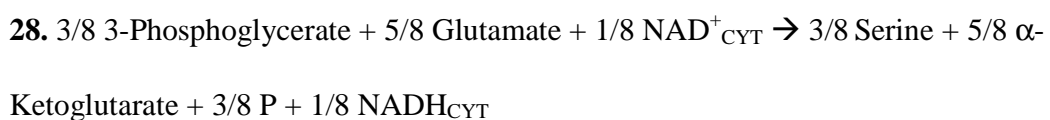
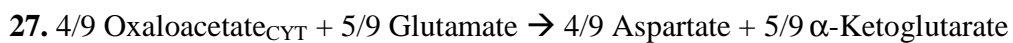
Anaplerotic reaction: pyruvate carboxylase



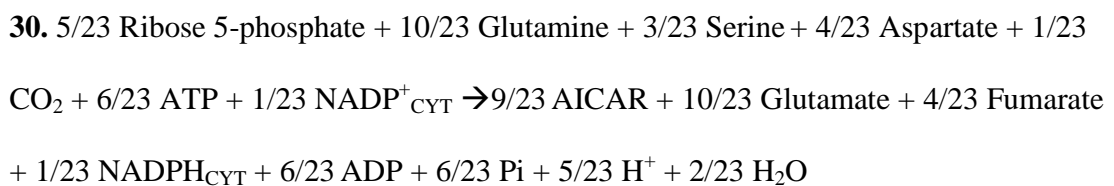
Carbohydrate synthesis



Nitrogen metabolism and amino acid biosynthesis



Synthesis of DNA, RNA, proteins, and lipids



31. 0.4579 AICAR + 0.4371 Glutamine + 0.0842 THF + 0.3313 Aspartate + 0.2544 Ribose 5-phosphate + 0.4625 ATP + 0.0509 NADPH_{CYT} + 0.1540 NAD⁺_{CYT} + 0.3301 H₂O → DNA + 0.4371 Glutamate + 0.1278 Fumarate + 0.0509 NADP⁺_{CYT} + 0.1540 NADH_{CYT} + 0.5166 H⁺ + 0.4625 ADP + 0.4625 Pi

32. 0.5112 AICAR + 0.5271 Glutamine + 0.0568 THF + 0.2993 Aspartate + 0.2400 Ribose 5-phosphate + 0.4890 ATP + 0.0568 NADP⁺_{CYT} + 0.1348 NAD⁺_{CYT} + 0.3427 H₂O → RNA + 0.5271 Glutamate + 0.1073 Fumarate + 0.1348 NADH_{CYT} + 0.0568 NADPH_{CYT} + 0.7080 H⁺ + 0.4890 ADP + 0.4890 Pi

33. 0.0263 Ribose 5-phosphate + 0.7189 Glutamate + 0.1311 Glutamine + 0.2319 Aspartate + 0.3944 Pyruvate + 0.0869 Serine + 0.0597 Erythrose 4-phosphate + 0.0895 Phosphoenolpyruvate + 1.0084 ATP + 0.0522 NADPH_{MIT} + 0.0742 NAD⁺_{MIT} + 0.0201 NADH_{CYT} + 0.0883 NADPH_{CYT} + 0.0083 SO₄⁻² + 0.7685 H₂O → Proteins + 0.5596 α-Ketoglutarate + 0.0518 Fumarate + 0.0044 Glyceraldehyde 3-phosphate + 0.1155 CO₂ + 0.0110 NH₄⁺ + 0.0124 THF + 0.0742 NADH_{MIT} + 1.0617 H⁺ + 0.0522 NADP⁺_{MIT} + 0.0201 NAD⁺_{CYT} + 0.0883 NADP⁺_{CYT} + 1.0084 ADP + 1.0084 Pi

34. 0.8326 Acetyl coenzyme A + 0.0662 Glyceraldehyde 3-phosphate + 0.1012 Serine + 0.4000 ATP + 0.7111 NADPH_{CYT} + 0.0259 H⁺ → Lipids + 0.0258 H₂O + 0.4000 ADP + 0.4000 Pi + 0.4163 Coenzyme A + 0.7111 NADP⁺_{CYT}

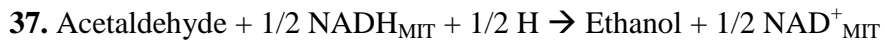
Maintenance ATP

35. ATP → "maintenance"

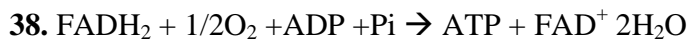
Oxaloacetate shuttle



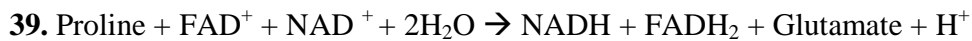
Mitochondrial synthesis of ethanol



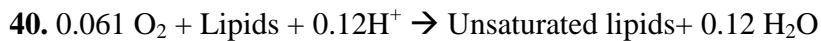
FAD oxidation



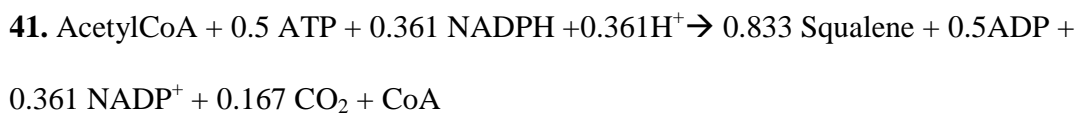
Proline consumption



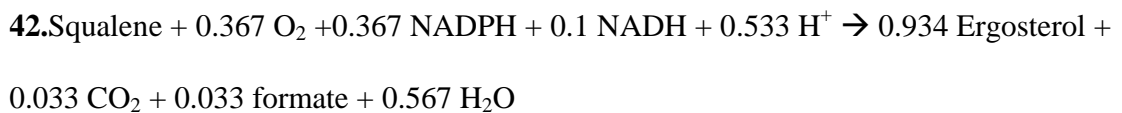
Unsaturated lipid synthesis



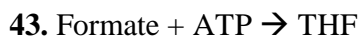
Squalene synthesis



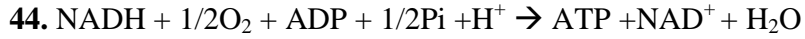
Ergosterol synthesis



Formate incorporation



Electron transport chain



Annexes B. Supplementary tables

Supplementary Table 1. Average fluxes for each reaction (numbered as in previous section) for the five dissolved oxygen conditions. Data in C-mmol (gDCW h)⁻¹

Dissolved Oxygen (μM)	0	1.2	2.7	5	21
01	43.56791	43.93017	37.45833	35.40776	21.62141
02	41.74124	42.05062	35.42772	33.4213	19.63494
03	42.27222	42.61684	35.99882	33.99629	20.20993
04	19.65378	19.9032	16.58607	15.9513	9.682103
05	40.91255	41.34309	34.71817	33.08311	19.92073
06	40.80399	41.23453	34.61269	32.97763	19.81525
07	40.72317	41.15371	34.53187	32.89681	19.73443
08	39.70785	40.01887	30.83968	27.55615	12.92306
09	26.37516	26.71167	22.28275	21.43511	13.07627
10	0.031122	0.01129	0.011266	0.022955	0.022955
11	1.482331	1.40522	1.413343	1.046845	0.422862
12	1.482331	1.40522	1.413343	1.046845	0.422862
13	0.911807	0.964684	0.96061	0.966462	0.966462
14	0.509793	0.539161	0.543223	0.546467	0.546467
15	0.337649	0.364081	0.367738	0.370658	0.370658
16	0.367146	0.557225	5.241644	10.17779	13.17587
17	0.057972	0.220897	4.236103	8.467075	11.03685
18	-0.40121	-0.26544	3.080556	6.606354	8.747821
19	-0.38068	-0.32281	1.617522	5.060879	6.848967
20	-0.32882	-0.27094	1.663335	5.106699	6.894788
21	-0.00027	0.01129	0.011266	0.022955	0.022955
22	0.256723	0.256723	0.25672	0.256719	0.256719
23	0.754398	0.805152	1.538157	0.915469	0.84057
24	0.914864	0.914864	1.07	1.02	2.588
25	1.156713	1.15673	1.139657	1.139674	1.139674
26	0.237184	0.237206	0.217369	0.217391	0.217391
27	0.485519	0.485544	0.464089	0.464115	0.464115

28	0.289491	0.289499	0.281267	0.281275	0.281275
29	0.270135	0.270143	0.262761	0.262769	0.262769
30	0.048963	0.04899	0.025329	0.025357	0.025357
31	0.006806	0.006819	0.006862	0.006875	0.006875
32	0.063172	0.063181	0.045031	0.04504	0.04504
33	0.864406	0.864403	0.864393	0.86439	0.86439
34	1.39E-07	1.39E-07	1.39E-07	1.39E-07	1.39E-07
35	11.20334	11.40328	10.86781	12.85686	10.18332
36	0.538614	0.589357	1.331898	0.709197	0.634299
37	0.065756	-0.04358	-1.73413	-3.08721	-4.4838
38	-0.09517	-0.1023	0.35558	1.21682	1.712242
39	6.7E-15	-0.108	-0.244	-0.242	-1.26E-14
40	-0.00596	-0.0058	-0.00635	-0.00618	-0.00618
41	2.2E-08	2.2E-08	2.2E-08	2.2E-08	2.20E-08
42	-0.00027	0.01129	0.011266	0.022955	0.022955
43	-0.00023	0.009405	0.009384	0.019121	0.019121
44	0.095335	0.1954	2.537532	4.469145	6.053723

Supplementary Table 2. Gene expression of key mitochondrial respiratory genes according to Affymetrix microarray data (Aceituno, et al., 2012).

Gene code	Gene name	Function	Dissolved oxygen concentration (μM)			
			0	1.2	2.7	5
YGL187C	COX4	Complex IV subunit	8.69	9.43	9.85	10.12
YNL052W	COX5A	Complex IV subunit	8.60	9.19	9.95	10.30
YJR048W	CYC1	Cytochrome c	6.55	5.49	7.09	8.67
YOR065W	CYT1	Complex III catalytic subunit	7.51	7.13	7.33	8.27
Average gene expression of the whole transcriptome			6.69	6.40	6.50	6.66

Data is deposited at Gene Expression Omnibus under the number GSE34964.

Annexes C. Succinic acid transport

The observed production rate of succinic acid (Table III.4a, main text) is the actual production rate only if there is no intracellular accumulation of the product, i.e., it is exported against concentration gradient. Since active succinic acid transporters in yeast are unknown, we evaluated a diffusion mechanism. In the first case, the diffusion is governed by the intracellular and extracellular pH. Since the pK_a of succinic acid is 4.21, assuming an intracellular pH of 5 (Walker, 1998) and extracellular pH of 3.5, most of the succinic acid should be in an anionic, monocarboxylic form that is unable to cross the membrane. This arises from the following calculations, using the equation for diffusion of weak acids in (Villadsen, et al., 2011).

$$\frac{C_{intracellular}}{C_{extracellular}} = \frac{1 + 10^{pH - pKa}}{1 + 10^{pH - pKa}}$$

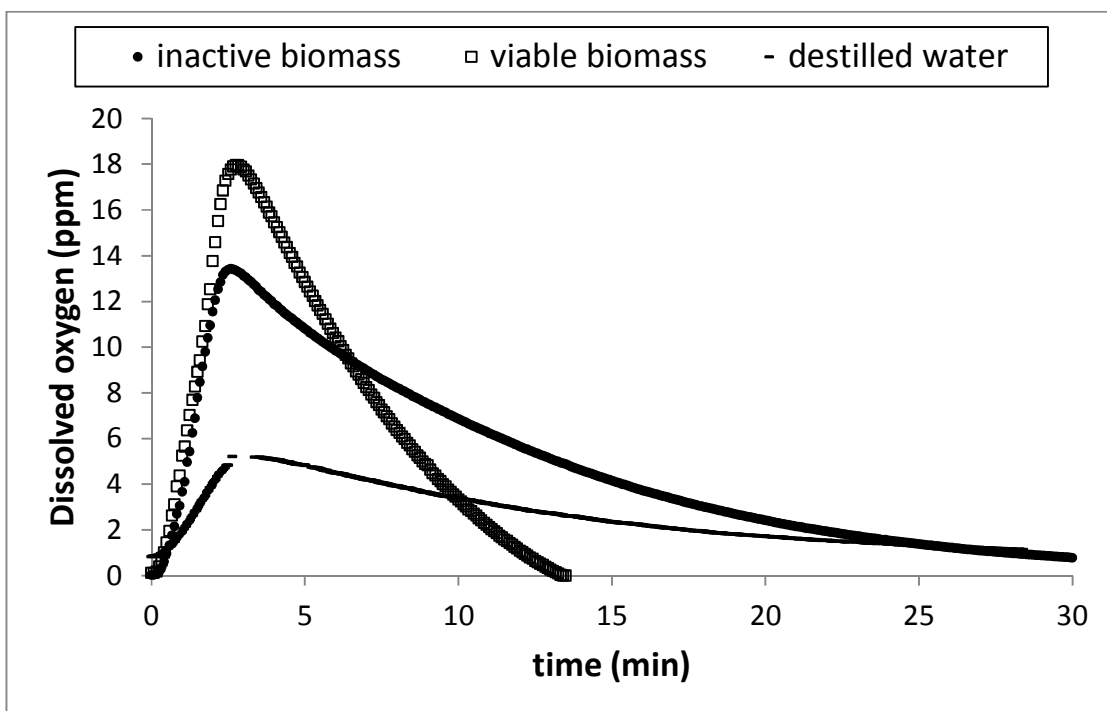
Replacing the values for compartment pH and pK_a , we obtain that the ratio intracellular/extracellular concentration is 6 at this pH conditions. Therefore, to achieve a production rate of succinic acid of $0.24 \text{ C-mmol (gDCW}^{-1} \text{ h)}^{-1}$, (the rate in the $4 \mu\text{M}$ of dissolved oxygen), which corresponds to an extracellular concentration of 2.54 mM , the cell should to accumulate 15.24 mM of intracellular succinic acid. This would correspond to an actual production rate of $1.44 \text{ C-mmol (gDCW h)}^{-1}$ of succinic acid, six-fold higher than the observed production rate.

To differentiate between active transport and passive diffusion, we carried out batch cultures of in presence of $0.2 \text{ g}\cdot\text{L}^{-1}$ exogenous succinic acid, with should inhibit diffusion but not active transport. These cultures were performed in 250 ml flasks filled with cMS300 medium up to 225 ml. They were inoculated and incubated in an orbital shaker at 150 RPM at 20°C . These cultures had aprox. $4 \mu\text{M}$ dissolved oxygen, resembling the 5% condition. We found that succinic acid is produced at roughly the same rate ($0.11 \text{ C-mmol (gDCW h)}^{-1}$) despite the exogenous succinic acid, giving evidence of active transport. Although there is no known transporter for succinic acid, we tested the Pdr12p transporter. This is an ATP-dependent transporter of the ABC family that is known to transport monocarboxylic acids and induced by succinic acid

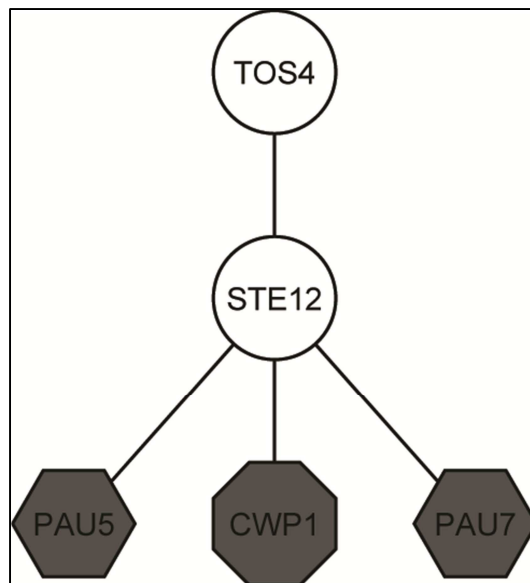
(Hatzixanthis, et al., 2003). We evaluated batch cultures of a *PDR12* null mutant in a BY4743 strain background; however, it produced succinic acid in the same amount as the control with 4 μ M dissolved oxygen. Despite this setback, we can conclude that succinic acid should be actively exported by a, so far, unknown transporter.

Annexes D. Supplementary figures

Supplementary figure 1: Dissolved oxygen dynamics after oxygen impulse with different compositions of culture media: distilled water (lines), viable biomass (open square) and heat inactivated biomass (close circle). In this experiment, the nitrogen gas feed was replaced with pure oxygen for 35 seconds. After this time, the nitrogen gas feed was restored.



Supplementary figure 3: Ste12p regulates the expression of mannoprotein genes: Master transcription factor and target genes are illustrated from the top to the bottom of the figure. Nodes were identified according to the cluster which they belong: Cluster 3 (grey octagon) and Cluster 4 (grey hexagon).



VII. REFERENCES

- Abramova, N., Sertil, O., Mehta, S., & Lowry, C. V. (2001). Reciprocal Regulation of Anaerobic and Aerobic Cell Wall Mannoprotein Gene Expression in *Saccharomyces cerevisiae*. *Journal of bacteriology*, 183(9), 2881–2887.
- Aceituno, F. F., Orellana, M., Torres, J., Mendoza, S., Slater, A. W., Melo, F., & Agosin, E. (2012). Oxygen response of the wine yeast *Saccharomyces cerevisiae* EC1118 grown under carbon-sufficient, nitrogen-limited enological conditions. *Applied and environmental microbiology*, 78(23), 8340–52.
- Acevedo, F., Gentina, J. C., & Illanes, A. (2004). *Fundamentos de Ingeniería Bioquímica* (pp. 124–147). Valparaíso: Ediciones Universitarias Valparaíso.
- Affymetrix. (2009). Gene Chip Expression Analysis Technical Manual.
- Alberty, R. A. (2006). *Biochemical thermodynamics : applications of Mathematica* (p. 464). Hoboken, N.J: Wiley-Interscience.
- Alexandre, H., Ansanay-Galeote, V., Dequin, S., & Blondin, B. (2001). Global gene expression during short-term ethanol stress in *Saccharomyces cerevisiae*. *FEBS letters*, 498(1), 98–103.
- Alexandre, H., & Charpentier, C. (1998). Biochemical aspects of stuck and sluggish fermentation in grape must. *Journal of Industrial Microbiology and Biotechnology*, 20(1), 20–27.
- Alexandre, H., Rousseaux, I., & Charpentier, C. (1994). Relationship between ethanol tolerance, lipid composition and plasma membrane fluidity in *Saccharomyces cerevisiae* and *Kloeckera apiculata*. *FEMS Microbiology Letters*, 124(1), 17–22.
- Atanasova, V., Fulcrand, H., Cheynier, V., & Moutounet, M. (2002). Effect of oxygenation on polyphenol changes occurring in the course of wine-making. *Analytica Chimica Acta*, 458(1), 15–27.
- Athenstaedt, K., & Daum, G. (1997). Biosynthesis of phosphatidic acid in lipid particles and endoplasmic reticulum of *Saccharomyces cerevisiae*. *Journal of bacteriology*, 179(24), 7611–7616.
- Bakker, B. M., Bro, C., Kötter, P., Luttik, M. a, van Dijken, J. P., & Pronk, J. T. (2000). The mitochondrial alcohol dehydrogenase Adh3p is involved in a redox shuttle in *Saccharomyces cerevisiae*. *Journal of bacteriology*, 182(17), 4730–7.
- Bakker, B. M., Overkamp, K. M., van Maris AJ, Kötter, P., Luttik, M. a, van Dijken JP, & Pronk, J. T. (2001). Stoichiometry and compartmentation of NADH metabolism in *Saccharomyces cerevisiae*. *FEMS microbiology reviews*, 25(1), 15–37.

- Bauer, F., & Pretorius, I. (2000). Yeast stress response and fermentation efficiency: how to survive the making of wine: a review. *South african journal for enology and Viticulture*, 21, 27–51.
- Bayly, J. C., Douglas, L. M., Pretorius, I. S., Bauer, F. F., & Dranginis, A. M. (2005). Characteristics of Flo11-dependent flocculation in *Saccharomyces cerevisiae*. *FEMS yeast research*, 5(12), 1151–6.
- Bell, W., Sun, W., Hohmann, S., Wera, S., Reinders, a, De Virgilio, C.,Thevelein, J. M. (1998). Composition and functional analysis of the *Saccharomyces cerevisiae* trehalose synthase complex. *The Journal of biological chemistry*, 273(50), 33311–9.
- Bisson, L. F. ., & Butzke, C. E. (2000). Diagnosis and Rectification of Stuck and Sluggish Fermentations. *American Journal of Enology and Viticulture*, 51(2), 168–177.
- Blateyron, L., & Sablayrolles, J. M. (2001). Stuck and slow fermentations in enology: statistical study of causes and effectiveness of combined additions of oxygen and diammonium phosphate. *Journal of bioscience and bioengineering*, 91(2), 184–9.
- Blüthgen, N., Brand, K., Cajavec, B., Swat, M., Herzel, H., & Beule, D. (2005). Biological profiling of gene groups utilizing Gene Ontology. *Genome Informatics*, 16, 106–115.
- Boer, V. M., Tai, S. L., Vuralhan, Z., Arifin, Y., Walsh, M. C., Piper, M. D. W. Daran, J.-M. (2007). Transcriptional responses of *Saccharomyces cerevisiae* to preferred and nonpreferred nitrogen sources in glucose-limited chemostat cultures. *FEMS yeast research*, 7(4), 604–20.
- Boubekeur, S., Camougrand, N., Bunoust, O., Rigoulet, M., & Gue, B. (2001). Participation of acetaldehyde dehydrogenases in ethanol and pyruvate metabolism of the yeast *Saccharomyces cerevisiae*. *European Journal of Biochemistry*, 268, 5057–5065.
- Boulton, R. B., Singleton, V. L., Bisson, L. F., & Kunkee, R. E. (1998). *Principles and Practices of Winemaking* (p. 604). Springer.
- Breitling, R., Armengaud, P., Amtmann, A., & Herzyk, P. (2004). Rank products: a simple, yet powerful, new method to detect differentially regulated genes in replicated microarray experiments. *FEBS letters*, 573(1-3), 83–92.
- Bunn, H. F., & Poyton, R. O. (1996). Oxygen Sensing and Molecular to Hypoxia. *physiological reviews*, 76(3), 839–885.
- Burke, P. V, Raitt, D. C., Allen, L. a, Kellogg, E. a, & Poyton, R. O. (1997). Effects of oxygen concentration on the expression of cytochrome c and cytochrome c oxidase genes in yeast. *The Journal of biological chemistry*, 272(23), 14705–12.
- Butcher, R. a, & Schreiber, S. L. (2004). Identification of Ald6p as the target of a class of small-molecule suppressors of FK506 and their use in network dissection. *Proceedings of the National Academy of Sciences of the United States of America*, 101(21), 7868–73.

- Camarasa, C., Grivet, J.-P., & Dequin, S. (2003). Investigation by ¹³C-NMR and tricarboxylic acid (TCA) deletion mutant analysis of pathways for succinate formation in *Saccharomyces cerevisiae* during anaerobic fermentation. *Microbiology*, *149*(9), 2669–2678.
- Carbon, S., Ireland, A., Mungall, C. J., Shu, S., Marshall, B., & Lewis, S. (2009). AmiGO: online access to ontology and annotation data. *Bioinformatics (Oxford, England)*, *25*(2), 288–9.
- Caridi, A. (2006). Enological functions of parietal yeast mannoproteins. *Antonie van Leeuwenhoek*, *89*(3-4), 417–22.
- Castellari, M., Arfelli, G., Riponi, C., & Amati, A. (1998). Evolution of phenolic compounds in red winemaking as affected by must oxygenation. *American Journal of Enology and Viticulture*, *49*(1), 91–94.
- Castrillo, J. I., Zeef, L. A., Hoyle, D. C., Zhang, N., Hayes, A., Gardner, D. C. J., Oliver, S. G. (2007). Growth control of the eukaryote cell: a systems biology study in yeast. *Journal of Biology*, *6*(4), 4.1–4.25.
- Causton, H. C., Ren, B., Koh, S. S., Harbison, C. T., Kanin, E., Jennings, E. G., Young, R. a. (2001). Remodeling of yeast genome expression in response to environmental changes. *Molecular biology of the cell*, *12*(2), 323–37.
- Chen, T., Li, F., & Chen, B.-S. (2009). Cross-talks of sensory transcription networks in response to various environmental stresses. *Interdisciplinary sciences, computational life sciences*, *1*(1), 46–54.
- Christie, K. R., Weng, S., Balakrishnan, R., Costanzo, M. C., Dolinski, K., Dwight, S. S., Cherry, J. M. (2004). Saccharomyces Genome Database (SGD) provides tools to identify and analyze sequences from *Saccharomyces cerevisiae* and related sequences from other organisms. *Nucleic acids research*, *32*(Database issue), D311–4.
- Conesa, A., Götz, S., García-Gómez, J. M., Terol, J., Talón, M., & Robles, M. (2005). Blast2GO: a universal tool for annotation, visualization and analysis in functional genomics research. *Bioinformatics (Oxford, England)*, *21*(18), 3674–6.
- Cot, M., Loret, M.-O., François, J., & Benbadis, L. (2007). Physiological behaviour of *Saccharomyces cerevisiae* in aerated fed-batch fermentation for high level production of bioethanol. *FEMS yeast research*, *7*(1), 22–32.
- Danilewicz, J. (2003). Review of reaction mechanisms of oxygen and proposed intermediate reduction products in wine: Central role of iron and copper. *American Journal of Enology and Viticulture*, *54*(2), 73–85.
- Davies, B. S. J., & Rine, J. (2006). A Role for Sterol Levels in Oxygen Sensing in *Saccharomyces cerevisiae*. *Genetics*, *174*(1), 191–201.
- De Deken, R. H. (1966). The Crabtree effect: a regulatory system in yeast. *Journal of general microbiology*, *44*(2), 149–56.

- De Groot, M. J. L., Daran-Lapujade, P., van Breukelen, B., Knijnenburg, T. a, de Hulster, E. a F., Reinders, M. J. T., ... Slijper, M. (2007). Quantitative proteomics and transcriptomics of anaerobic and aerobic yeast cultures reveals post-transcriptional regulation of key cellular processes. *Microbiology (Reading, England)*, 153(Pt 11), 3864–78.
- Decottignies, A., Evain, A., & Ghislain, M. (2004). Binding of Cdc48p to a ubiquitin-related UBX domain from novel yeast proteins involved in intracellular proteolysis and sporulation. *Yeast (Chichester, England)*, 21(2), 127–39.
- Devatine, A., Chiciuc, I., Poupot, C., & Mietton-Peuchot, M. (2007). Micro-oxygenation of wine in presence of dissolved carbon dioxide. *Chemical Engineering Science*, 62(17), 4579–4588.
- Dhar, R., Sägesser, R., Weikert, C., Yuan, J., & Wagner, A. (2011). Adaptation of *Saccharomyces cerevisiae* to saline stress through laboratory evolution. *Journal of evolutionary biology*, 24(5), 1135–53.
- Dikicioglu, D., Karabekmez, E., Rash, B., Pir, P., Kirdar, B., & Oliver, S. G. (2011). How yeast re-programmes its transcriptional profile in response to different nutrient impulses. *BMC systems biology*, 5(1), 148.
- Dinh, T. N., Nagahisa, K., Hirasawa, T., Furusawa, C., & Shimizu, H. (2008). Adaptation of *Saccharomyces cerevisiae* cells to high ethanol concentration and changes in fatty acid composition of membrane and cell size. *PloS one*, 3(7), e2623.
- Dukes, B. C., & Butzke, C. E. (1998). Rapid Determination of Primary Amino Acids in Grape Juice Using an o-Phthaldialdehyde/N-Acetyl-L-Cysteine Spectrophotometric Assay. *American Journal of Enology and Viticulture*, 49, 125–134.
- Dupin, I. V., Stockdale, V. J., Williams, P. J., Jones, G. P., Markides, a J., & Waters, E. J. (2000). *Saccharomyces cerevisiae* mannoproteins that protect wine from protein haze: evaluation of extraction methods and immunolocalization. *Journal of agricultural and food chemistry*, 48(4), 1086–95.
- DuToit, W., Marais, J., Pretorius, I., & DuToit, M. (2006). Oxygen in must and wine: A review. *S. Afr. J. Enol. Vitic*, 27(1), 76–94.
- Ehsani, M., Fernández, M. R., Biosca, J. a, Julien, A., & Dequin, S. (2009). Engineering of 2,3-butanediol dehydrogenase to reduce acetoin formation by glycerol-overproducing, low-alcohol *Saccharomyces cerevisiae*. *Applied and environmental microbiology*, 75(10), 3196–205.
- Eide, D. (1998). The molecular biology of metal ion transport in *Saccharomyces cerevisiae*. *Annual review of nutrition*, 18, 441–469.
- Erasmus, D., Vandermerwe, G., & Vanvuuren, H. (2003). Genome-wide expression analyses: Metabolic adaptation of to high sugar stress. *FEMS Yeast Research*, 3(4), 375–399.
- Estruch, F. (2000). Stress-controlled transcription factors, stress-induced genes and stress tolerance in budding yeast. *FEMS microbiology reviews*, 24(4), 469–86.

Fornairon-Bonnefond, C., Demaretz, V., Rosenfeld, E., & Salmon, J.-M. (2002). Oxygen addition and sterol synthesis in *Saccharomyces cerevisiae* during enological fermentation. *Journal of bioscience and bioengineering*, 93(2), 176–82.

Gancedo, J. M. (1998). Yeast carbon catabolite repression. *Microbiology and molecular biology reviews : MMBR*, 62(2), 334–61.

Gasch, a P., Spellman, P. T., Kao, C. M., Carmel-Harel, O., Eisen, M. B., Storz, G., Brown, P. O. (2000). Genomic expression programs in the response of yeast cells to environmental changes. *Molecular biology of the cell*, 11(12), 4241–57.

Gentleman, R. C., Carey, V. J., Bates, D. M., Bolstad, B., Dettling, M., Dudoit, S., Zhang, J. (2004). Bioconductor: open software development for computational biology and bioinformatics. *Genome biology*, 5(10), R80.

Georis, I., Feller, A., Vierendeels, F., & Dubois, E. (2009). The yeast GATA factor Gat1 occupies a central position in nitrogen catabolite repression-sensitive gene activation. *Molecular and cellular biology*, 29(13), 3803–15.

Gombert, A., Dos Santos, M., Christensen, B., & Nielsen, J. (2001). Network identification and flux quantification in the central metabolism of *Saccharomyces cerevisiae* under different conditions of glucose repression. *Journal of bacteriology*, 183(4), 1441–1451.

Gonzalez-Ramos, D., Cebollero, E., & Gonzalez, R. (2008). A recombinant *Saccharomyces cerevisiae* strain overproducing mannoproteins stabilizes wine against protein haze. *Applied and environmental microbiology*, 74(17), 5533–40.

Grabowska, D., & Chelstowska, A. (2003). The ALD6 gene product is indispensable for providing NADPH in yeast cells lacking glucose-6-phosphate dehydrogenase activity. *The Journal of biological chemistry*, 278(16), 13984–8.

Green, R., Lesage, G., Sdicu, A.-M., Menard, P., & Bussey, H. (2003). A synthetic analysis of the *Saccharomyces cerevisiae* stress sensor Mid2p, and identification of a Mid2p-interacting protein, Zeo1p, that modulates the PKC1-MPK1 cell integrity pathway. *Microbiology*, 149(9), 2487–2499.

Hatzixanthis, K., Mollapour, M., Seymour, I., Bauer, B. E., Krapf, G., Schüller, C., Piper, P. W. (2003). Moderately lipophilic carboxylate compounds are the selective inducers of the *Saccharomyces cerevisiae* Pdr12p ATP-binding cassette transporter. *Yeast (Chichester, England)*, 20(7), 575–85.

Hayes, A., Zhang, N., Wu, J., Butler, P. R., Hauser, N. C., Hoheisel, J. D., Oliver, S. G. (2002). Hybridization array technology coupled with chemostat culture: Tools to interrogate gene expression in *Saccharomyces cerevisiae*. *Methods (San Diego, Calif.)*, 26(3), 281–90.

Hickman, M. J., & Winston, F. (2007). Heme levels switch the function of Hap1 of *Saccharomyces cerevisiae* between transcriptional activator and transcriptional repressor. *Molecular and cellular biology*, 27(21), 7414–24.

- Hon, T., Dodd, A., Dirmeier, R., Gorman, N., Sinclair, P. R., Zhang, L., & Poyton, R. O. (2003). A mechanism of oxygen sensing in yeast. Multiple oxygen-responsive steps in the heme biosynthetic pathway affect Hap1 activity. *The Journal of biological chemistry*, 278(50), 50771–80.
- Hon, T., Lee, H. C., Hu, Z., Iyer, V. R., & Zhang, L. (2005). The heme activator protein Hap1 represses transcription by a heme-independent mechanism in *Saccharomyces cerevisiae*. *Genetics*, 169(3), 1343–52.
- Hoskisson, P. a., & Hobbs, G. (2005). Continuous culture--making a comeback? *Microbiology (Reading, England)*, 151(Pt 10), 3153–9.
- Ingledeu, WM, & Magnus, C. (1987). Influence of oxygen on proline utilization during the wine fermentation. *American Journal of Enology and Viticulture*, 38(3), 246–248.
- Ingledeu, WM, & Kunkee, R. (1985). Factors Influencing Sluggish Fermentations of Grape Juice. *American Journal of Enology and Viticulture*, 36(1), 65–76.
- Jamieson, D. J. (1998). Oxidative stress responses of the yeast *Saccharomyces cerevisiae*. *Yeast (Chichester, England)*, 14(16), 1511–27.
- Jothi, R., Balaji, S., Wuster, A., Grochow, J. a, Gsponer, J., Przytycka, T. M., Babu, M. M. (2009). Genomic analysis reveals a tight link between transcription factor dynamics and regulatory network architecture. *Molecular systems biology*, 5(294), 294.
- Jouhten, P., Rintala, E., Huuskonen, A., Tamminen, A., Toivari, M., Wiebe, M., Maaheimo, H. (2008). Oxygen dependence of metabolic fluxes and energy generation of *Saccharomyces cerevisiae* CEN.PK113-1A. *BMC systems biology*, 2, 60.
- Julien, A., Roustan, J., & Dulau, L. (2000). Comparison of nitrogen and oxygen demands of enological yeasts: technological consequences. *American Journal of Enology and Viticulture*, 51(3), 215–222.
- Kapat, A., Jung, J. K., & Park, Y. H. (2001). Enhancement of glucose oxidase production in batch cultivation of recombinant *Saccharomyces cerevisiae*: optimization of oxygen transfer condition. *Journal of applied microbiology*, 90(2), 216–22.
- Keng, T. (1992). HAP1 and ROX1 form a regulatory pathway in the repression of HEM13 transcription in *Saccharomyces cerevisiae*. *Molecular and cellular biology*, 12(6), 2616–2623.
- Klis, F. M., Boorsma, A., & De Groot, P. W. J. (2006). Cell wall construction in *Saccharomyces cerevisiae*. *Yeast (Chichester, England)*, 23(3), 185–202.
- Knijnenburg, T. a, Daran, J.-M. G., van den Broek, M. a, Daran-Lapujade, P. A., de Winde, J. H., Pronk, J. T., ... Wessels, L. F. a. (2009). Combinatorial effects of environmental parameters on transcriptional regulation in *Saccharomyces cerevisiae*: a quantitative analysis of a compendium of chemostat-based transcriptome data. *BMC genomics*, 10, 53.

- Kobayashi, N., Mcclanahan, T. K., Simon, J. R., Treger, J. M., & Mcentee, K. (1996). Structure and Functional Analysis of the Multistress Response Gene DDR2 from *Saccharomyces cerevisiae*. *Biochemical and Biophysical Research Communications*, 229(2), 540–547.
- Kresnowati, M. T. a P., van Winden, W. a, Almering, M. J. H., ten Pierick, A., Ras, C., Knijnenburg, T. a, Daran, J. M. (2006). When transcriptome meets metabolome: fast cellular responses of yeast to sudden relief of glucose limitation. *Molecular systems biology*, 2, 49.
- Kwast, K. E., Burke, P. V., & Poyton, R. O. (1998). Oxygen sensing and the transcriptional regulation of oxygen-responsive genes in yeast. *The Journal of experimental biology*, 201(Pt 8), 1177–95.
- Kwast, K., Lai, L., Menda, N., James III, D., Aref, S., & Burke, P. V. (2002). Genomic analyses of anaerobically induced genes in *Saccharomyces cerevisiae*: functional roles of Rox1 and other factors in mediating the anoxic response. *Journal of bacteriology*, 184(1), 250–265.
- Lai, L.-C., & Kosorukoff, A. (2005). Remodeling of the transcriptome during short-term anaerobiosis in *Saccharomyces cerevisiae*: differential response and role of Msn2 and/or Msn4 and other factors in. *Molecular and cellular biology*, 25(10), 4075–4091.
- Lai, L.-C., Kosorukoff, A. L., Burke, P. V., & Kwast, K. E. (2006). Metabolic-state-dependent remodeling of the transcriptome in response to anoxia and subsequent reoxygenation in *Saccharomyces cerevisiae*. *Eukaryotic cell*, 5(9), 1468–89.
- Landolfo, S., Zara, G., Zara, S., Budroni, M., Ciani, M., & Mannazzu, I. (2010). Oleic acid and ergosterol supplementation mitigates oxidative stress in wine strains of *Saccharomyces cerevisiae*. *International journal of food microbiology*, 141(3), 229–235.
- Larsson, C., von Stockar, U., Marison, I., & Gustafsson, L. (1993). Growth and metabolism of *Saccharomyces cerevisiae* in chemostat cultures under carbon-, nitrogen-, or carbon- and nitrogen-limiting conditions. *Journal of bacteriology*, 175(15), 4809–16.
- Letunic, I., & Bork, P. (2007). Interactive Tree Of Life (iTOL): an online tool for phylogenetic tree display and annotation. *Bioinformatics (Oxford, England)*, 23(1), 127–8.
- Levin, D. E. (2011). Regulation of cell wall biogenesis in *Saccharomyces cerevisiae*: the cell wall integrity signaling pathway. *Genetics*, 189(4), 1145–75.
- Li, L., Ye, Y., Pan, L., Zhu, Y., Zheng, S., & Lin, Y. (2009). The induction of trehalose and glycerol in *Saccharomyces cerevisiae* in response to various stresses. *Biochemical and biophysical research communications*, 387(4), 778–83.
- Liao, J. C., Boscolo, R., Yang, Y.-L., Tran, L. M., Sabatti, C., & Roychowdhury, V. P. (2003). Network component analysis: reconstruction of regulatory signals in biological systems. *Proceedings of the National Academy of Sciences of the United States of America*, 100(26), 15522–7.

- Lisman, Q., Urli-Stam, D., & Holthuis, J. C. M. (2004). HOR7, a multicopy suppressor of the Ca²⁺-induced growth defect in sphingolipid mannosyltransferase-deficient yeast. *The Journal of biological chemistry*, 279(35), 36390–6.
- Liu, H., Sañuda-Peña, M. C., Harvey-White, J. D., Kalra, S., & Cohen, S. A. (1998). Determination of submicromolar concentrations of neurotransmitter aminoacids by fluorescence detection using a modification of the 6-aminoquinolyl-N-hydroxysuccinimidyl carbamate method for aminoacid analysis. *Journal of Chromatography A*, 828(1-2), 383–395.
- Lorenz, M. C., & Heitman, J. (1998). Regulators of pseudohyphal differentiation in *Saccharomyces cerevisiae* identified through multicopy suppressor analysis in ammonium permease mutant strains. *Genetics*, 150(4), 1443–57.
- Luo, Z., & van Vuuren, H. J. J. (2008). Stress-induced production, processing and stability of a seripauperin protein, Pau5p, in *Saccharomyces cerevisiae*. *FEMS yeast research*, 8(3), 374–85.
- Luo, Z., & van Vuuren, H. J. J. (2009). Functional analyses of PAU genes in *Saccharomyces cerevisiae*. *Microbiology (Reading, England)*, 155(Pt 12), 4036–49.
- Lupiañez, J. A., Machado, A., Nuñez de Castro, I., & Mayor, F. (1974). Succinic acid production by yeasts grown under different hypoxic conditions. *Molecular and cellular biochemistry*, 3(2), 113–116.
- Marks, V. D., Ho Sui, S. J., Erasmus, D., van der Merwe, G. K., Brumm, J., Wasserman, W. W., van Vuuren, H. J. J. (2008). Dynamics of the yeast transcriptome during wine fermentation reveals a novel fermentation stress response. *FEMS yeast research*, 8(1), 35–52.
- Martínez-Pastor, M. T., Marchler, G., Schüller, C., Marchler-Bauer, a, Ruis, H., & Estruch, F. (1996). The *Saccharomyces cerevisiae* zinc finger proteins Msn2p and Msn4p are required for transcriptional induction through the stress response element (STRE). *The EMBO journal*, 15(9), 2227–35.
- Mashego, M. R., Jansen, M. L. a, Vinke, J. L., van Gulik, W. M., & Heijnen, J. J. (2005). Changes in the metabolome of *Saccharomyces cerevisiae* associated with evolution in aerobic glucose-limited chemostats. *FEMS yeast research*, 5(4-5), 419–30.
- Mateles, R. I., & Battat, E. (1975). Continuous Culture Used for Media Optimization. *Applied Microbiology*, 28(6), 901–905.
- Matys, V., Fricke, E., Geffers, R., Gößling, E., Haubrock, M., Hehl, R., Wingender, E. (2003). TRANSFAC(R): transcriptional regulation, from patterns to profiles. *Nucleic Acids Research*, 31(1), 374–378.
- Morano, K. a, Grant, C. M., & Moye-Rowley, W. S. (2012). The response to heat shock and oxidative stress in *Saccharomyces cerevisiae*. *Genetics*, 190(4), 1157–95.
- Morgan, B. a, Banks, G. R., Toone, W. M., Raitt, D., Kuge, S., & Johnston, L. H. (1997). The Skn7 response regulator controls gene expression in the oxidative stress response of the budding yeast *Saccharomyces cerevisiae*. *The EMBO journal*, 16(5), 1035–44.

- Murray, D. B., Haynes, K., & Tomita, M. (2011). Redox regulation in respiring *Saccharomyces cerevisiae*. *Biochimica et biophysica acta*, *1810*(10), 945–58.
- Ng, C.-H., Tan, S.-X., Perrone, G. G., Thorpe, G. W., Higgins, V. J., & Dawes, I. W. (2008). Adaptation to hydrogen peroxide in *Saccharomyces cerevisiae*: the role of NADPH-generating systems and the SKN7 transcription factor. *Free radical biology & medicine*, *44*(6), 1131–45.
- Ni, L., Bruce, C., & Hart, C. (2009). Dynamic and complex transcription factor binding during an inducible response in yeast. *Genes & Development*, *23*(11), 1351–1363.
- Nissen, T. L., Schulze, U., Nielsen, J., & Villadsen, J. (1997). Flux distributions in anaerobic, glucose-limited continuous cultures of *Saccharomyces cerevisiae*. *Microbiology (Reading, England)*, *143* (Pt 1), 203–18.
- Novo, M., Bigey, F., Beyne, E., Galeote, V., Gavory, F., Mallet, S., Dequin, S. (2009). Eukaryote-to-eukaryote gene transfer events revealed by the genome sequence of the wine yeast *Saccharomyces cerevisiae* EC1118. *Proceedings of the National Academy of Sciences of the United States of America*, *106*(38), 16333–8.
- Nylund, J.-E., & Wallander, H. (1992). Ergosterol Analysis as a Means of Quantifying Mycorrhizal Biomass. *Methods in Microbiology*, *24*, 77–88.
- Oszmianski, J., Moutounet, M., & Polyme, L. (1996). Iron-Catalyzed Oxidation of (+) - Catechin in Model Systems. *Journal of agricultural and food chemistry*, *44*, 1712–1715.
- Pahlman, I.-L., Gustafsson, L., Rigoulet, M., & Larsson, C. (2001). Cytosolic redox metabolism in aerobic chemostat cultures of *Saccharomyces cerevisiae*. *Yeast*, *18*, 611–620.
- Palmieri, L., Runswick, M. J., Fiermonte, G., Walker, J. E., & Palmieri, F. (2000). Yeast mitochondrial carriers: bacterial expression, biochemical identification and metabolic significance. *Journal of bioenergetics and biomembranes*, *32*(1), 67–77.
- Parish, M., Wollan, D., & Paul, R. (2000). Micro-oxygenation-a review. *Australian Grapegrower and Winemaker*, *438*, 47–50.
- Pearson, R. K., Zylkin, T., Schwaber, J. S., & Gonye, G. E. (2004). Quantitative Evaluation of Clustering Results Using Computational Negative Controls. In M. W. Berry, U. Dayal, C. Kamath, & D. Skillicorn (Eds.), *Fourth SIAM International Conference on Data Mining*. (p. 537). Lake Buena Vista, Florida.: Society for Industrial and Applied Mathematics.
- Pereira, M. D., Eleutherio, E. C., & Panek, a D. (2001). Acquisition of tolerance against oxidative damage in *Saccharomyces cerevisiae*. *BMC microbiology*, *1*(11), 1–10.
- Pérez-Magariño, S., Sánchez-Iglesias, M., Ortega-Heras, M., González-Huerta, C., & González-Sanjosé, M. L. (2007). Colour stabilization of red wines by microoxygenation treatment before malolactic fermentation. *Food Chemistry*, *101*(3), 881–893.

- Piper, M. D. W., Daran-Lapujade, P., Bro, C., Regenber, B., Knudsen, S., Nielsen, J., & Pronk, J. T. (2002). Reproducibility of oligonucleotide microarray transcriptome analyses. An interlaboratory comparison using chemostat cultures of *Saccharomyces cerevisiae*. *The Journal of biological chemistry*, 277(40), 37001–8.
- Pizarro, F. J., Jewett, M. C., Nielsen, J., & Agosin, E. (2008). Growth temperature exerts differential physiological and transcriptional responses in laboratory and wine strains of *Saccharomyces cerevisiae*. *Applied and environmental microbiology*, 74(20), 6358–68.
- Pizarro, F., Varela, C., Marabit, C., Bruno, C., Perez-Correa, R., & Agosin, E. (2007). Coupling kinetic expressions and metabolic networks for predicting wine fermentations. *Biotechnology and Bioengineering*, 98(5), 986–998.
- Plakunov, V. K., & Shelemekh, O. V. (2009). Mechanisms of oxygen regulation in microorganisms. *Microbiology*, 78(5), 535–546.
- Poyton, R. O. (1999). Models for oxygen sensing in yeast: implications for oxygen-regulated gene expression in higher eucaryotes. *Respiration physiology*, 115(2), 119–33.
- Pronk, J. T., Steensma, H., & van Dijken JP. (1996). Pyruvate Metabolism in *S. cerevisiae*. *Yeast*, 12, 1607–1633.
- Pujol-Carrion, N., Belli, G., Herrero, E., Nogues, A., & de la Torre-Ruiz, M. A. (2006). Glutaredoxins Grx3 and Grx4 regulate nuclear localisation of Aft1 and the oxidative stress response in *Saccharomyces cerevisiae*. *Journal of cell science*, 119(Pt 21), 4554–64.
- Pyrzyńska, K. (2004). Analytical Methods for the Determination of Trace Metals in Wine. *Critical Reviews in Analytical Chemistry*, 34(2), 69–83.
- R Development Core, T. (2006). R: A Language and Environment for Statistical Computing. In *R Foundation for Statistical Computing*. Vienna.
- Rachidi, N., Martinez, M. J., Barre, P., & Blondin, B. (2000). *Saccharomyces cerevisiae* PAU genes are induced by anaerobiosis. *Molecular microbiology*, 35(6), 1421–30.
- Raitt, D. C., Johnson, a L., Erkin, a M., Makino, K., Morgan, B., Gross, D. S., & Johnston, L. H. (2000). The Skn7 response regulator of *Saccharomyces cerevisiae* interacts with Hsf1 in vivo and is required for the induction of heat shock genes by oxidative stress. *Molecular biology of the cell*, 11(7), 2335–47.
- Regenber, B., Grotkjaer, T., Winther, O., Fausbøll, A., Akesson, M., Bro, C., Nielsen, J. (2006). Growth-rate regulated genes have profound impact on interpretation of transcriptome profiling in *Saccharomyces cerevisiae*. *Genome biology*, 7(11), R107.
- Rep, M., Krantz, M., Thevelein, J. M., & Hohmann, S. (2000). The Transcriptional Response of *Saccharomyces cerevisiae* to osmotic shock. *Journal of Biological Chemistry*, 275(12), 8290–8300.

- Ribereau-Gayon, J. (1933). *Contribution à l'étude des oxidations et réductions dans les vins. Application à l'étude de vieillissement et des casses*. Delmas Bordeaux.
- Ribereau-Gayon, P., Dubourdieu, D., Donèche, B., & Lonvaud, A. (2006). *Handbook of Enology, The Microbiology of Wine and Vinifications, Volume 1* (Second Edi., p. 512). Wiley.
- Rigoulet, M., Aguilaniu, H., Avéret, N., Bunoust, O., Camougrand, N., Grandier-Vazeille, X., Gustafsson, L. (2004). Organization and regulation of the cytosolic NADH metabolism in the yeast *Saccharomyces cerevisiae*. *Molecular and cellular biochemistry*, 256-257(1-2), 73–81.
- Rintala, E., Toivari, M., Pitkänen, J.-P., Wiebe, M. G., Ruohonen, L., & Penttilä, M. (2009). Low oxygen levels as a trigger for enhancement of respiratory metabolism in *Saccharomyces cerevisiae*. *BMC genomics*, 10, 461.
- Rosenfeld, E., & Beauvoit, B. (2003). Role of the non respiratory pathways in the utilization of molecular oxygen by *Saccharomyces cerevisiae*. *Yeast*, 20, 1115–1144.
- Rosenfeld, E., Beauvoit, B., & Blondin, B. (2003). Oxygen consumption by anaerobic *Saccharomyces cerevisiae* under enological conditions: effect on fermentation kinetics. *Applied and environmental microbiology*, 69(1), 113–121.
- Rosenfeld, E., Beauvoit, B., Rigoulet, M., & Salmon, J.-M. (2002). Non-respiratory oxygen consumption pathways in anaerobically-grown *Saccharomyces cerevisiae*: evidence and partial characterization. *Yeast (Chichester, England)*, 19(15), 1299–321.
- Rosenfeld, E., Schaeffer, J., Beauvoit, B., & Salmon, J.-M. (2004). Isolation and properties of promitochondria from anaerobic stationary-phase yeast cells. *Antonie van Leeuwenhoek*, 85(1), 9–21.
- Rossignol, T., Postaire, O., Storaï, J., & Blondin, B. (2006). Analysis of the genomic response of a wine yeast to rehydration and inoculation. *Applied Microbiology and Biotechnology*, 71(5), 699–712.
- Rossignol, Tristan, Dulau, L., Julien, A., & Blondin, B. (2003). Genome-wide monitoring of wine yeast gene expression during alcoholic fermentation. *Yeast (Chichester, England)*, 20(16), 1369–85.
- Rossouw, D., Jacobson, D., & Bauer, F. F. (2012). Transcriptional regulation and the diversification of metabolism in wine yeast strains. *Genetics*, 190(1), 251–61.
- Rossouw, D., Olivares-Hernandes, R., Nielsen, J., & Bauer, F. F. (2009). Comparative transcriptomic approach to investigate differences in wine yeast physiology and metabolism during fermentation. *Applied and environmental microbiology*, 75(20), 6600–12.
- Saa, P., Moenne, M. I., Perez-Correa, R., & Agosin, E. (2012). Modeling oxygen dissolution and biological uptake during pulse oxygen additions in oenological fermentations. *Bioprocess and Biosystems Engineering*, 35(7), 1167–1178.

- Sablayrolles, J.-M., Dubois, C., Manginot, C., Roustan, J.-L., & Barre, P. (1996). Effectiveness of combined ammoniacal nitrogen and oxygen additions for completion of sluggish and stuck wine fermentations. *Journal of Fermentation and Bioengineering*, 82(4), 377–381.
- Salmanowicz, B., Nylund, J.-E., & Wallander, H. (1990). High performance liquid chromatography - Assay of ergosterol: A technique to estimate fungal biomass in roots with ectomycorrhiza. *Agriculture, Ecosystems & Environment*, 28(1-4), 437–440.
- Salmon, J. M., & Barre, P. (1998). Improvement of nitrogen assimilation and fermentation kinetics under enological conditions by derepression of alternative nitrogen-assimilatory pathways in an industrial *Saccharomyces cerevisiae* strain. *Applied and environmental microbiology*, 64(10), 3831–7.
- Salmon, J.-M. (2006). Interactions between yeast, oxygen and polyphenols during alcoholic fermentations: Practical implications. *LWT - Food Science and Technology*, 39(9), 959–965.
- Salmon, J.-M., Fornairon-Bonnefond, C., & Barre, P. (1998). Determination of Oxygen Utilization Pathways in an Industrial Strain of *Saccharomyces cerevisiae* during Enological Fermentation. *Journal of Fermentation and Bioengineering*, 86(2), 154–163.
- Sánchez, Ó., & Cardona, C. (2008). Trends in biotechnological production of fuel ethanol from different feedstocks. *Bioresource technology*, 99(13), 5270–95.
- Sánchez-Iglesias, M., González-Sanjosé, M. L., Pérez-Magariño, S., Ortega-Heras, M., & González-Huerta, C. (2009). Effect of micro-oxygenation and wood type on the phenolic composition and color of an aged red wine. *Journal of agricultural and food chemistry*, 57(24), 11498–509.
- Schmidtke, L. M., Clark, A. C., & Scollary, G. R. (2011). Micro-oxygenation of red wine: techniques, applications, and outcomes. *Critical reviews in food science and nutrition*, 51(2), 115–31.
- Shakoury-Elizeh, M., Tiedeman, J., Rashford, J., Ferea, T., Demeter, J., Garcia, E., Philpott, C. (2004). Transcriptional remodeling in response to iron deprivation in *Saccharomyces cerevisiae*. *Molecular biology of the cell*, 15, 1233–1243.
- Singh, J., Kumar, D., Ramakrishnan, N., Jervis, J., Garst, J. F., Slaughter, S. M., Helm, R. F. (2005). Transcriptional Response of *Saccharomyces cerevisiae* to Desiccation and Rehydration. *Applied and environmental microbiology*, 71(12), 8752–8763.
- Smoot, M. E., Ono, K., Ruscheinski, J., Wang, P.-L., & Ideker, T. (2011). Cytoscape 2.8: new features for data integration and network visualization. *Bioinformatics (Oxford, England)*, 27(3), 431–2.
- Sokal, R. R., & Rohlf, F. J. (1962). The comparison of dendrograms by objective methods. *Taxon*, 11, 33–40.
- Stephanopoulos, G., Aristidou, A., & Nielsen, J. (1998). *Metabolic Engineering Principles and Methodologies* (p. 725). Academic Press.

- Swan, T. M., & Watson, K. (1998). Stress tolerance in a yeast sterol auxotroph: role of ergosterol, heat shock proteins and trehalose. *FEMS microbiology letters*, *169*(1), 191–7.
- Tai, S. L., Boer, V. M., Daran-Lapujade, P., Walsh, M. C., de Winde, J. H., Daran, J.-M., & Pronk, J. T. (2005). Two-dimensional transcriptome analysis in chemostat cultures. Combinatorial effects of oxygen availability and macronutrient limitation in *Saccharomyces cerevisiae*. *The Journal of biological chemistry*, *280*(1), 437–47.
- Teixeira, M. C., Monteiro, P., Jain, P., Tenreiro, S., Fernandes, A. R., Mira, N. P., Sá-Correia, I. (2006). The YEASTRACT database: a tool for the analysis of transcription regulatory associations in *Saccharomyces cerevisiae*. *Nucleic acids research*, *34*(Database issue), D446–51.
- Ter Linde, J J M, Régnacq, M., & Steensma, H. Y. (2003). Transcriptional regulation of YML083c under aerobic and anaerobic conditions. *Yeast (Chichester, England)*, *20*(5), 439–54.
- Ter Linde, J. J., Liang, H., Davis, R. W., Steensma, H. Y., van Dijken, J. P., & Pronk, J. T. (1999). Genome-wide transcriptional analysis of aerobic and anaerobic chemostat cultures of *Saccharomyces cerevisiae*. *Journal of bacteriology*, *181*(24), 7409–13.
- Ter Linde, José J M, & Steensma, H. Y. (2002). A microarray-assisted screen for potential Hap1 and Rox1 target genes in *Saccharomyces cerevisiae*. *Yeast (Chichester, England)*, *19*(10), 825–40.
- Valero, E., Millán, C., & Ortega, J. M. (2001). Influence of oxygen addition during growth phase on the biosynthesis of lipids in *Saccharomyces cerevisiae* (M(3)30-9) in enological fermentations. *Journal of bioscience and bioengineering*, *92*(1), 33–8.
- Valero, E., Moyano, L., Millan, M., Medina, M., & Ortega, J. (2002). Higher alcohols and esters production by *Saccharomyces cerevisiae*. Influence of the initial oxygenation of the grape must. *Food Chemistry*, *78*, 57–61.
- Van den Brink, J., Daran-Lapujade, P., Pronk, J. T., & de Winde, J. H. (2008). New insights into the *Saccharomyces cerevisiae* fermentation switch: dynamic transcriptional response to anaerobicity and glucose-excess. *BMC genomics*, *9*, 100.
- Van Dijken, J. P., & Scheffers, W. A. (1986). Redox balances in the metabolism of sugars by yeasts. *FEMS microbiology reviews*, *32*, 199–224.
- Varela, C., Cárdenas, J., Melo, F., & Agosin, E. (2005). Quantitative analysis of wine yeast gene expression profiles under winemaking conditions. *Yeast (Chichester, England)*, *22*(5), 369–83.
- Varela, C., Pizarro, F., & Agosin, E. (2004). Biomass Content Governs Fermentation Rate in Nitrogen-Deficient Wine Musts. *Applied and environmental microbiology*, *70*(6), 3392–3400.
- Vargas, F., Aceituno, F., & Agosin, E. (2010). Biochemistry and Molecular Biology of Yeast Alcoholic Fermentation. In C. G. Dussap (Ed.), *Comprehensive Food Fermentation and Biotechnology*. New Delhi, India.: Asiatech Publishers.

- Varma, A., & Palsson, B. O. (1994). Metabolic Flux Balancing: Basic Concepts, Scientific and Practical Use. *Nature Biotechnology*, 12(10), 994–998.
- Vemuri, G. N., Eiteman, M. a, McEwen, J. E., Olsson, L., & Nielsen, J. (2007). Increasing NADH oxidation reduces overflow metabolism in *Saccharomyces cerevisiae*. *Proceedings of the National Academy of Sciences of the United States of America*, 104(7), 2402–7.
- Verduyn, C. (1991). Physiology of yeasts in relation to biomass yields. *Antonie van Leeuwenhoek*, 60, 325–353.
- Villadsen, J., Nielsen, J., & Lidén, G. (2011). *Bioreaction Engineering Principles* (Third edit., p. 561p). Springer.
- Villas-Bôas, S. G., Højer-Pedersen, J., Akesson, M., Smedsgaard, J., & Nielsen, J. (2005). Global metabolite analysis of yeast: evaluation of sample preparation methods. *Yeast (Chichester, England)*, 22(14), 1155–69.
- Visser, W., Scheffers, W. a, Batenburg-van der Vegte, W. H., & van Dijken, J. P. (1990). Oxygen requirements of yeasts. *Applied and environmental microbiology*, 56(12), 3785–92.
- Von Jagow, G., & Klingenberg, M. (1970). Pathways of Hydrogen in Mitochondria of *Saccharomyces carlsbergensis*. *European Journal of Biochemistry*, 12, 583–592.
- Walker, G. (1998). *Yeast physiology and biotechnology*. John Wiley and Sons.
- Wanduragala, S., Sanyal, N., Liang, X., & Becker, D. F. (2010). Purification and characterization of Put1p from *Saccharomyces cerevisiae*. *Archives of biochemistry and biophysics*, 498(2), 136–42.
- Wang, N. S., & Stephanopoulos, G. (1983). Application of macroscopic balances to the identification of gross measurement errors. *Biotechnology and Bioengineering*, 25(9), 2177–2208.
- Wang, S. S., & Brandriss, M. C. (1987). Proline utilization in *Saccharomyces cerevisiae*: sequence, regulation, and mitochondrial localization of the PUT1 gene product. *Molecular and cellular biology*, 7(12), 4431–40.
- Waterhouse, A. L., & Laurie, V. F. (2006). Oxidation of Wine Phenolics : A Critical Evaluation and Hypotheses. *American Journal of Enology and Viticulture*, 57(3), 306–313.
- Wiebe, M. G., Rintala, E., Tamminen, A., Simolin, H., Salusjärvi, L., Toivari, M., Penttilä, M. (2008). Central carbon metabolism of *Saccharomyces cerevisiae* in anaerobic, oxygen-limited and fully aerobic steady-state conditions and following a shift to anaerobic conditions. *FEMS yeast research*, 8(1), 140–54.
- Yale, J., & Bohnert, H. J. (2001). Transcript expression in *Saccharomyces cerevisiae* at high salinity. *The Journal of biological chemistry*, 276(19), 15996–6007.

- Yao, R., Zhang, Z., An, X., Bucci, B., Perlstein, D. L., Stubbe, J., & Huang, M. (2003). Subcellular localization of yeast ribonucleotide reductase regulated by the DNA replication and damage checkpoint pathways. *Proceedings of the National Academy of Sciences of the United States of America*, *100*(11), 6628–33.
- You, K. M., Rosenfield, C., & Knipple, D. C. (2003). Ethanol Tolerance in the Yeast *Saccharomyces cerevisiae* Is Dependent on Cellular Oleic Acid Content. *Applied and environmental microbiology*, *69*(3), 1499–1503.
- Zhuang, K., Vemuri, G. N., & Mahadevan, R. (2011). Economics of membrane occupancy and respiro-fermentation. *Molecular systems biology*, *7*(500), 1–9.
- Zitomer, R. S., Limbach, M. P., Rodriguez-Torres, a M., Balasubramanian, B., Deckert, J., & Snow, P. M. (1997). Approaches to the study of Rox1 repression of the hypoxic genes in the yeast *Saccharomyces cerevisiae*. *Methods*, *11*(3), 279–88.
- Zitomer, R. S., & Lowry, C. V. (1992). Regulation of gene expression by oxygen in *Saccharomyces cerevisiae*. *Microbiological reviews*, *56*(1), 1–11.
- Zoecklein, B. W., Carey, R., & Sullivan, P. (2002). Current theory and applications of microoxygenation. *Wine East*, *30*(3), 28–34.
- Zu, T., Verna, J., & Ballester, R. (2001). Mutations in WSC genes for putative stress receptors result in sensitivity to multiple stress conditions and impairment of Rlm1-dependent gene expression in *Saccharomyces cerevisiae*. *Molecular Genetics and Genomics*, *266*(1), 142–155.
- Zuzuarregui, A., Monteoliva, L., & Gil, C. (2006). Transcriptomic and proteomic approach for understanding the molecular basis of adaptation of *Saccharomyces cerevisiae* to wine fermentation. *Applied and environmental microbiology*, *72*(1), 836–847.